Electrocardiology Modeling After Pulsed Field Ablation Relying on Asymptotic analysis

Workshop Toulouse 2023
Mathematics of electrical imaging: modeling, theory and implementation

Annabelle Collin*,

* University of Bordeaux (IMB), CNRS, Inria center at the university of Bordeaux, Bordeaux INP

In strong collaboration with **IHU Liryc** (Bordeaux)

Bordeaux INP ENSEIRB MATMECA

Inria

université de BORDEAUX

liryc L'institut des maladies du rythme cardiaque

University Hospital Institute

Electrocardiology (or cardiac electrophysiology)

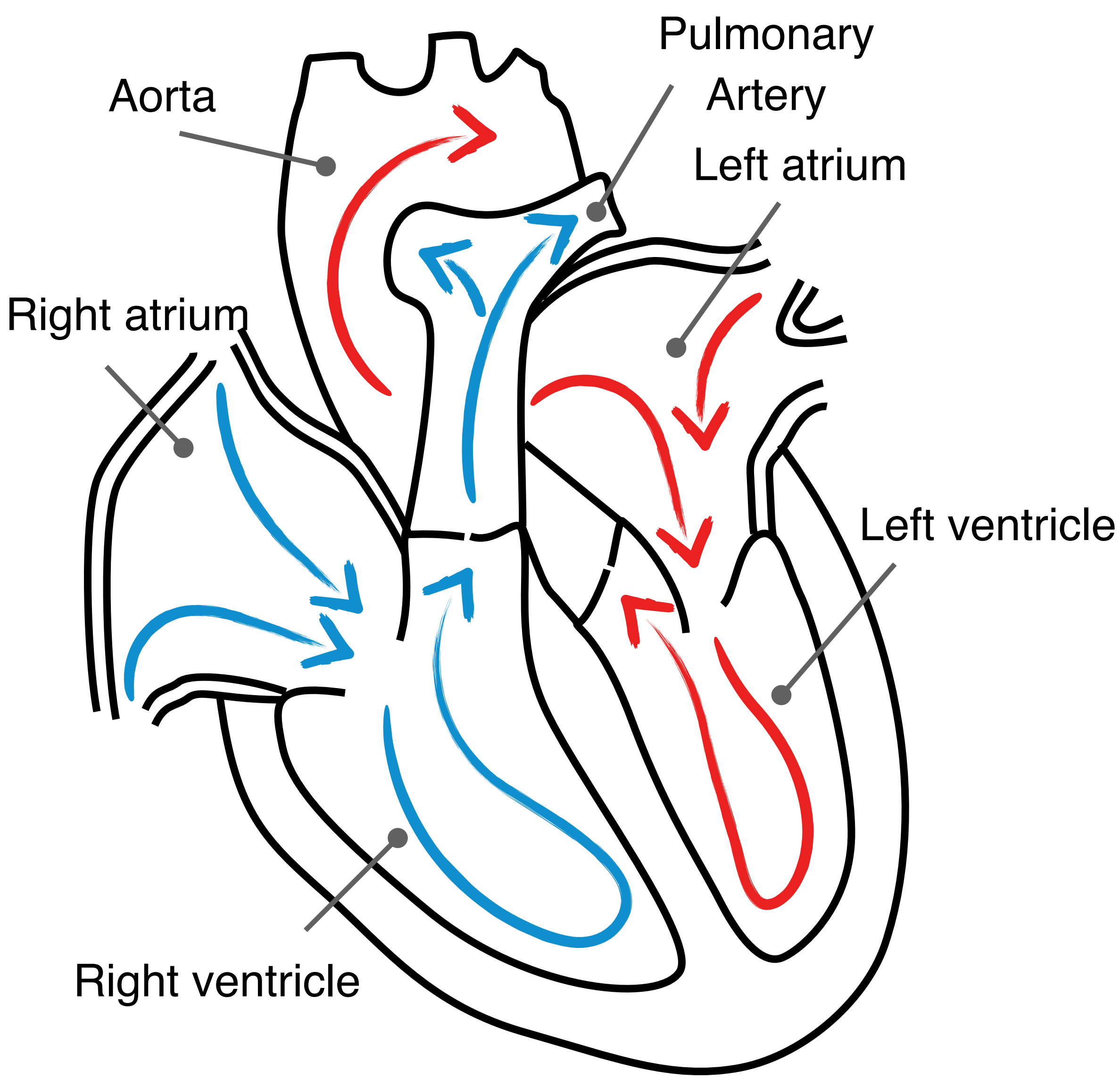

Blood circulation in the heart

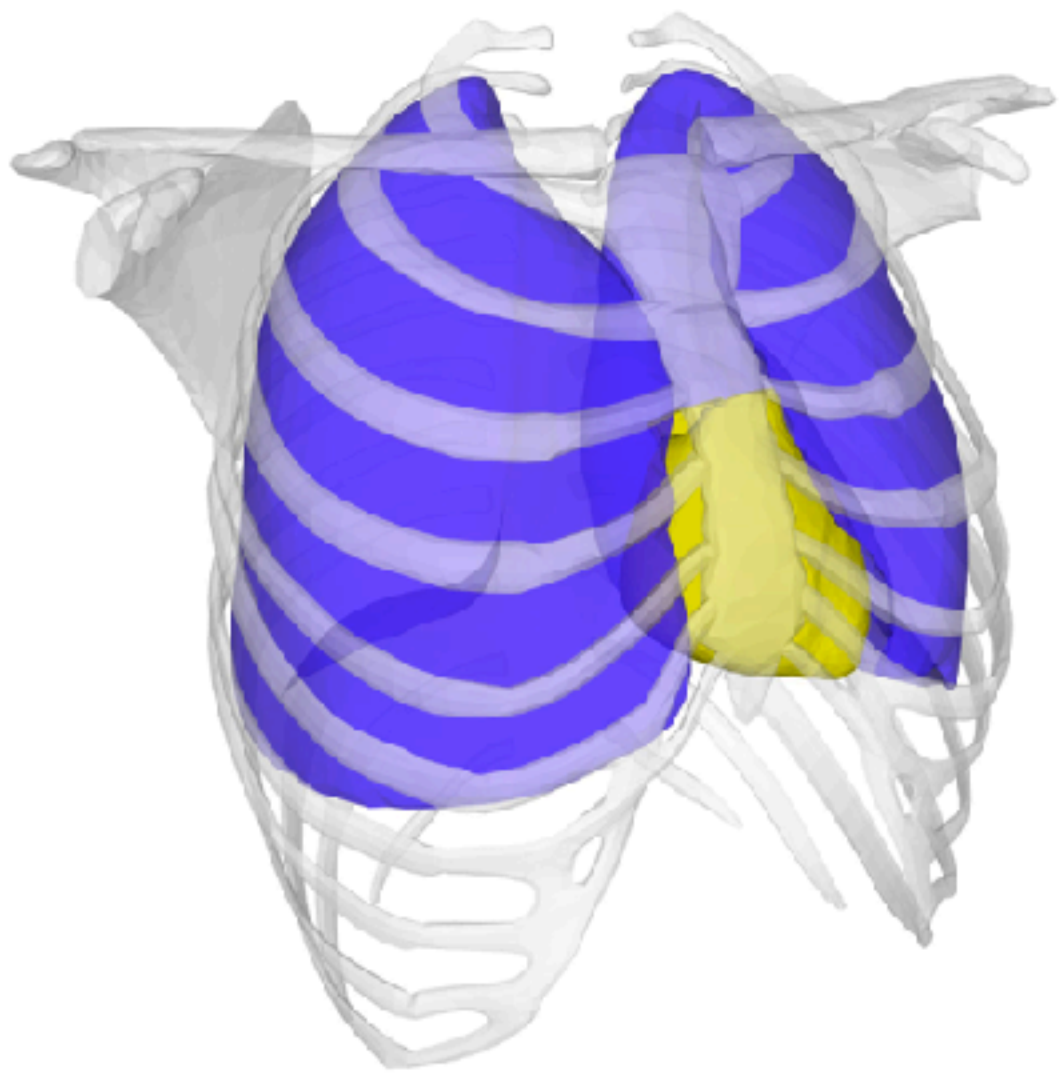

Electrical activity = origin of the mechanical activity

Electrocardiology (or cardiac electrophysiology)

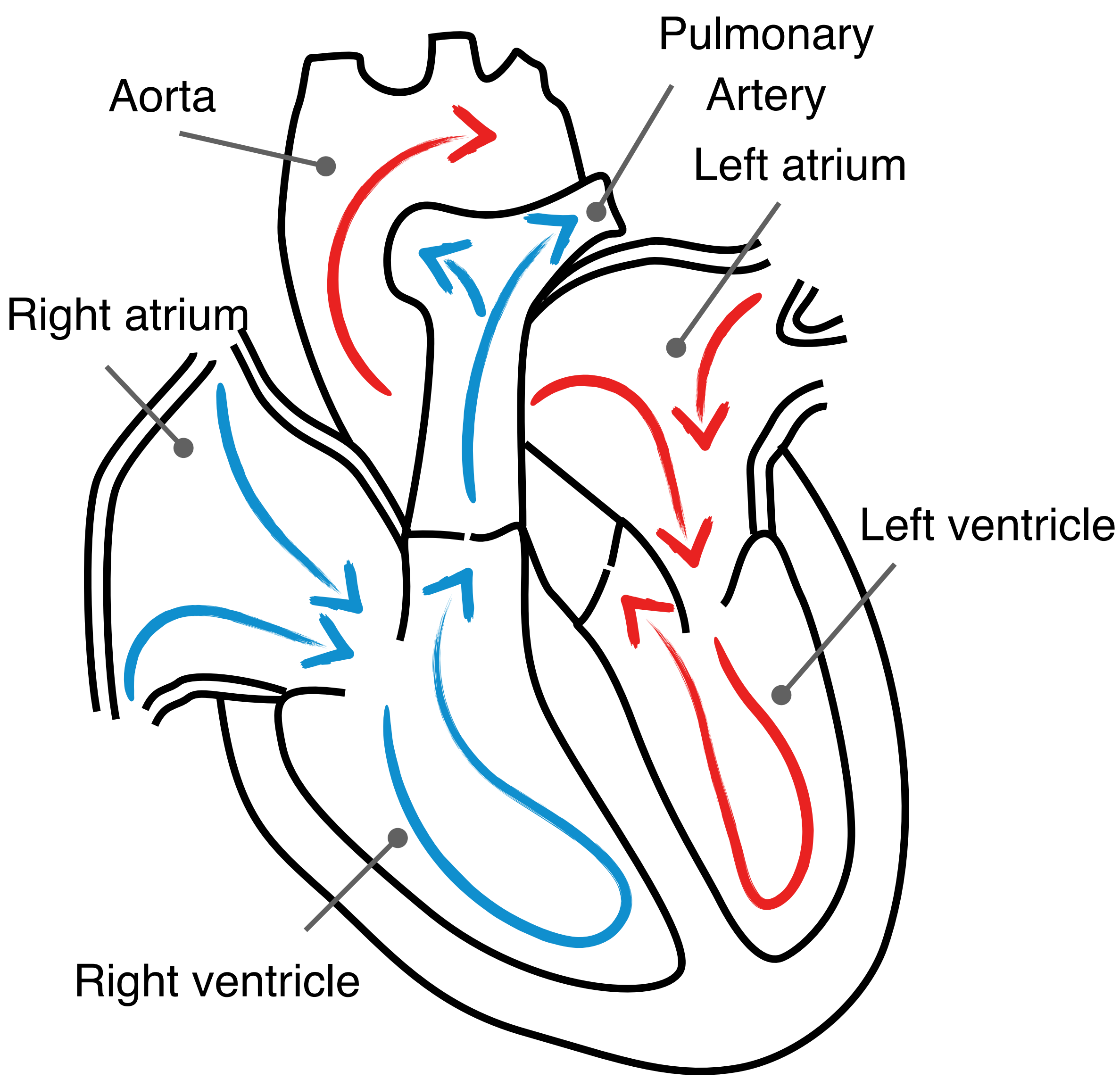

Blood circulation in the heart

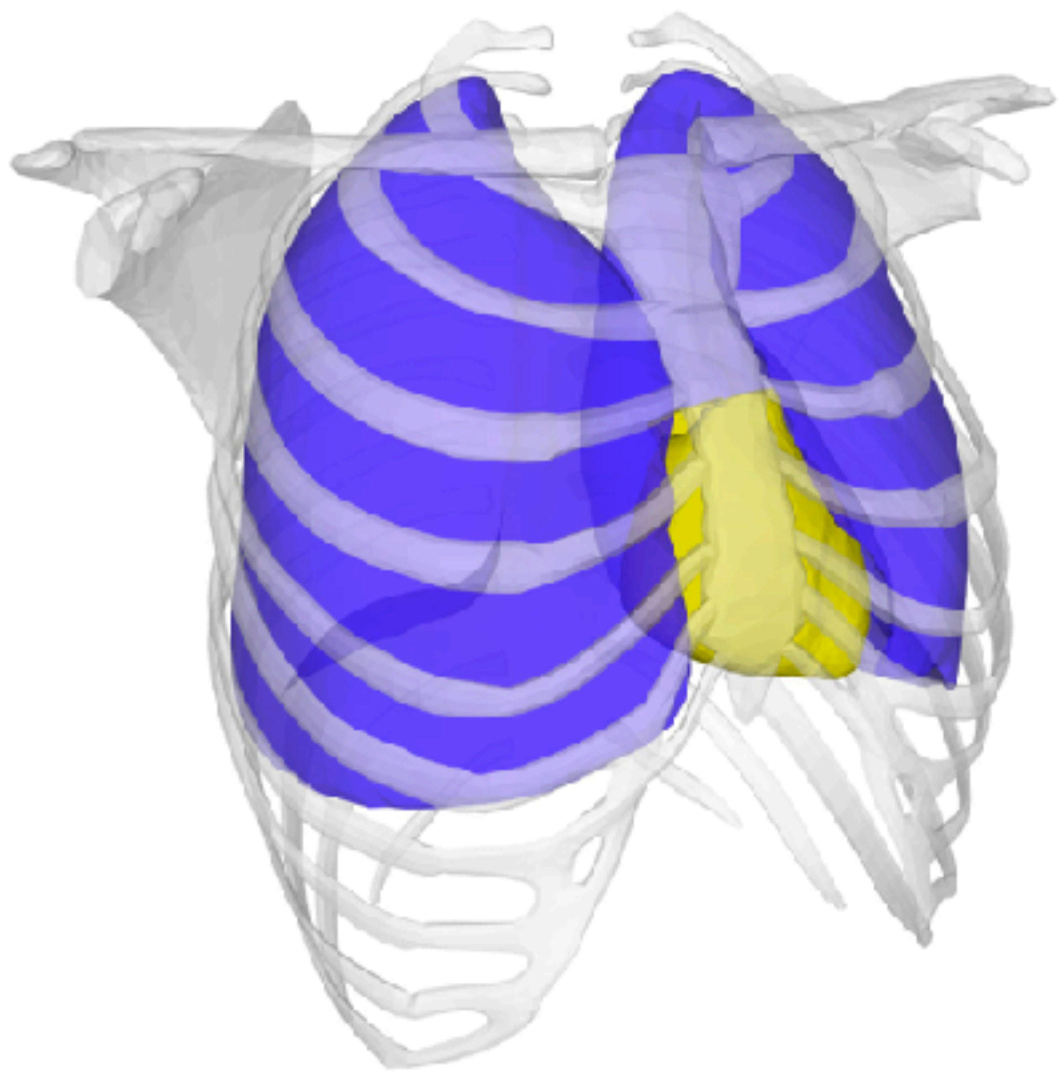

Electrical activity = origin of the mechanical activity

Mathematical model

- Bidomain model

$$A_m(C_m\partial_t v_m + I_{ion}(v_m, \cdots)) - \nabla\cdot(\sigma_i\cdot\nabla v_m) - \nabla\cdot(\sigma_i\cdot\nabla u_e) = 0,\ \ \Omega,$$
$$\nabla\cdot((\sigma_i+\sigma_e)\cdot\nabla u_e) + \nabla\cdot(\sigma_i\cdot\nabla v_m) = 0,\ \ \Omega\,.$$

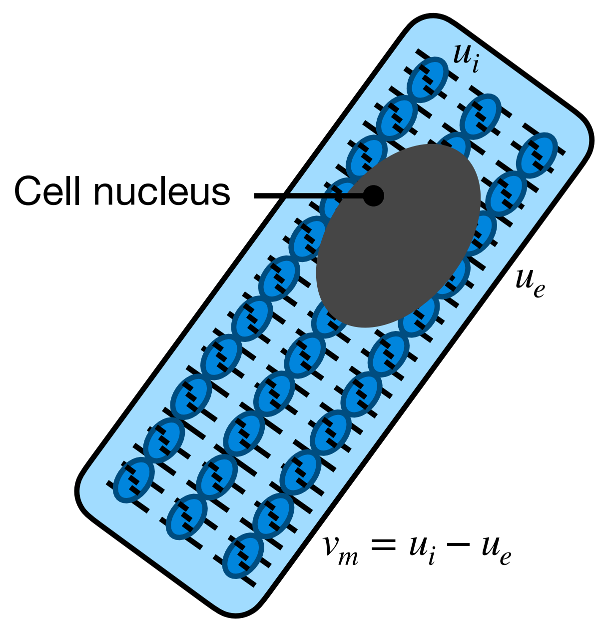

Unknowns

Transmembrane, extra- and intra-cellular potentials

Reaction term

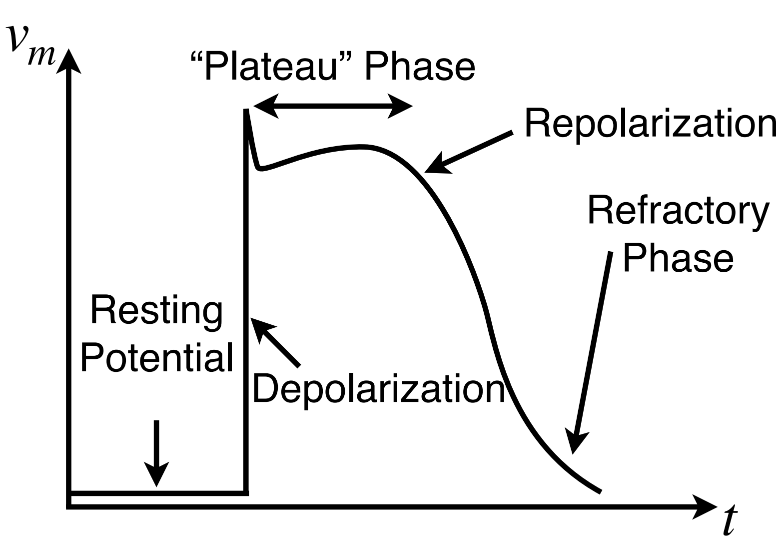

Diffusion term

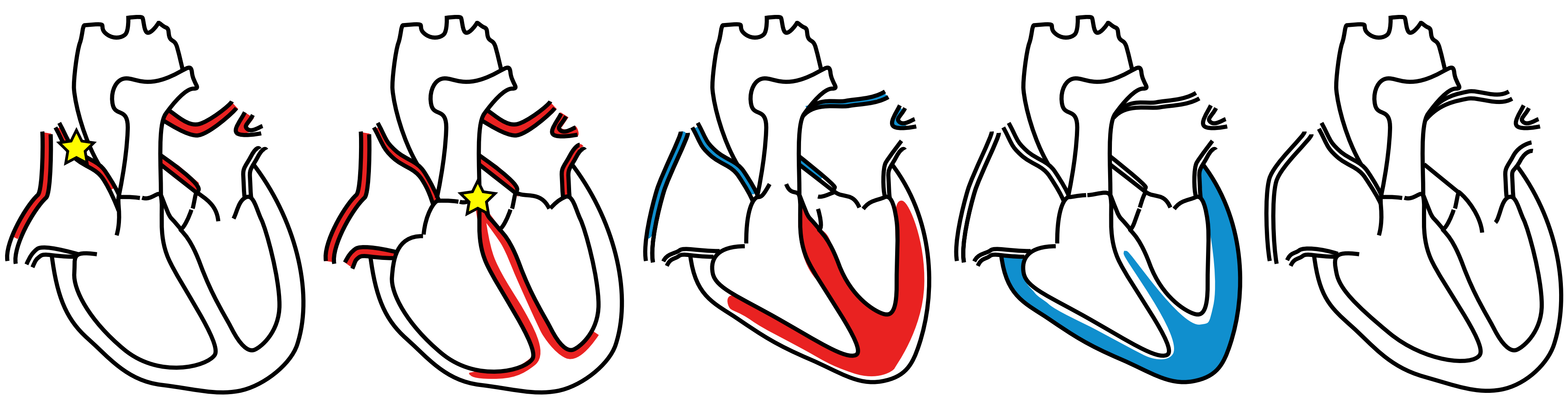

An example of pathology: Atrial fibrillation

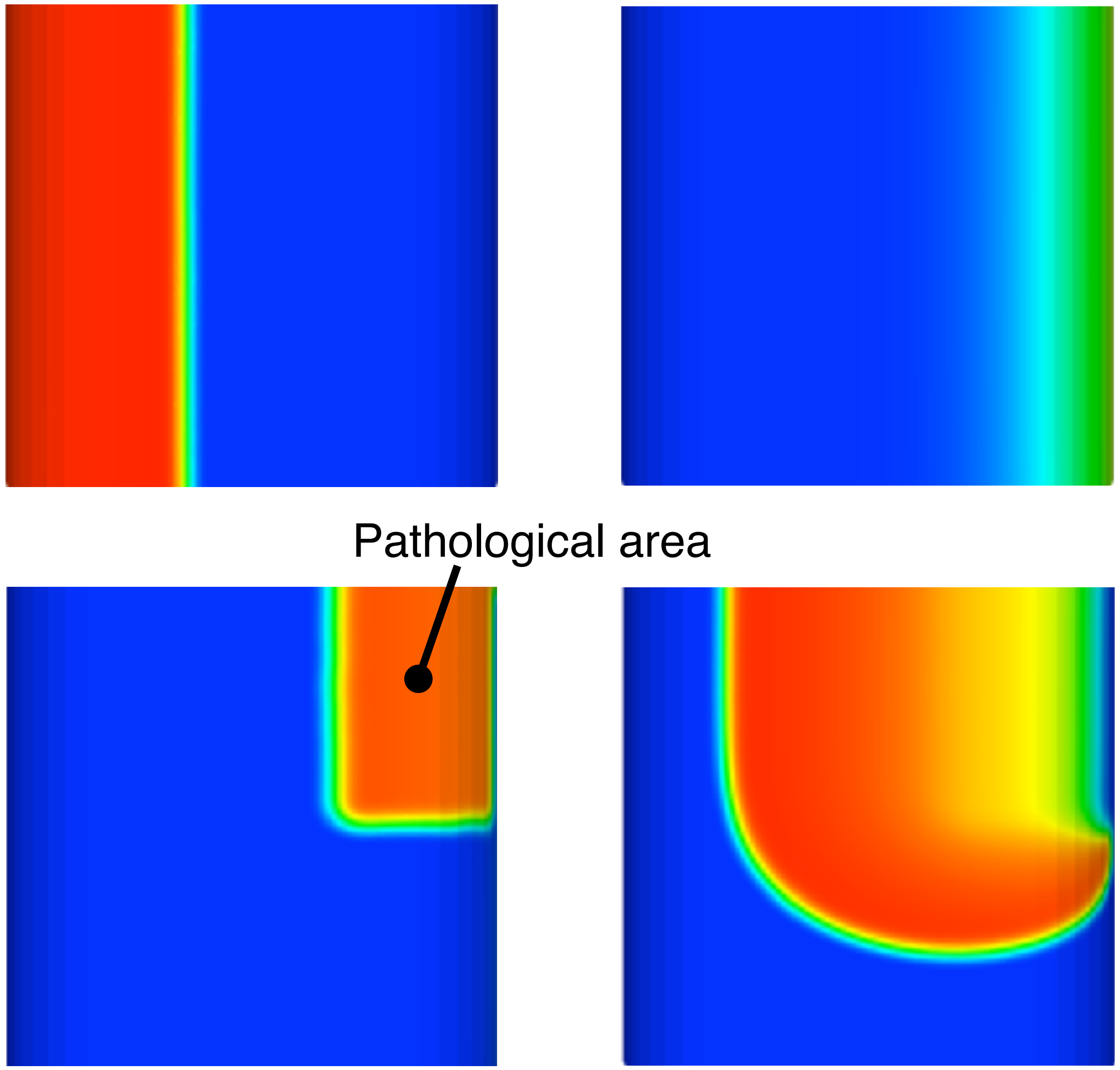

Standard S1 - S2 protocol

An example of pathology: Atrial fibrillation

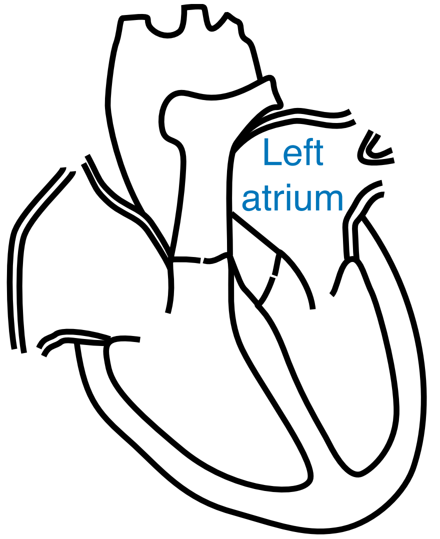

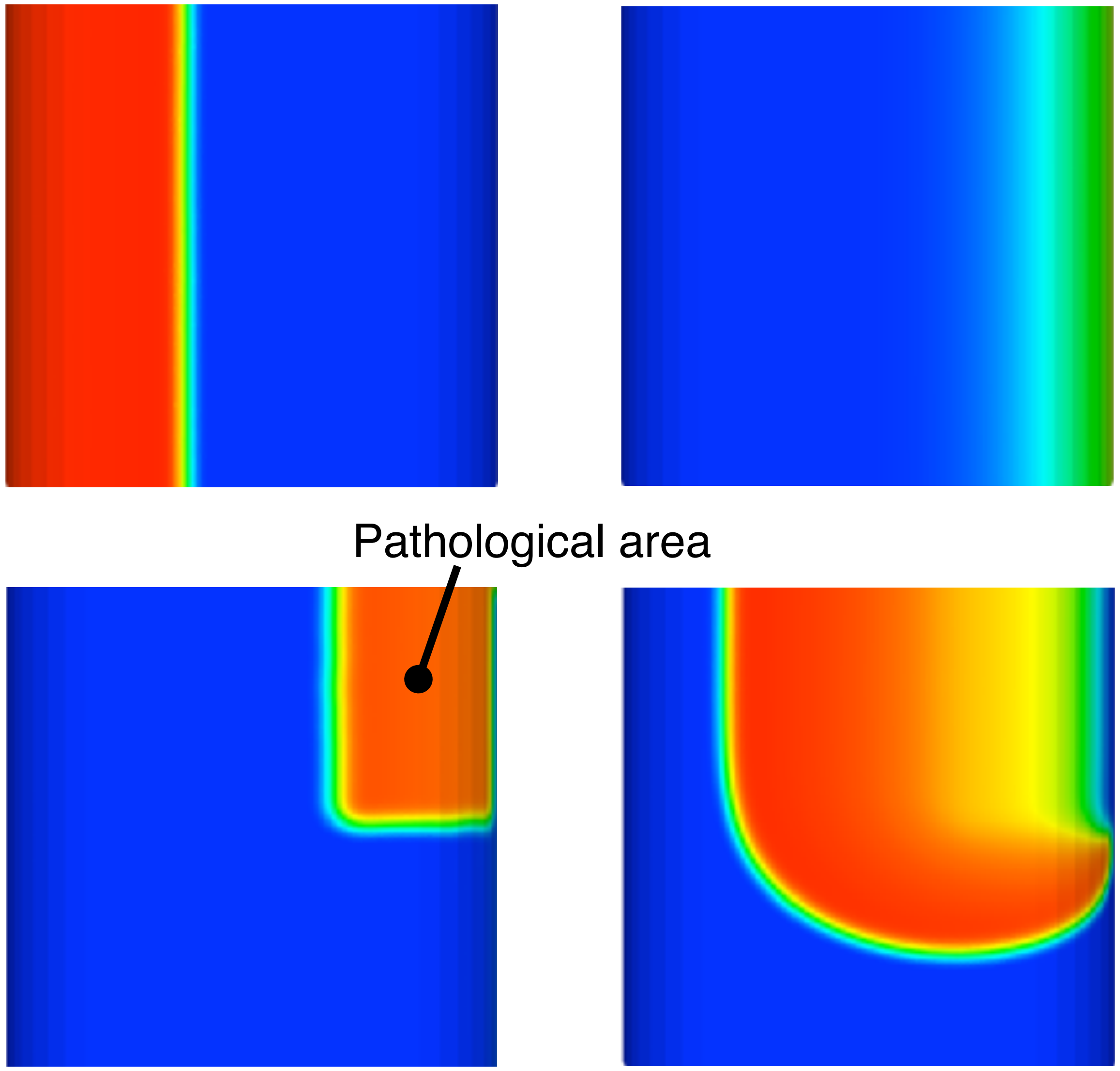

Standard S1 - S2 protocol

An example of pathology: Atrial fibrillation

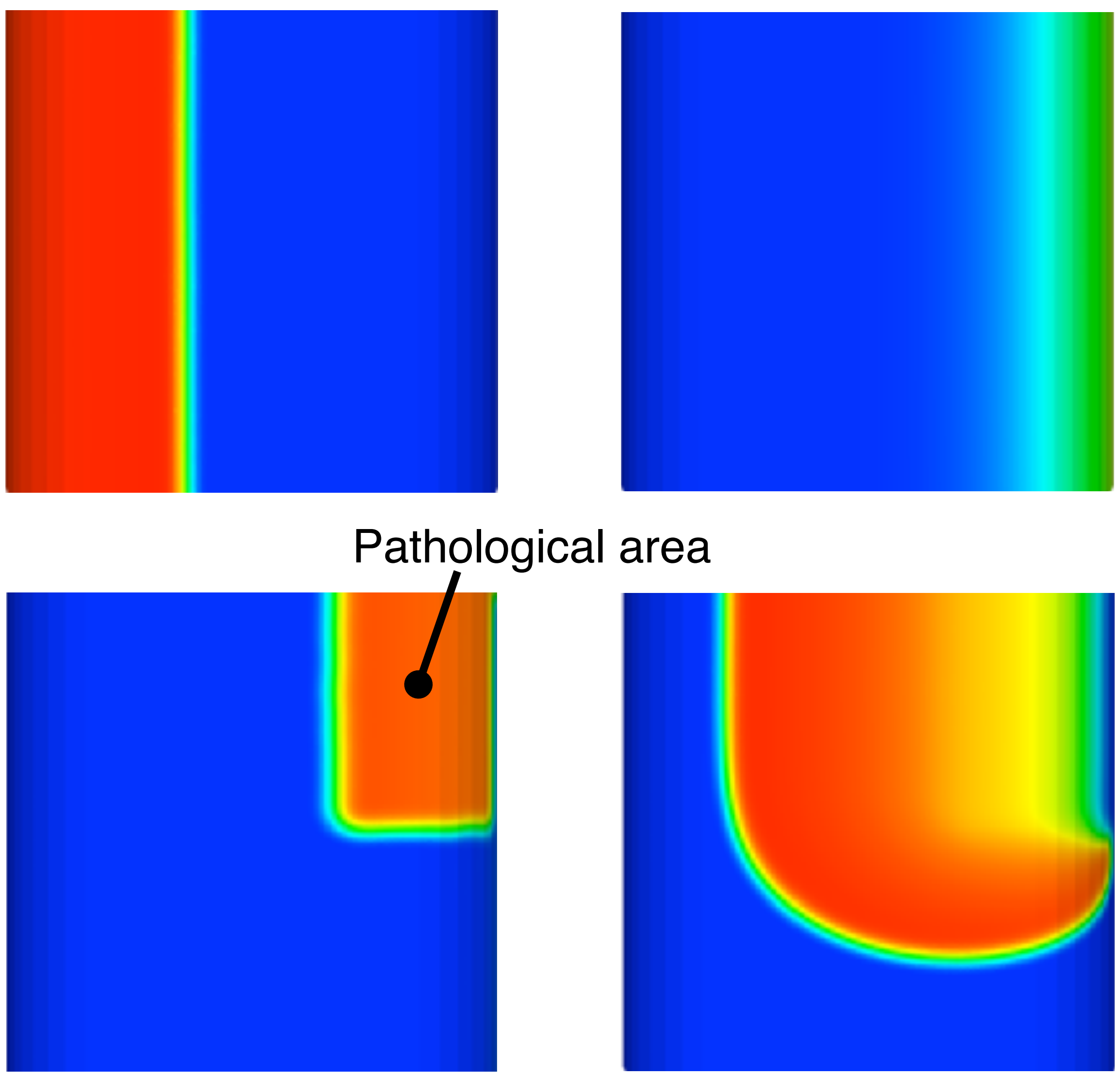

Standard S1 - S2 protocol

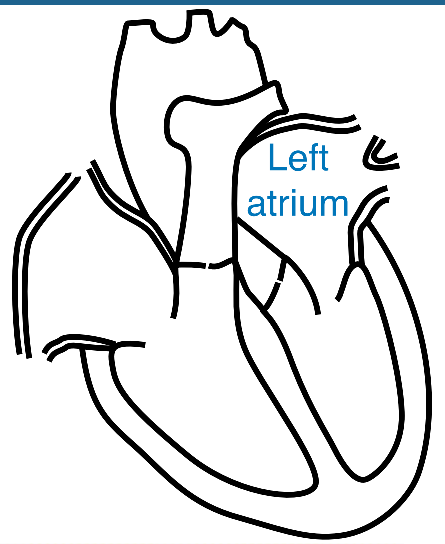

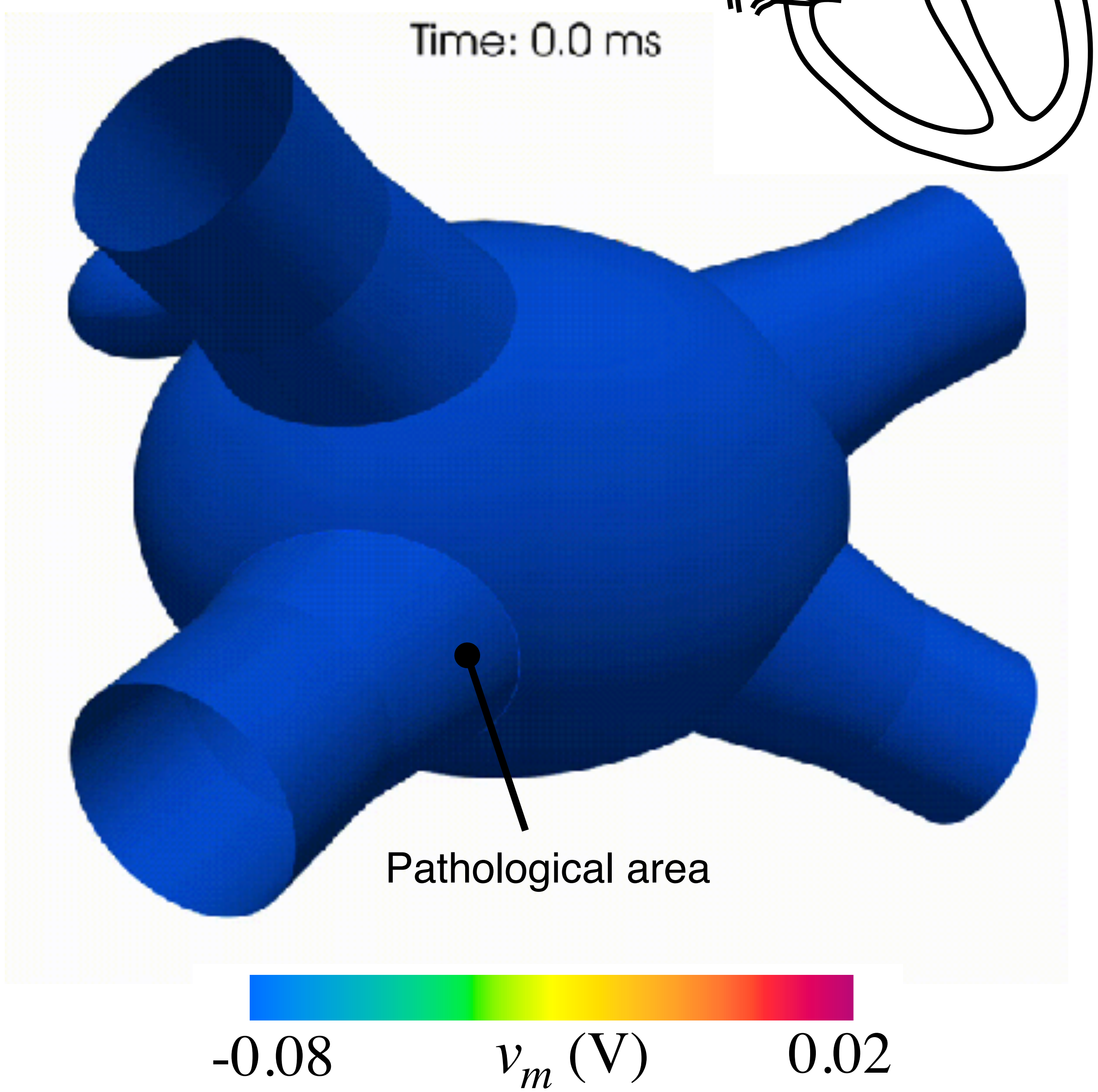

An example of pathology: Atrial fibrillation

- (At least) isolation of the 4 pulmonary veins.
- How? By cardiac ablation.

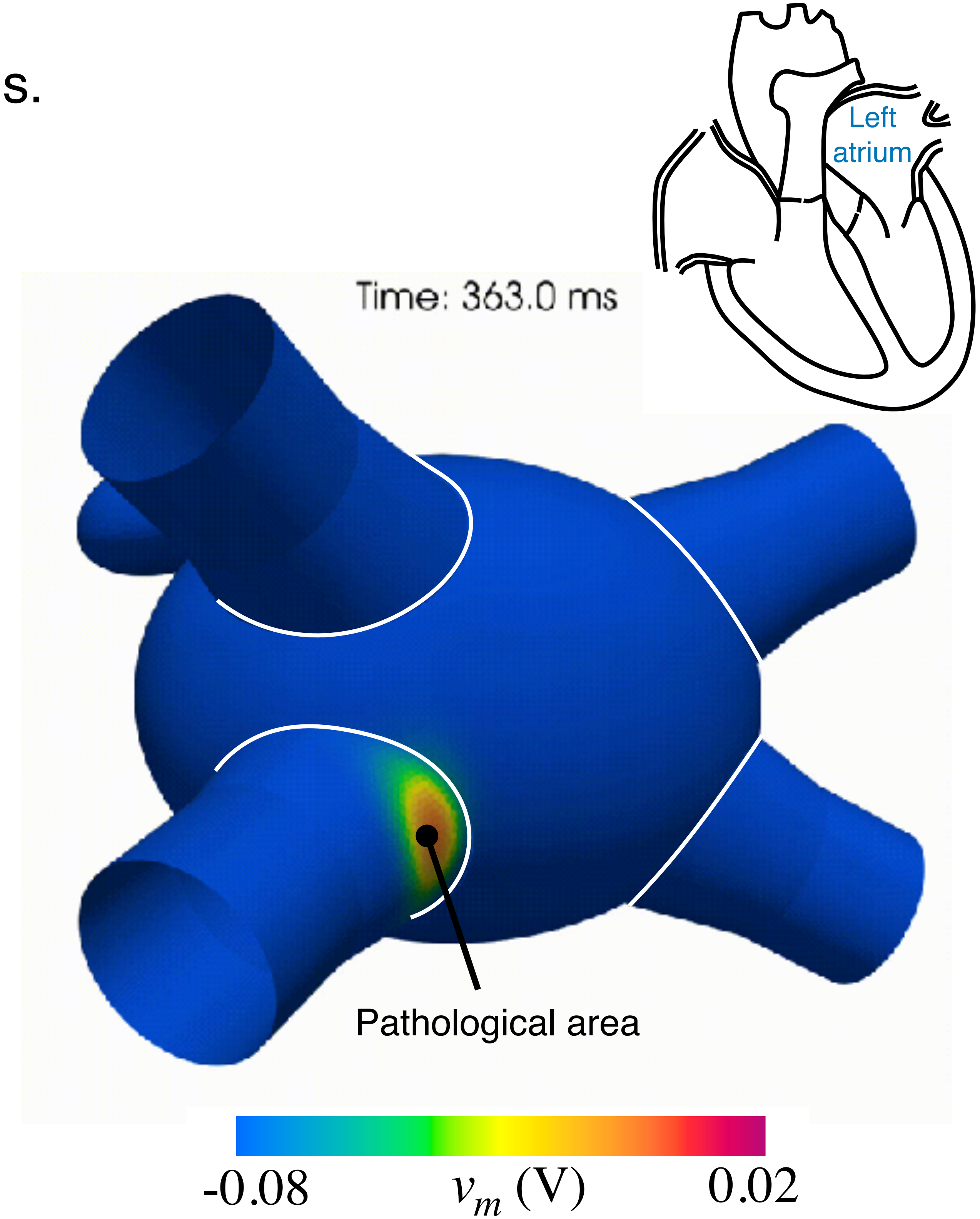

An example of pathology: Atrial fibrillation

- (At least) isolation of the 4 pulmonary veins.
- How? By cardiac ablation.
- Classical technique:
  Radio-Frequency Ablation (RFA).

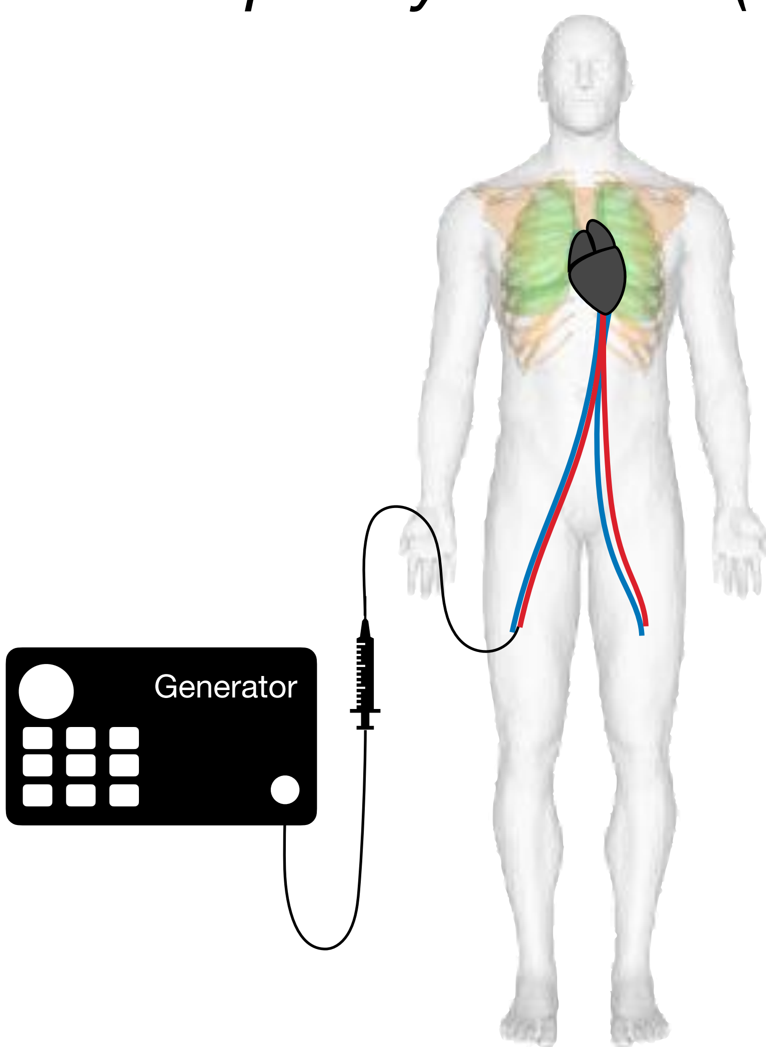

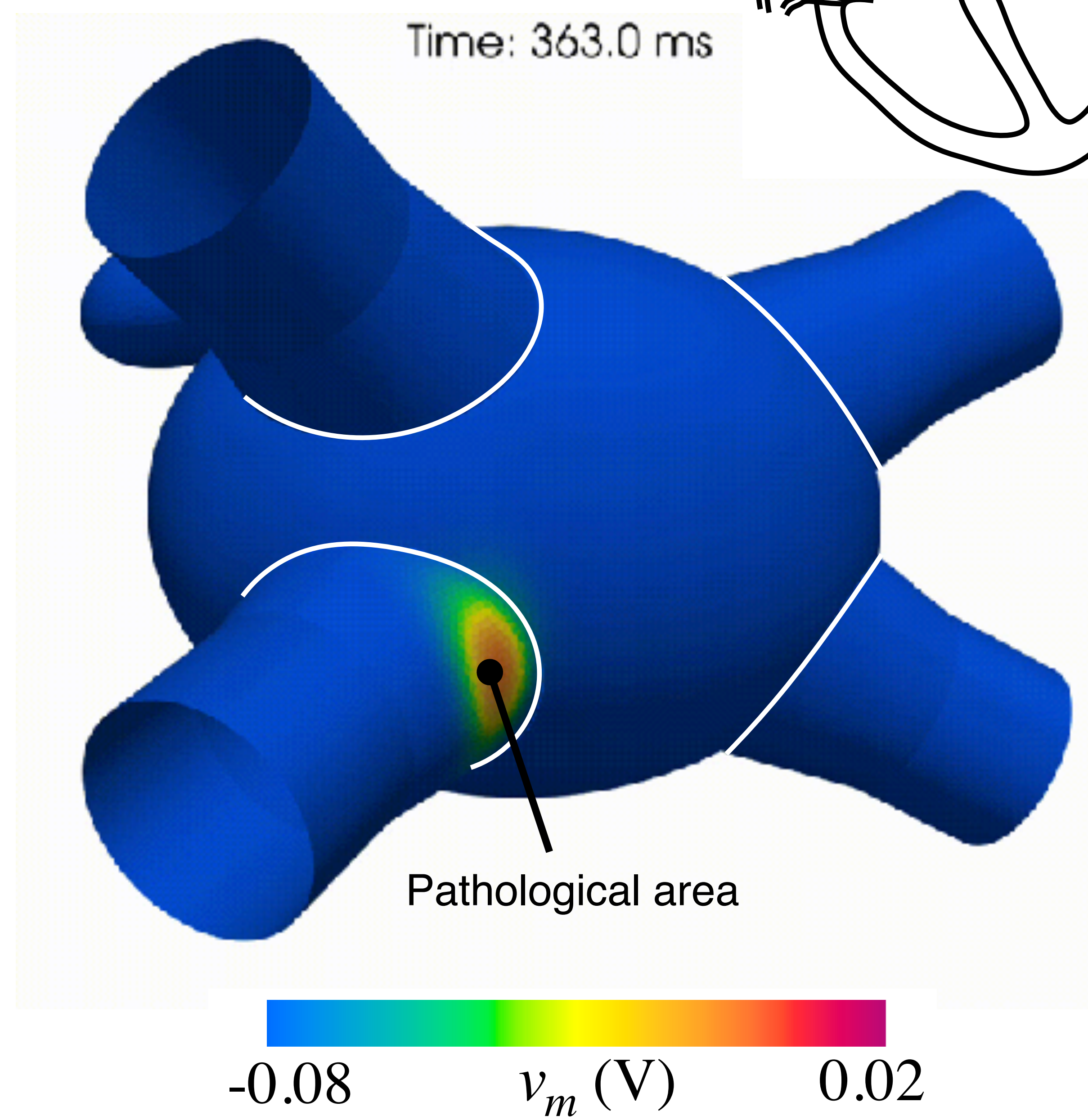

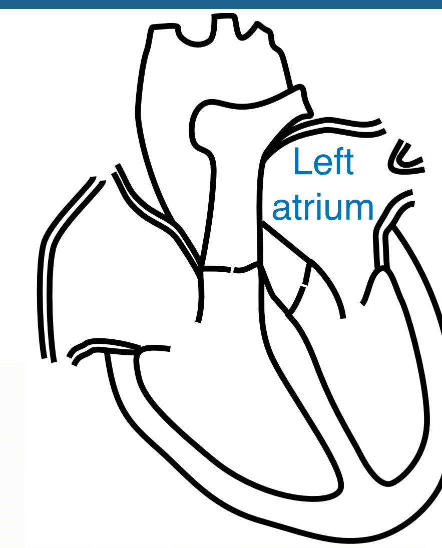

An example of pathology: Atrial fibrillation

- (At least) isolation of the 4 pulmonary veins.
- How? By cardiac ablation.
- Classical technique:
  Radio-Frequency Ablation (RFA).
- Clinics disadvantages [1]: damage to adjacent structures (lungs, phrenic nerve, oesophagus) and risk of “steam pop” mainly due to heat diffusion.

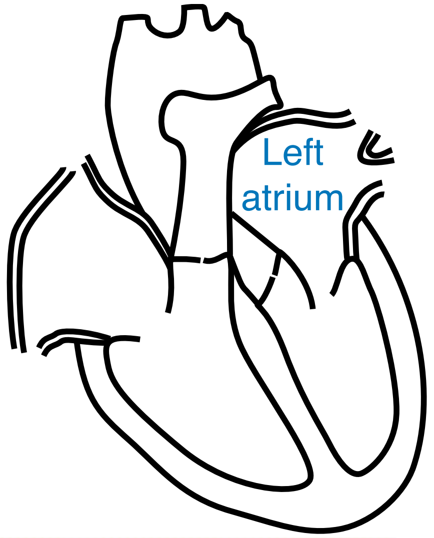

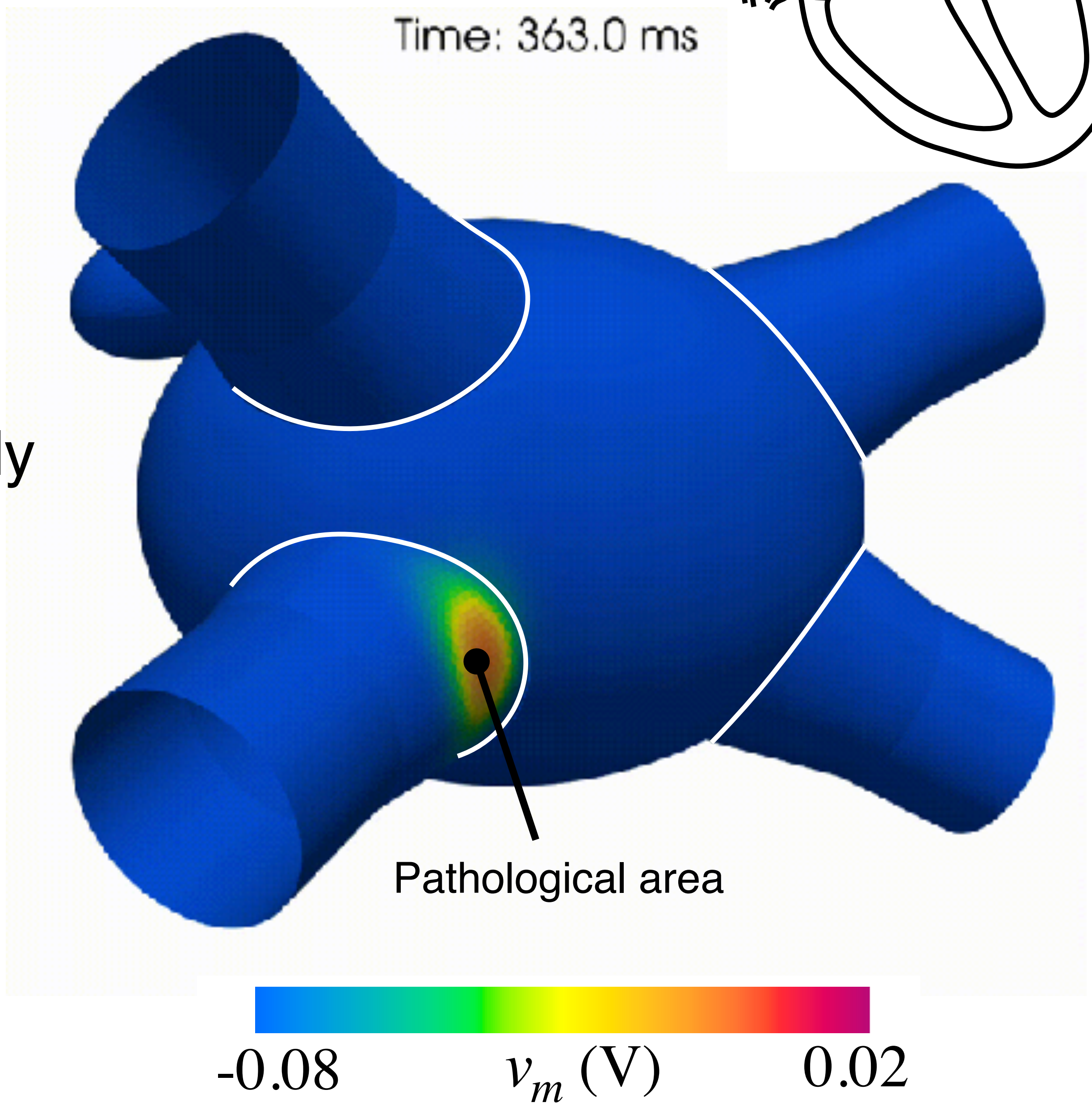

[1] Wojtaszczyk A, Caluori G, Pešl M, et al. Irreversible electroporation ablation for atrial fibrillation. J Cardiovasc Electrophysiol 2018; 29: 643–651.

An example of pathology: Atrial fibrillation

- (At least) isolation of the 4 pulmonary veins.
- How? By cardiac ablation.
- Classical technique:
  Radio-Frequency Ablation (RFA).
- Clinics disadvantages [1]: damage to adjacent structures (lungs, phrenic nerve, oesophagus) and risk of "steam pop" mainly due to heat diffusion.
- Novel non-thermal ablation technique:
  Pulsed electric Field Ablation (PFA), which takes advantage of irreversible electroporation.

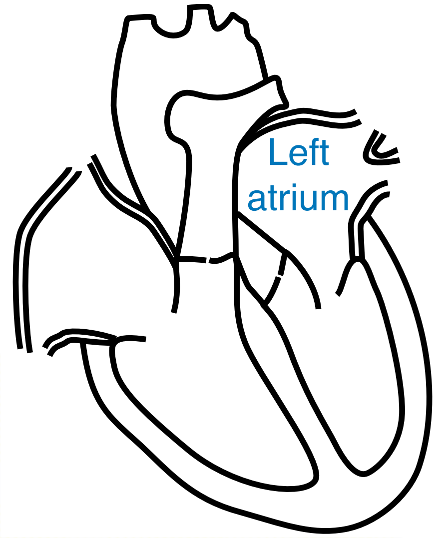

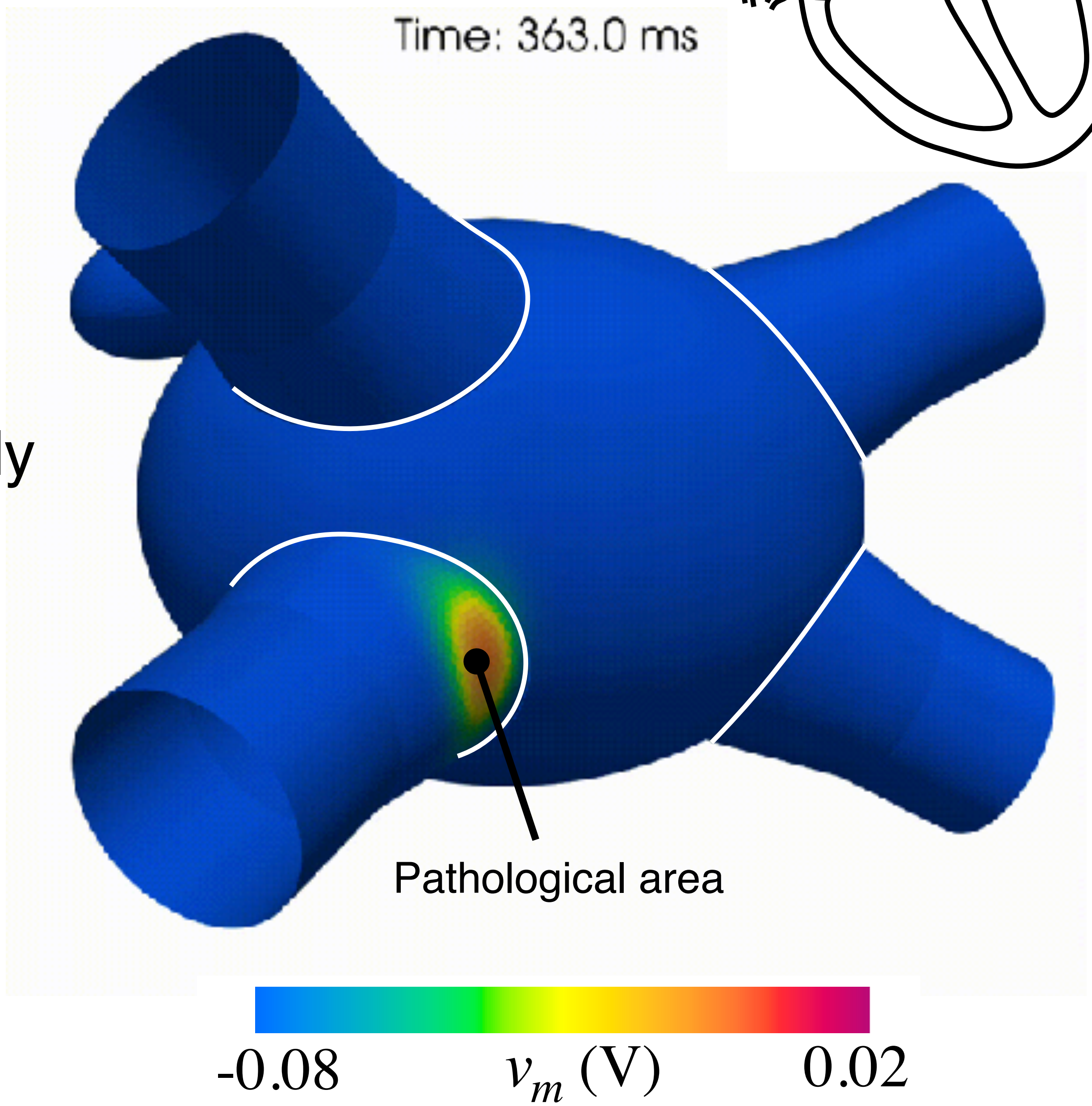

[1] Wojtaszczyk A, Caluori G, Pešl M, et al. Irreversible electroporation ablation for atrial fibrillation. J Cardiovasc Electrophysiol 2018; 29: 643–651.

What is electroporation?

Cell

Radius ~ 5 to 10 μm

Intra-cellular conductivity σ_c ~ 0.5 to 1 S.m^{-1}

Intra-cellular conductivity σ_e ~ 1 to 1.5 S.m^{-1}

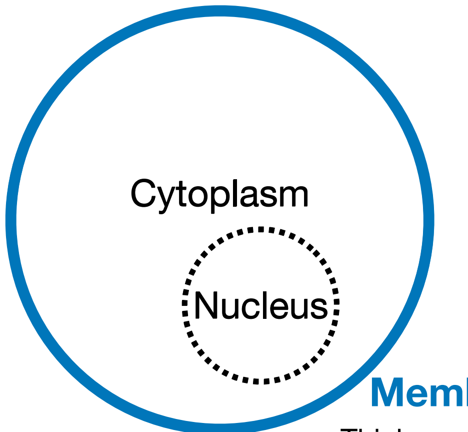

Membrane

Thickness $h \sim$ 5nm

Permitivity $\varepsilon \sim 4.5\varepsilon_0$

Capacitance C_m

Conductance S_m

What is electroporation?

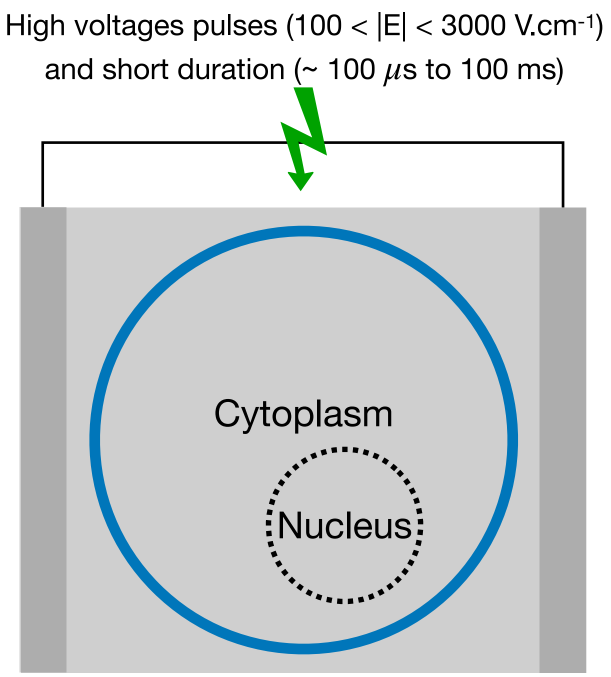

What is electroporation?

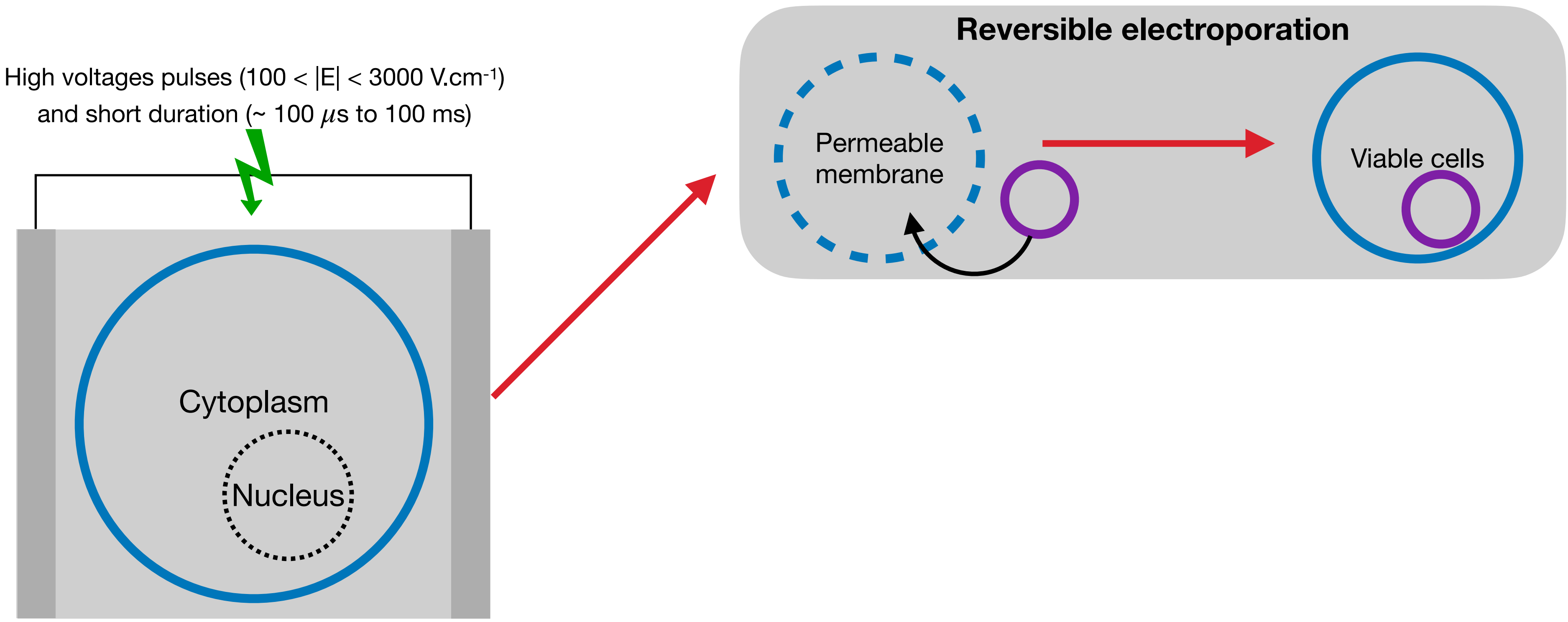

What is electroporation?

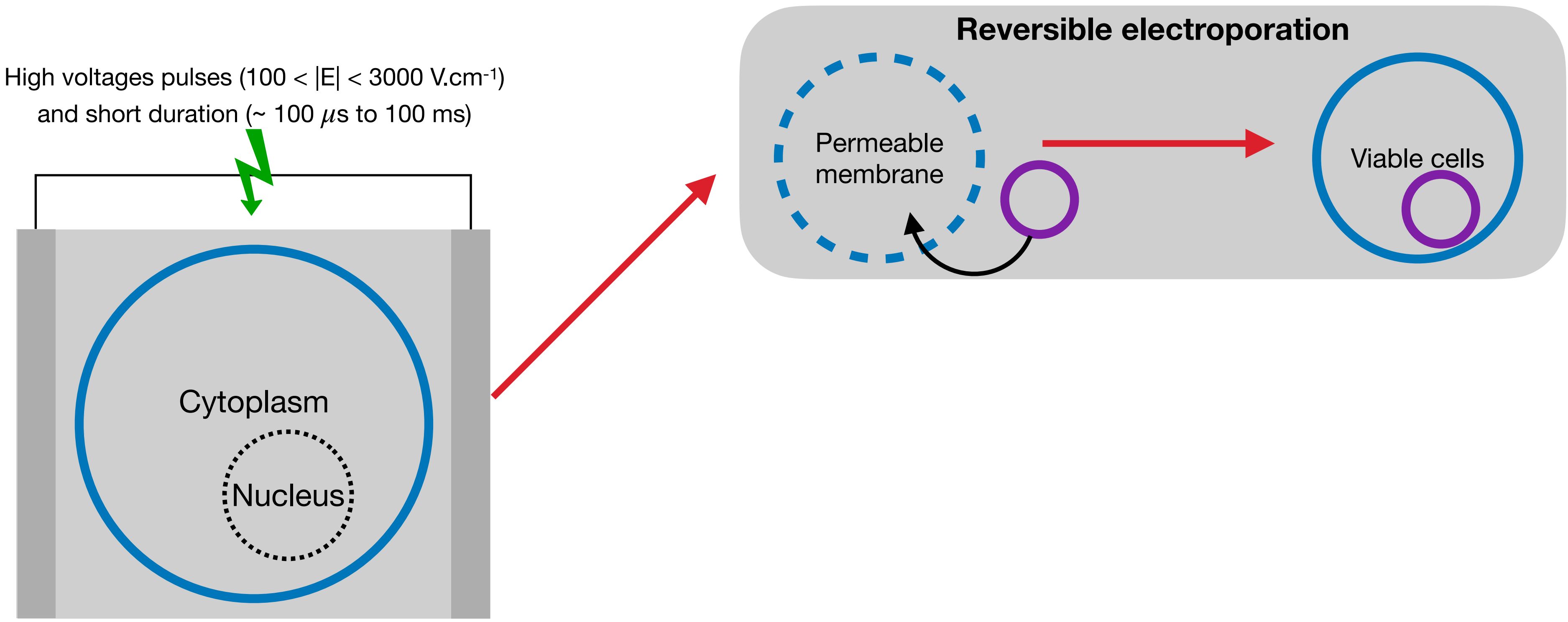

Applications (in oncology):

- In vitro gene transfection
- Electrochemotherapy

What is electroporation?

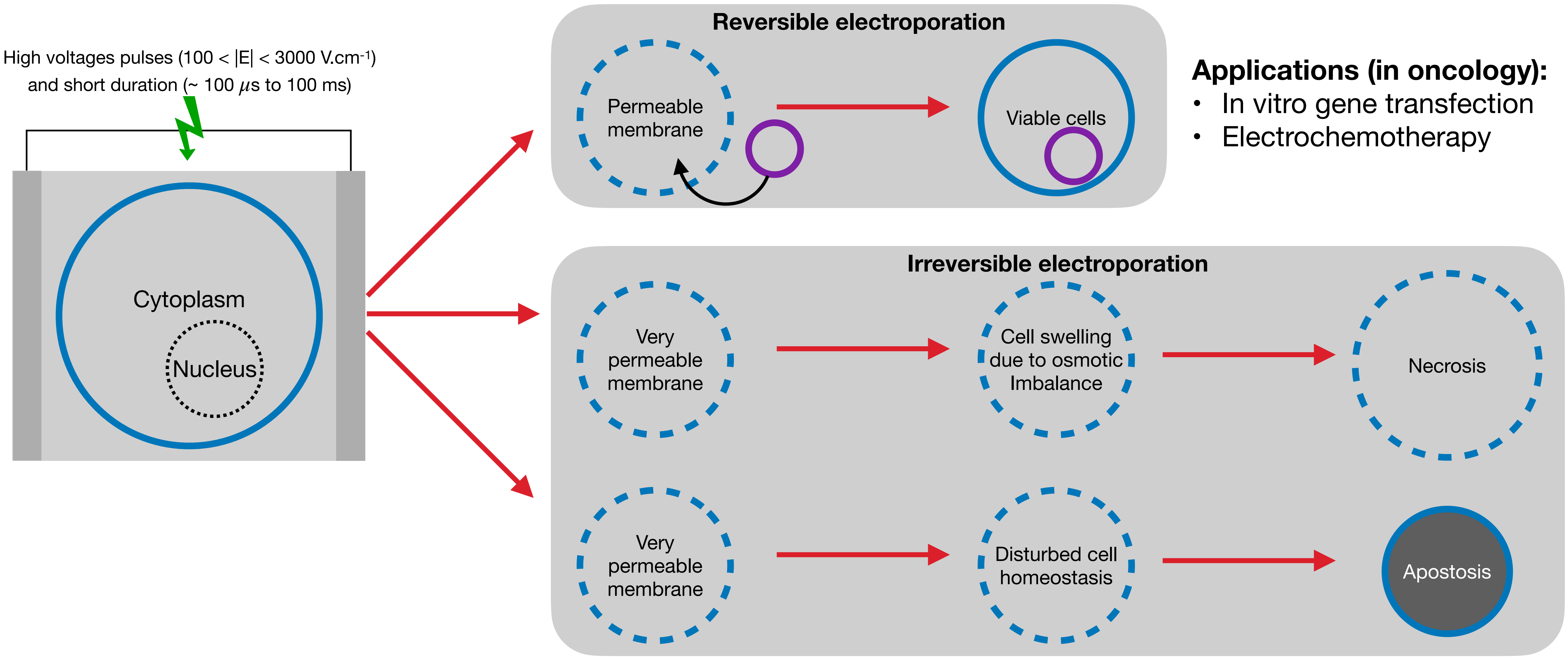

Applications (in oncology):
- In vitro gene transfection
- Electrochemotherapy

What is electroporation?

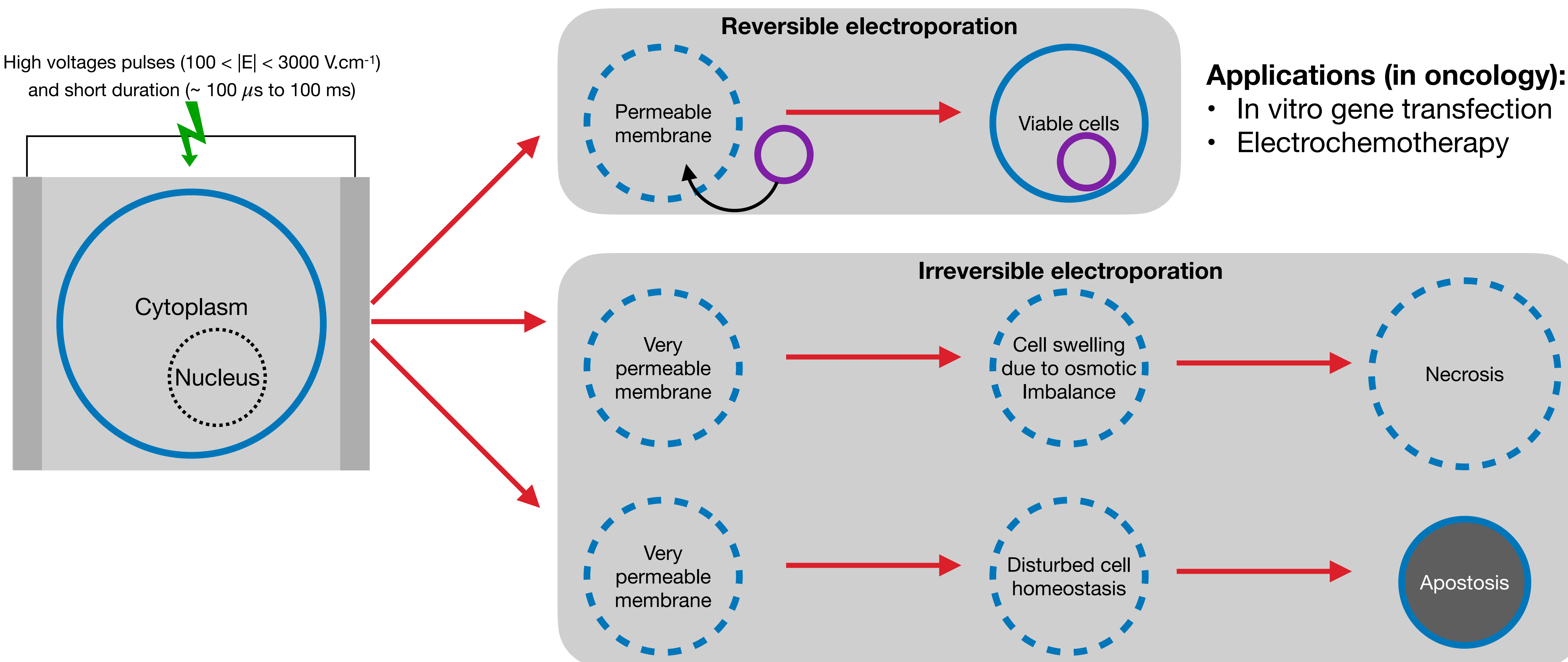

Applications (in oncology):
- In vitro gene transfection
- Electrochemotherapy

Application:
- Tumoral ablation
- Cardiac ablation

Cardiac Expertise

- Modeling expertise:
  2-scale homogenization, existence & uniqueness, numerical simulations (healthy and pathological cases)

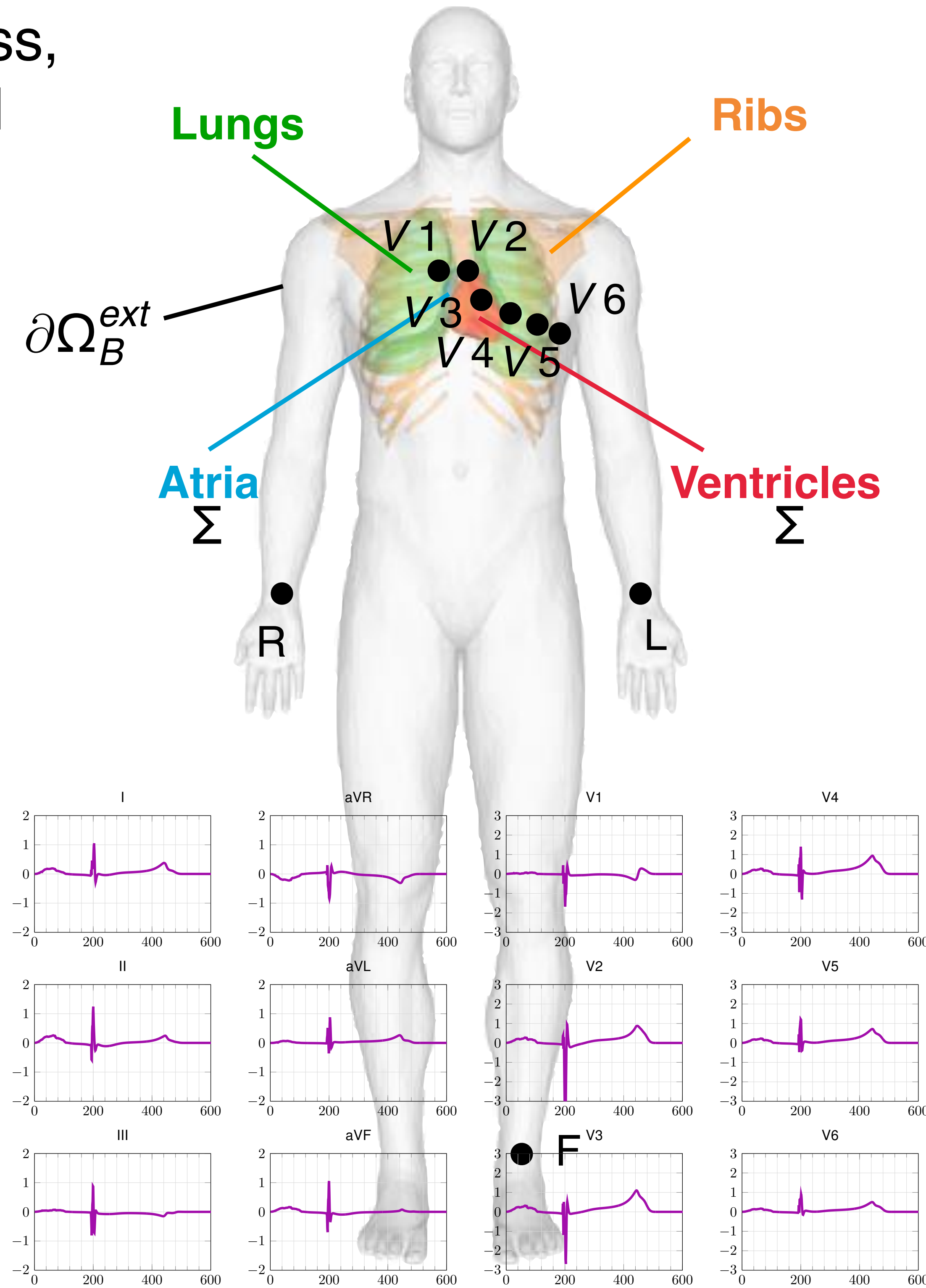

[1] A. Collin and S. Imperiale. Mathematical analysis and 2-scale convergence of a heterogeneous microscopic bidomain model. M3AS 2018.
[2] D. Chapelle, A. Collin, and J.-F. Gerbeau. A surface-based electrophysiology model relying on asymptotic analysis and motivated by cardiac atria modeling. M3AS, 2013.
[3] A. Collin, J.-F. Gerbeau, M. Hocini, M. Haïssaguerre, and D. Chapelle. Surface-based electrophysi- ology modeling and assessment of physiological simulations in atria. FIMH 2013.
[4] E. Schenone, A. Collin, and J.-F. Gerbeau. Numerical simulation of electrocardiograms for full c4rdiac cycles in healthy and pathological conditions. *International Journal for Numerical Methods in Biomedical Engineering*, 2015.

Cardiac Expertise

- Modeling expertise:
  2-scale homogenization, existence & uniqueness, numerical simulations (healthy and pathological cases)

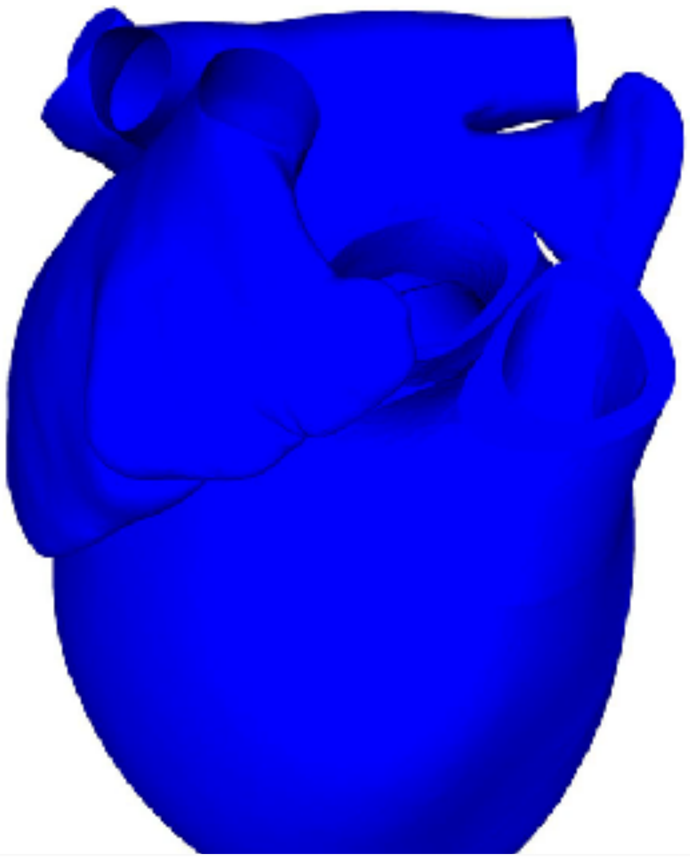

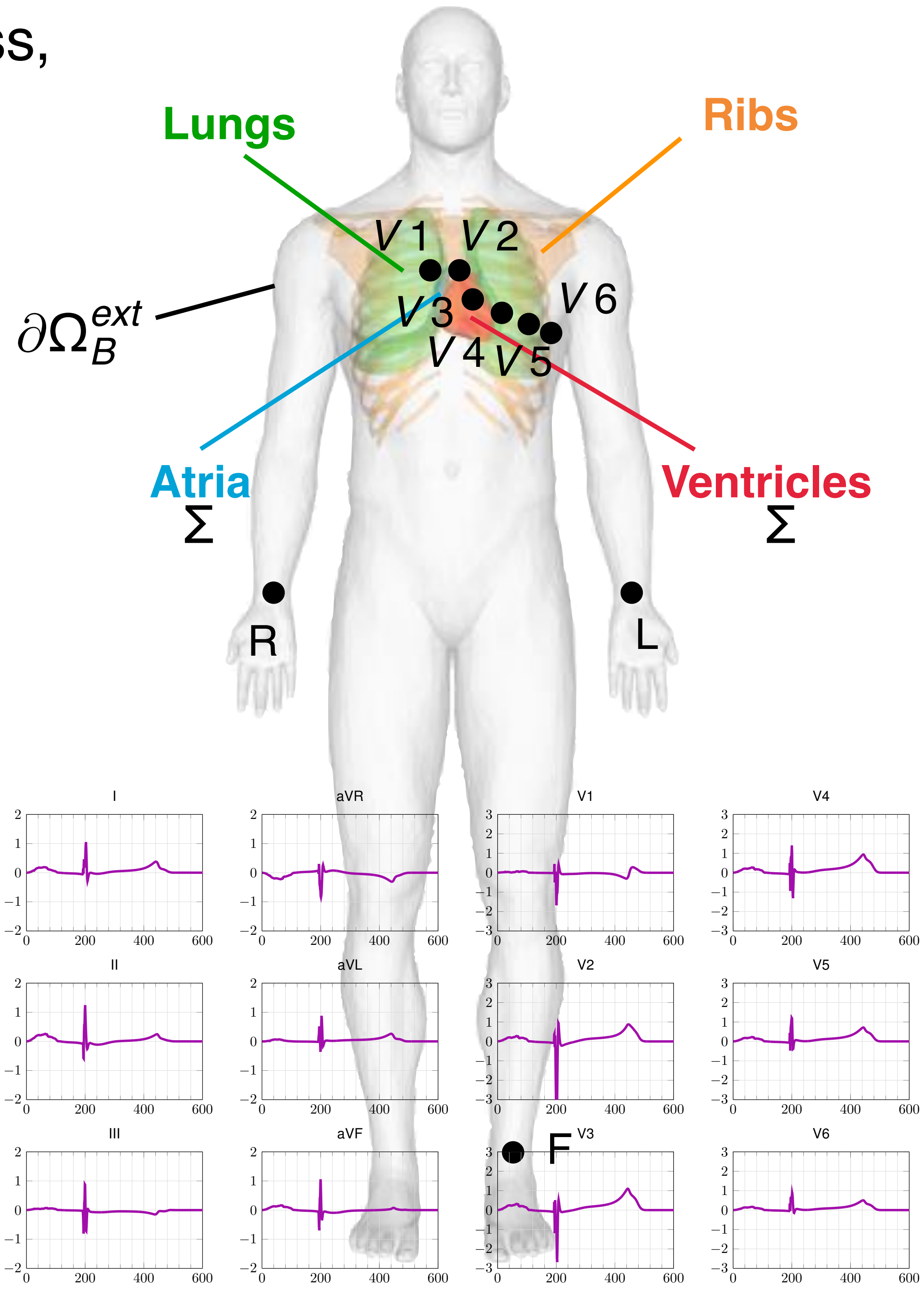

[1] A. Collin and S. Imperiale. Mathematical analysis and 2-scale convergence of a heterogeneous microscopic bidomain model. M3AS 2018.
[2] D. Chapelle, A. Collin, and J.-F. Gerbeau. A surface-based electrophysiology model relying on asymptotic analysis and motivated by cardiac atria modeling. M3AS, 2013.
[3] A. Collin, J.-F. Gerbeau, M. Hocini, M. Haïssaguerre, and D. Chapelle. Surface-based electrophysi- ology modeling and assessment of physiological simulations in atria. FIMH 2013.
[4] E. Schenone, A. Collin, and J.-F. Gerbeau. Numerical simulation of electrocardiograms for full c4rdiac cycles in healthy and pathological conditions. *International Journal for Numerical Methods in Biomedical Engineering*, 2015.

Cardiac Expertise

- Data assimilation expertise

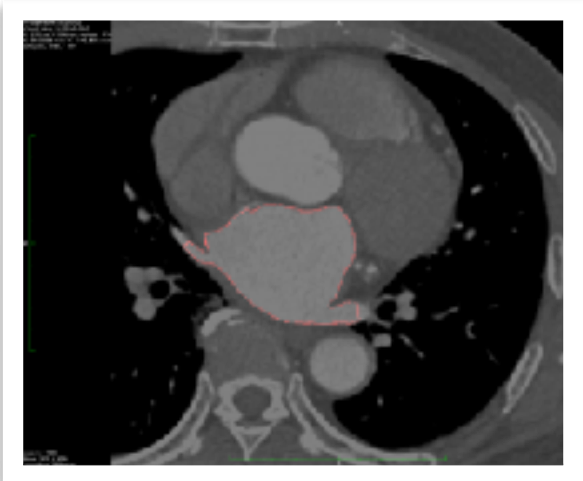

Images (CT, MRI)

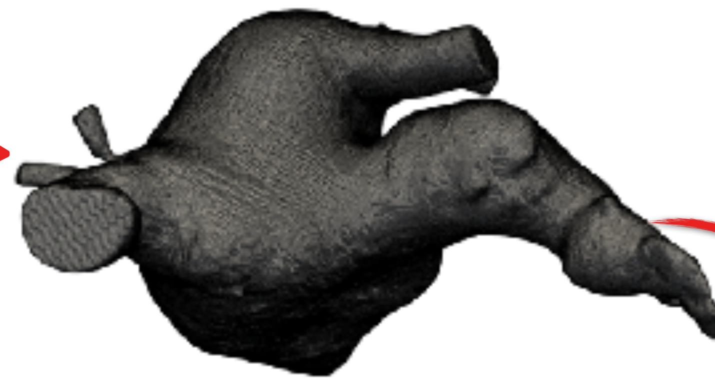

Anatomy

Computing inverse problem

Electrodes vest (multiple surface ECG recordings)

DATA

Maps of electrical activation (isochrones)

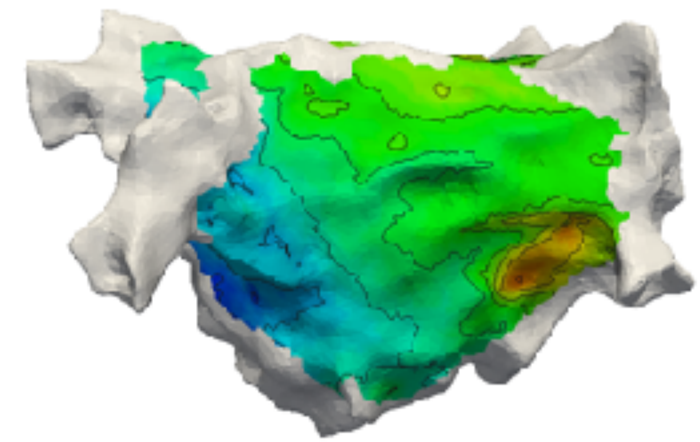

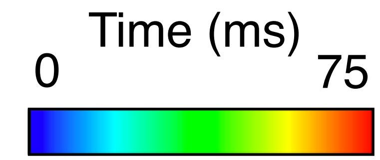

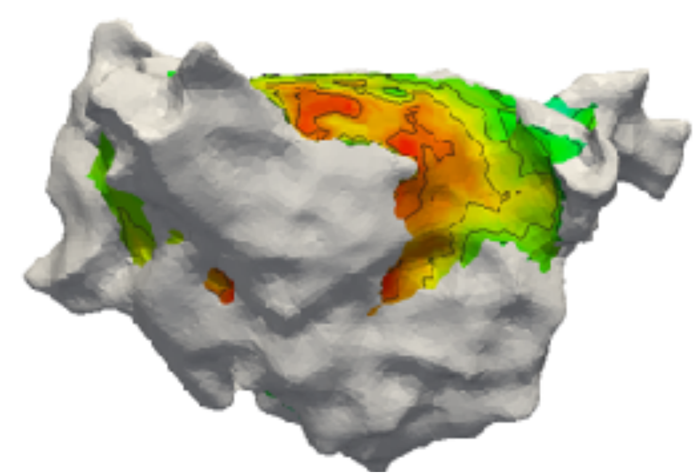

CHU Bordeaux

Data assimilation expertise

- Minimize a least squared criterion with respect to the uncertainties under the constraint of the model dynamics

- Many available methods: adjoint method, stochastic algorithms etc …

Data assimilation expertise

- Minimize a least squared criterion with respect to the uncertainties under the constraint of the model dynamics
- Many available methods: adjoint method, stochastic algorithms etc …

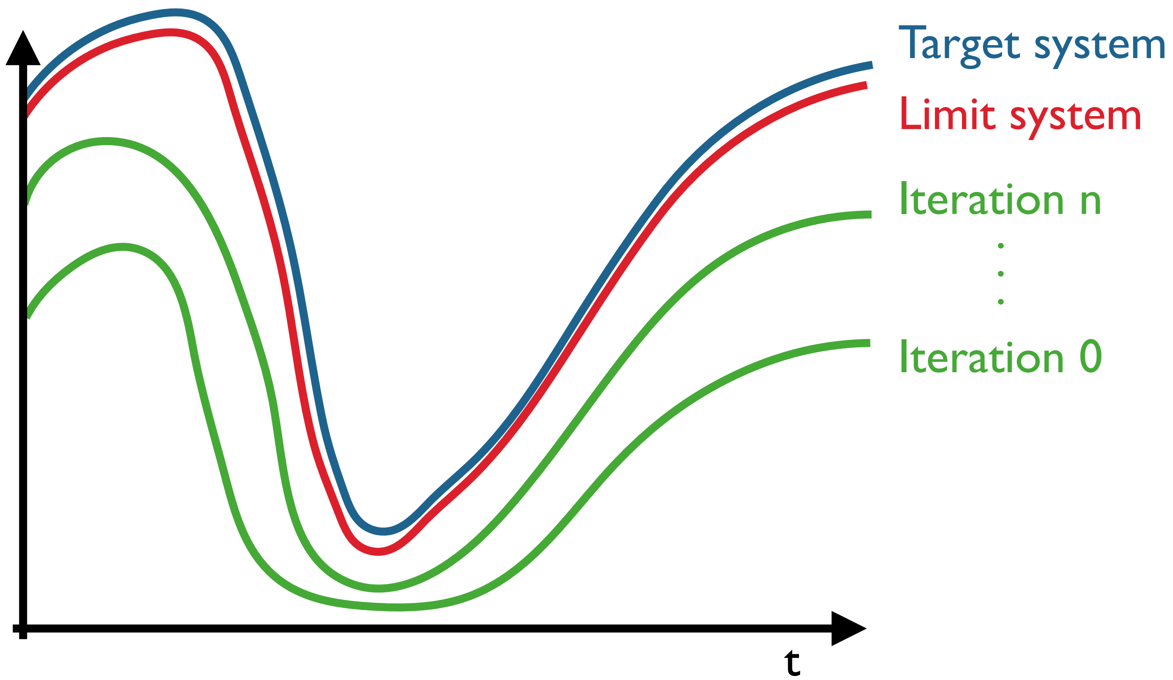

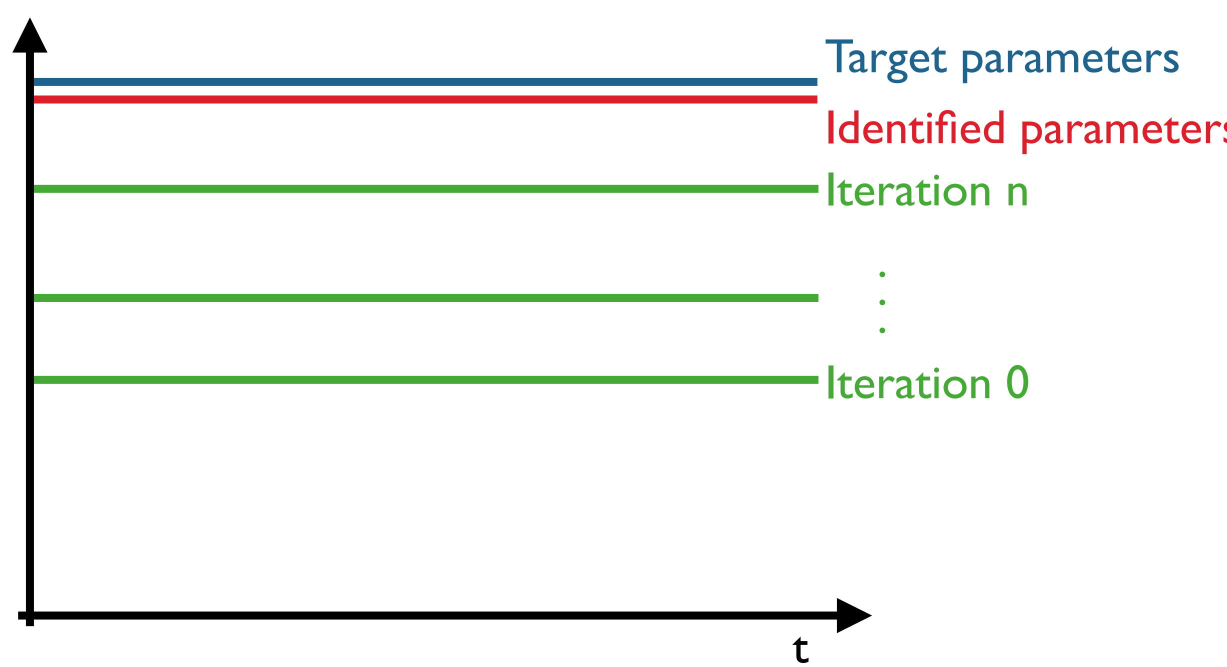

Data assimilation expertise

- Sequential strategy
- Design a *Luenberger observer* to correct the dynamics

$$\dot{u}(t) = A(t, u(t), \theta)$$
$$u(0) = u^\diamond + \xi_u$$
$$\theta = \theta^\diamond + \xi_\theta$$

$$\dot{\hat{u}}(t) = A(t, \hat{u}(t), \theta) + G^u(D(z_u(t), \hat{u}(t)))$$
$$\dot{\hat{\theta}}(t) = G^\theta(D(z_u(t), \hat{u}(t)))$$
$$\hat{u}(0) = u^\diamond,$$
$$\hat{\theta}(0) = \theta^\diamond$$

Objective:

Find G^u and G^θ such that: $\|\hat{u}(t) - u(t)\| \to 0$ and $\|\hat{\theta}(t) - \theta\| \to 0$

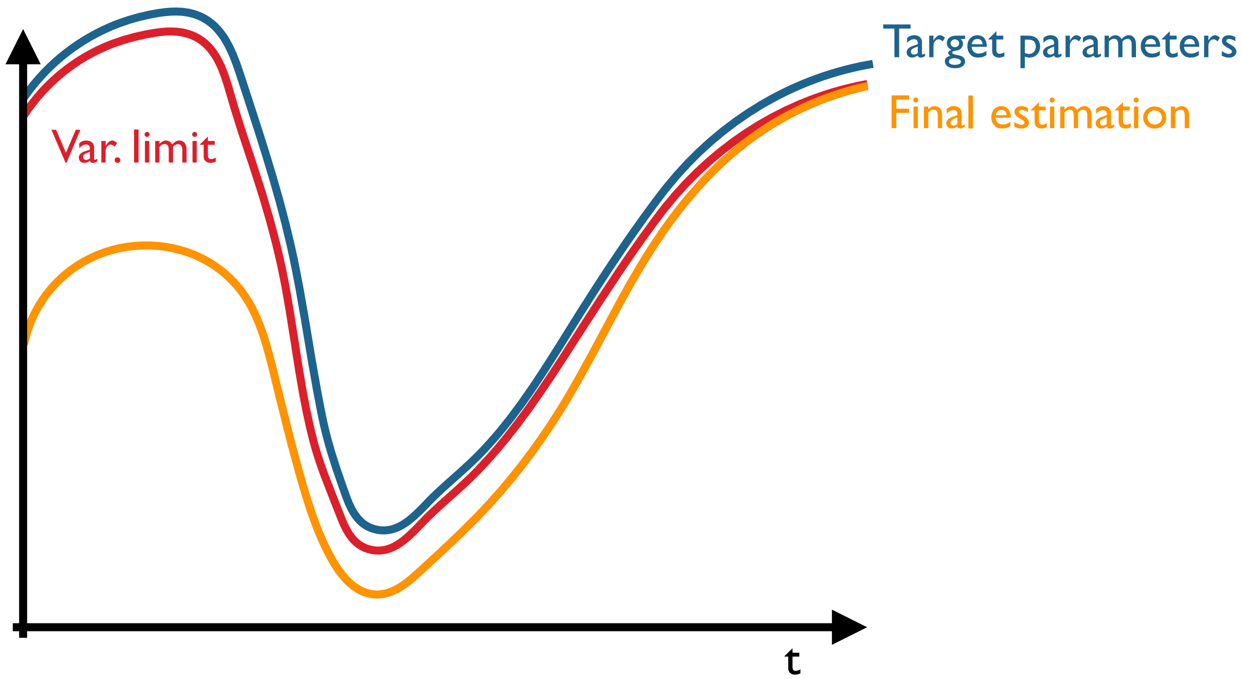

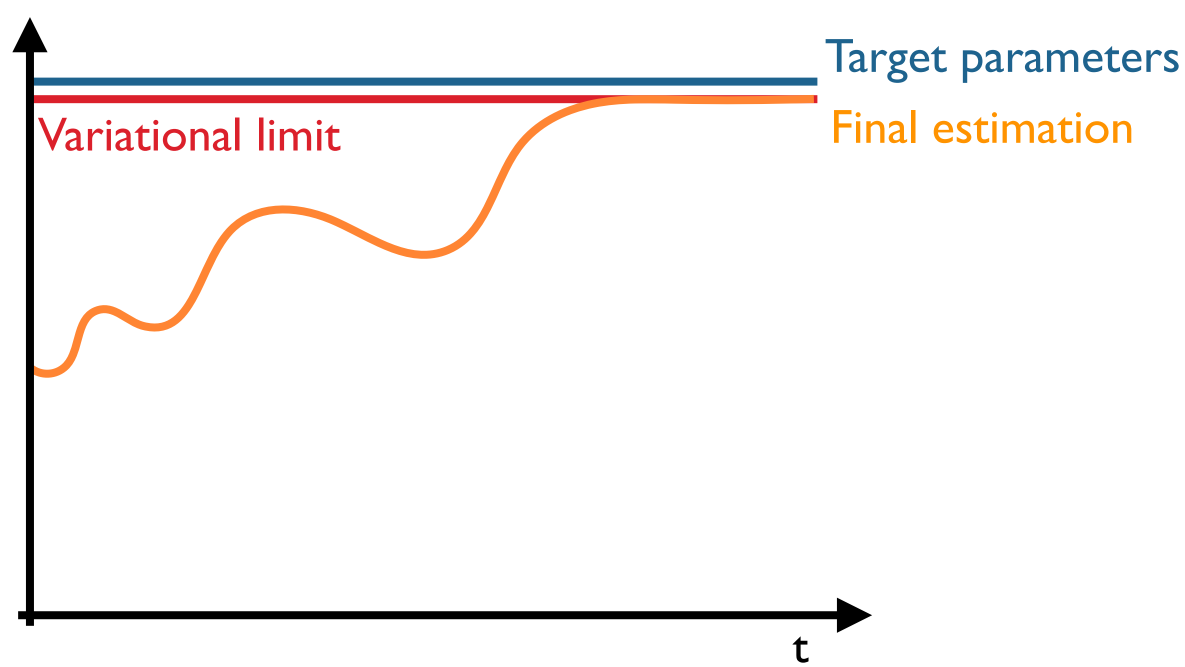

Data assimilation expertise

- Define a Luenberger observer (based on shape and topological derivatives) only to deal with the state error

Target system:

$$\partial_t u + \nabla \cdot (\sigma \nabla u) = f(u)$$
$$u(0) = u_0^\diamond + \xi_u$$

Observer system:

$$\partial_t \hat{u} + \nabla \cdot (\sigma \nabla \hat{u}) = f(\hat{u}) + g(\hat{u}, z_u)$$
$$\hat{u}(0) = u_0^\diamond$$
$$g(u, z_u) = \gamma_{sh}(x)\delta(u - c_{th})(-(z_u - C_{in})^2 + (z_u - C_{out})^2),$$
$$C_{in} = \frac{\int_{u>c_{th}} z_u}{\int_{u>c_{th}}} \text{ and } C_{out} = \frac{\int_{u<c_{th}} z_u}{\int_{u<c_{th}}}$$

Proposition The data correction stabilises the observer on the target trajectory for sufficiently small errors.

[1] A. Collin, D. Chapelle, and P. Moireau. A Luenberger observer for reaction–diffusion models with front position data. JCP 2015.
[2] A. Collin, D. Chapelle, and P. Moireau. Sequential state estimation for electrophysiology models with front level-set data using topological gradient derivations. FIMH 2015.

Data assimilation expertise

- 1D example

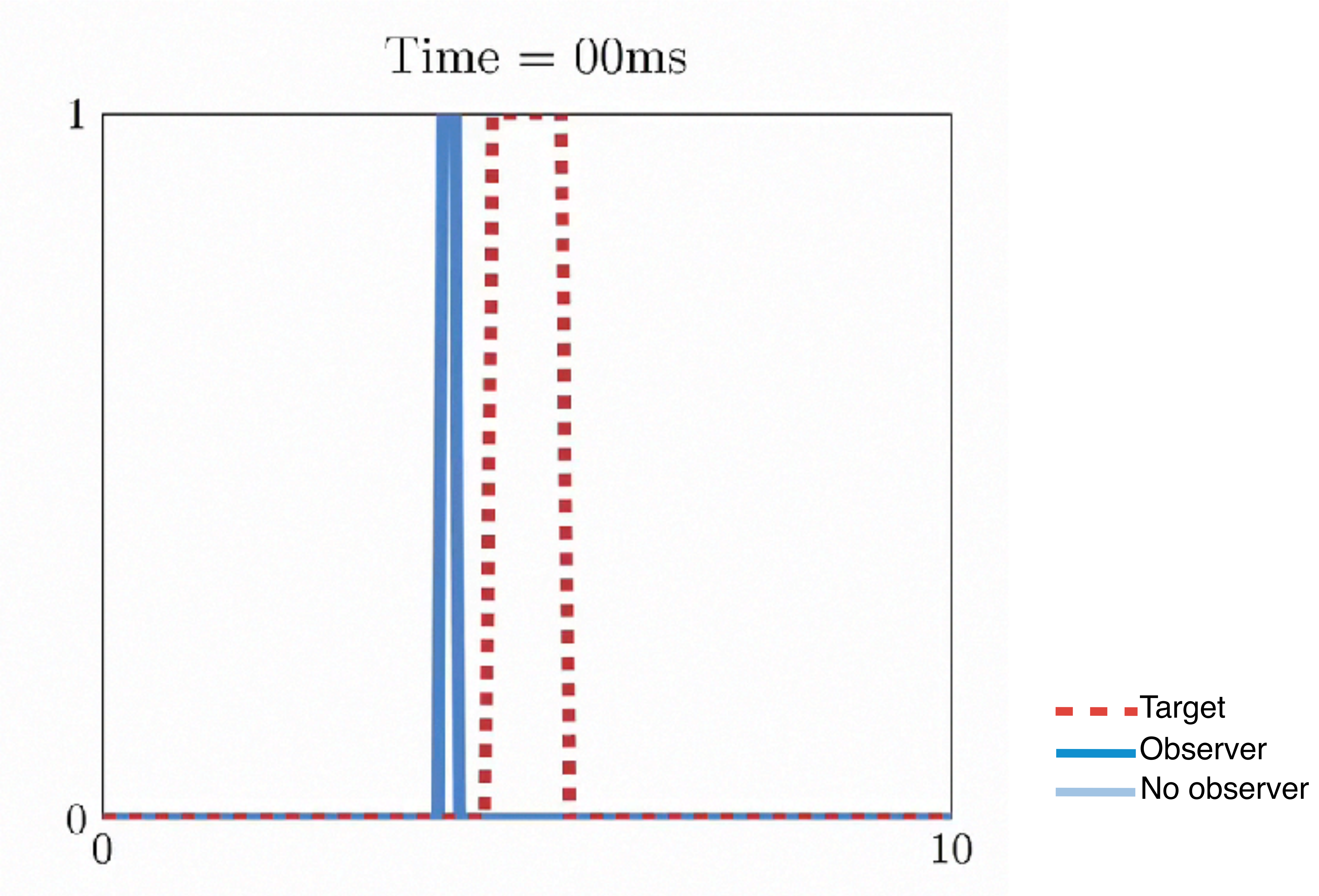

Data assimilation expertise

- 1D example

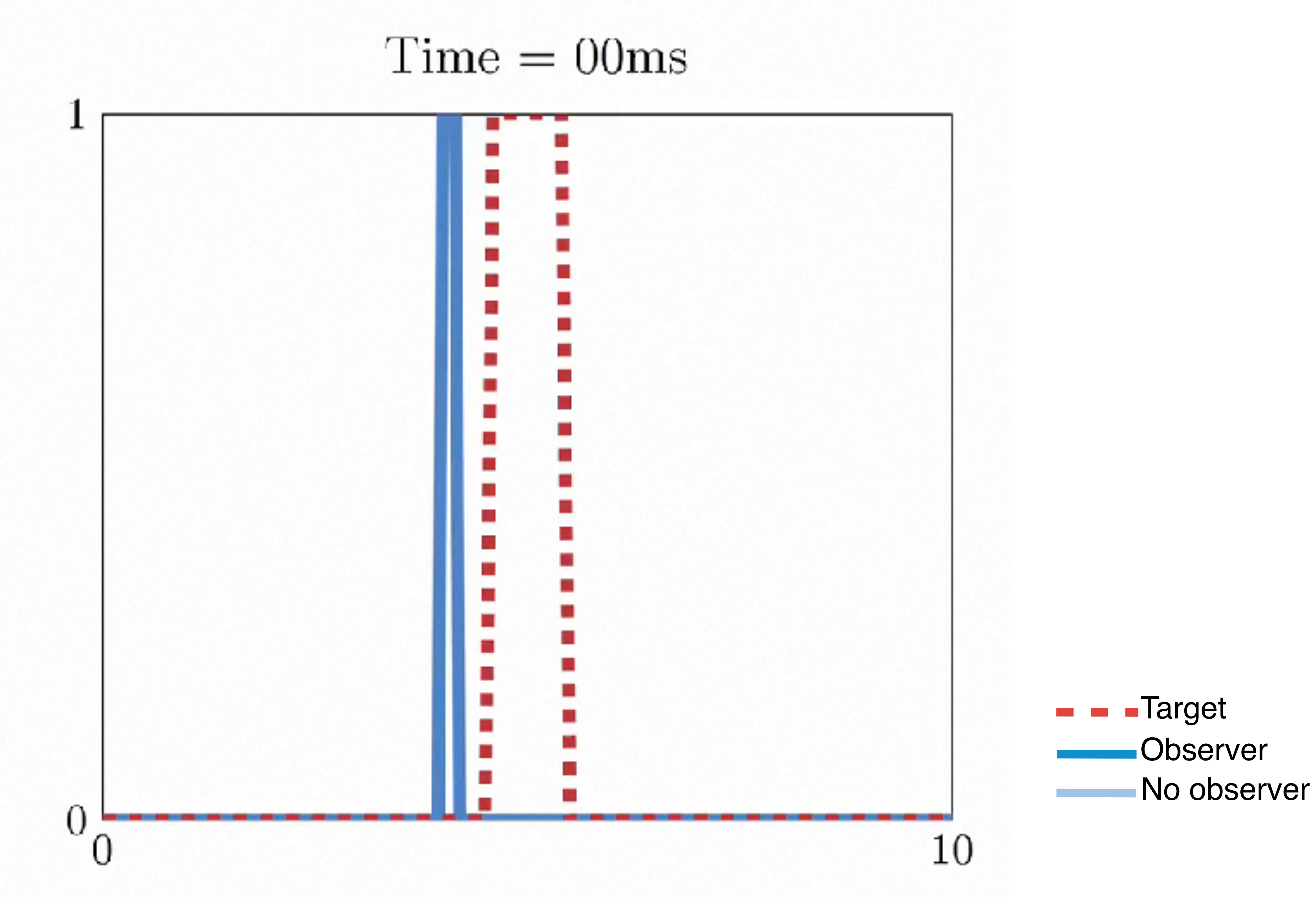

Data assimilation expertise

- 1D example

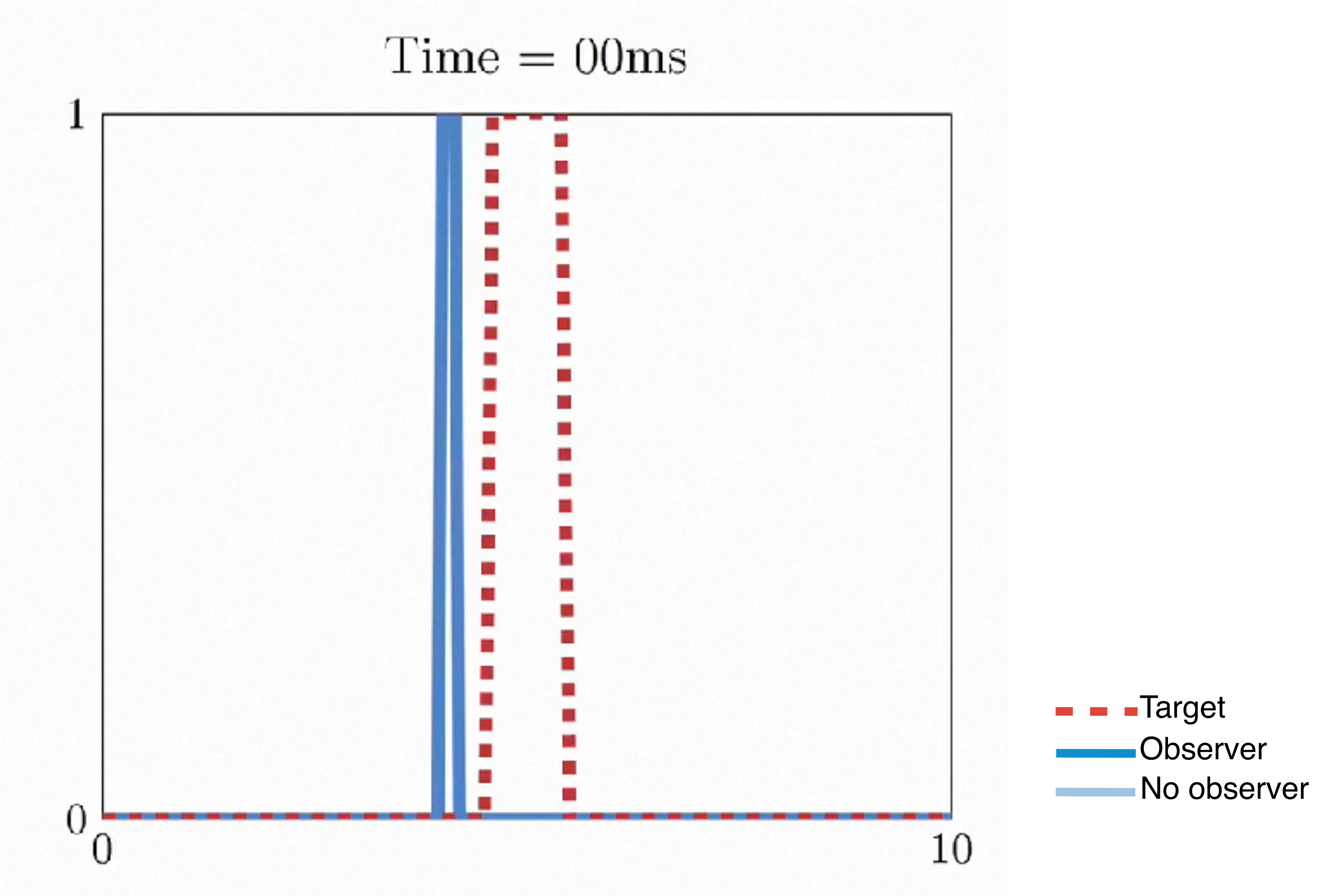

Data assimilation expertise

- Combine this state observer with a parameter observer

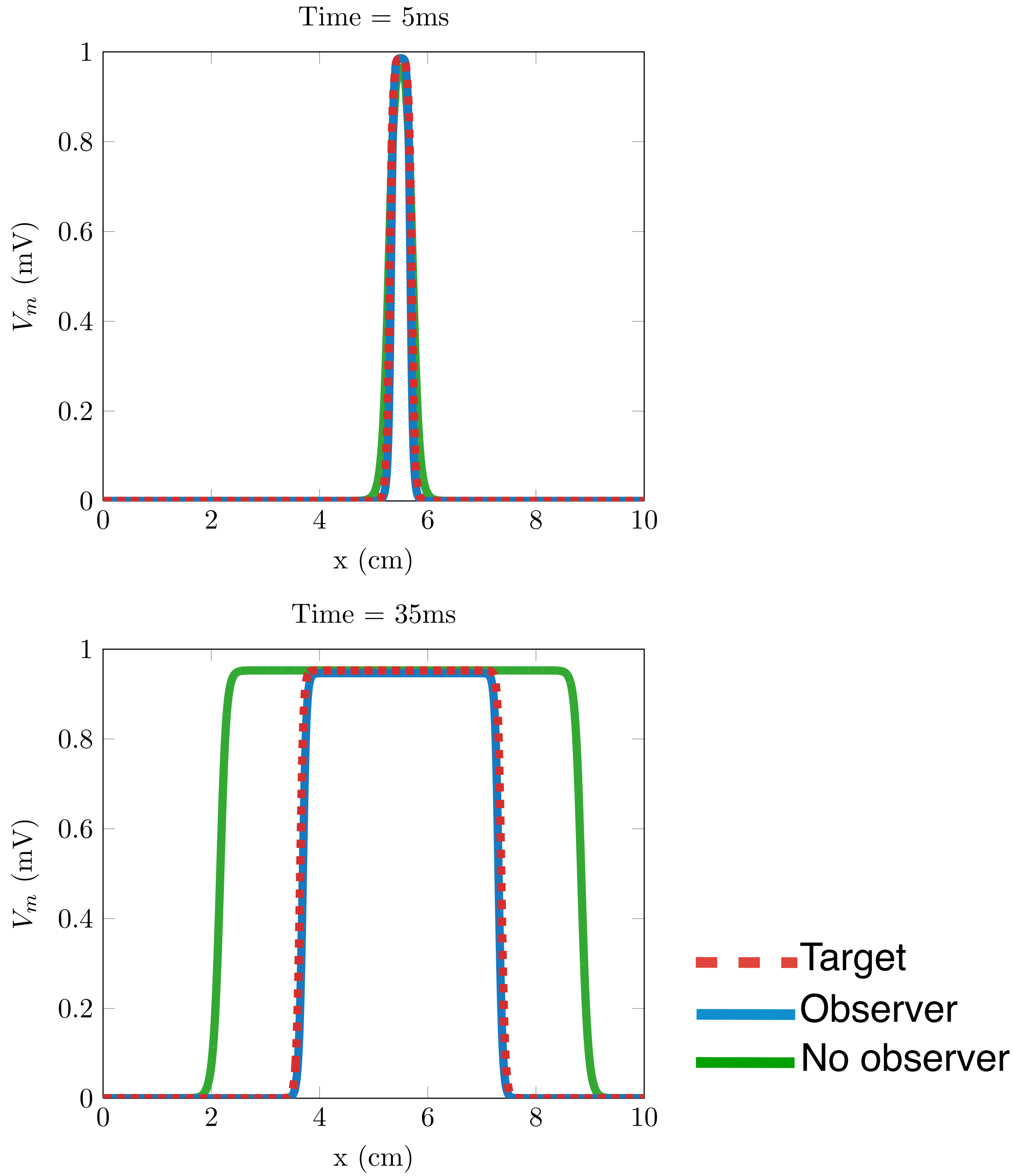

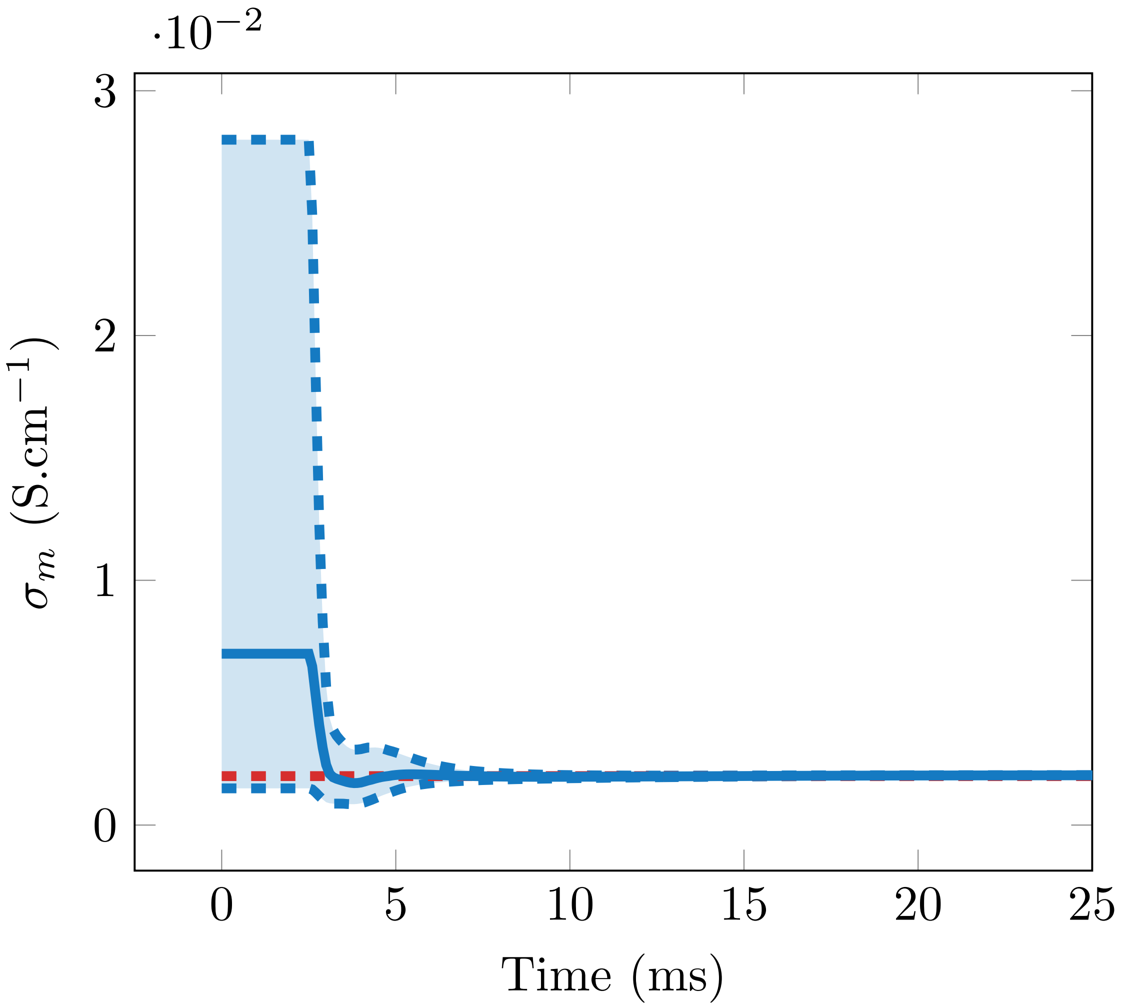

Data assimilation expertise

- Combine this state observer with a parameter observer

Target
Observer
No observer

Data assimilation expertise

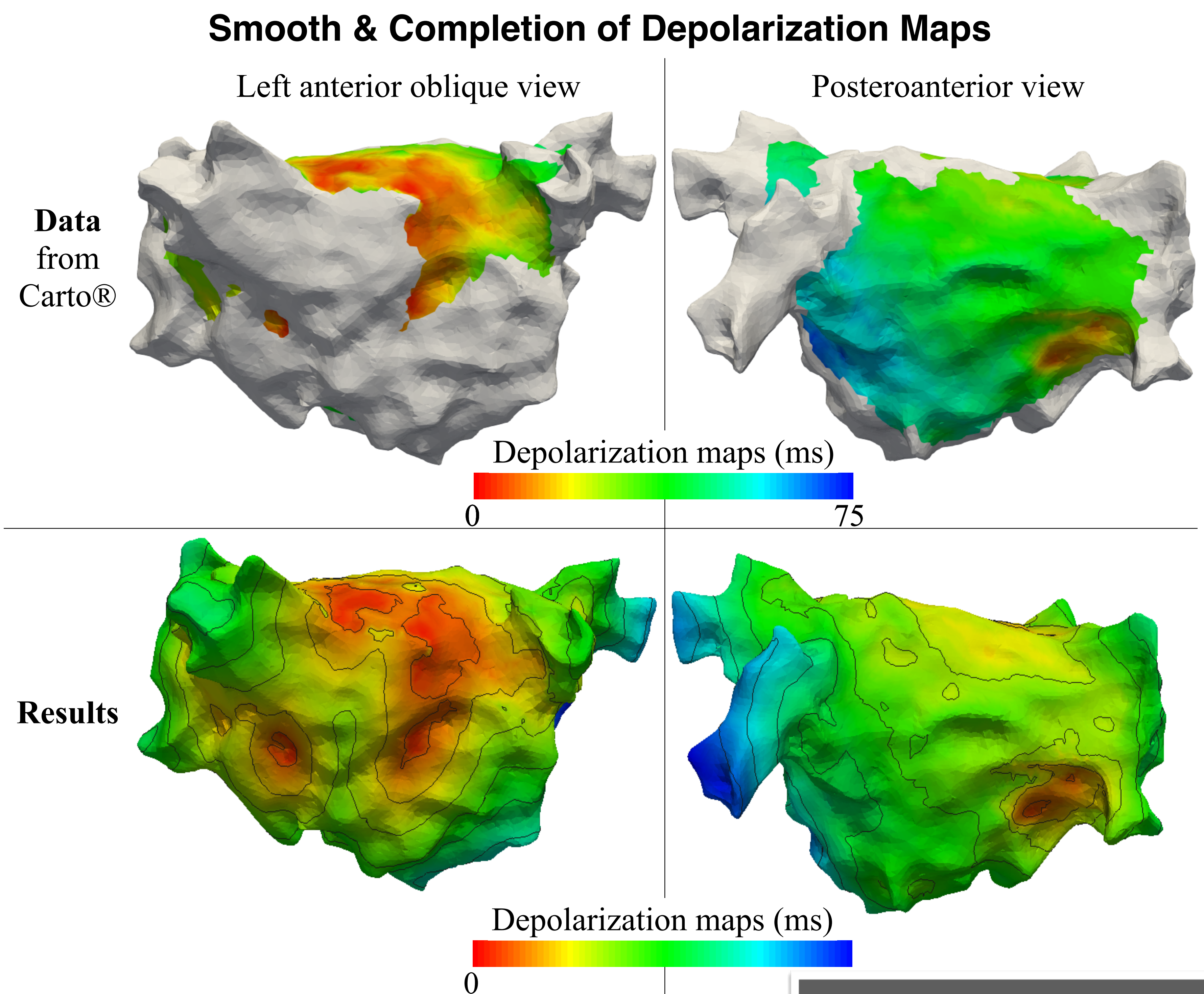

[1] A. Gérard, A. Collin, G. Bureau, P. Moireau, and Y. Coudière. Model assessment through data assimilation of realistic data in cardiac electrophysiology. FIMH 2023.

Electroporation Expertise

One axis of Monc Inria Team (Clair Poignard):

- Modeling cell scale
- Modeling tissue scale
- Comparison and parameters estimation with impedance measurements (biological, patients data)
- Combine with impact on tumor growth

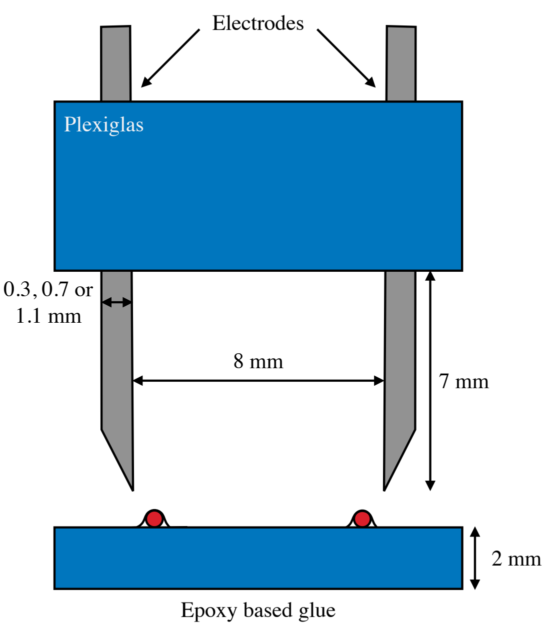

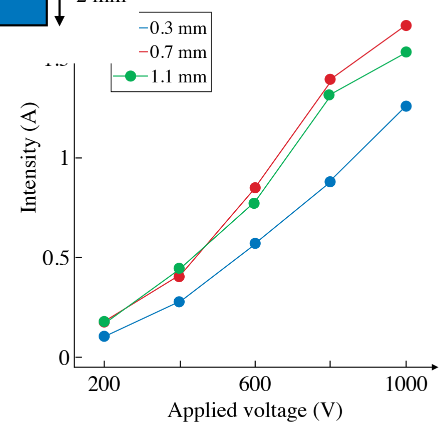

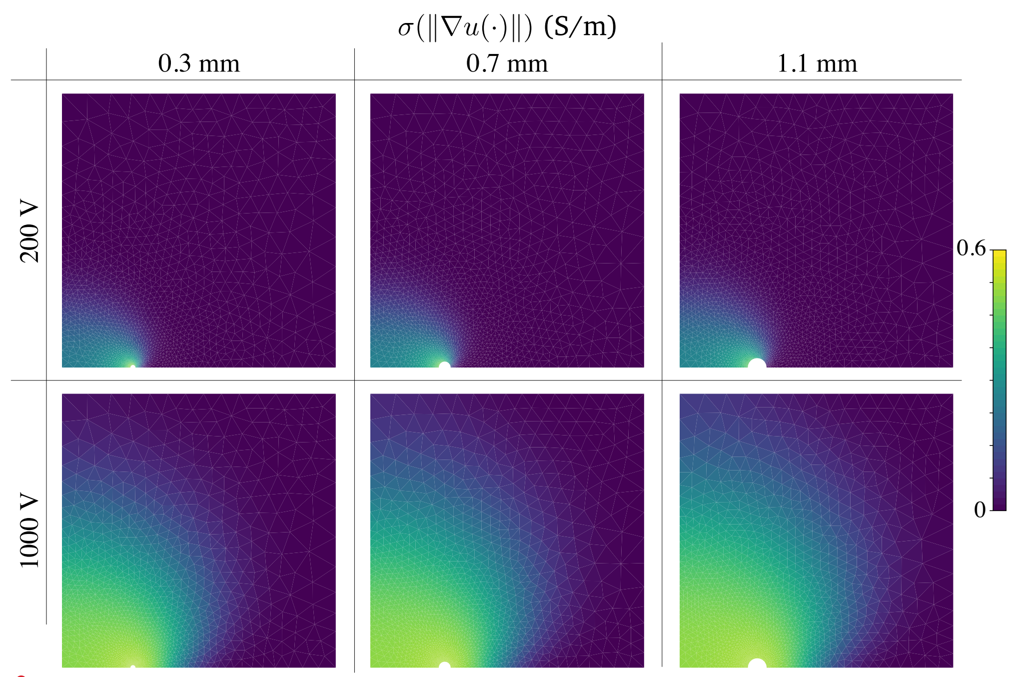

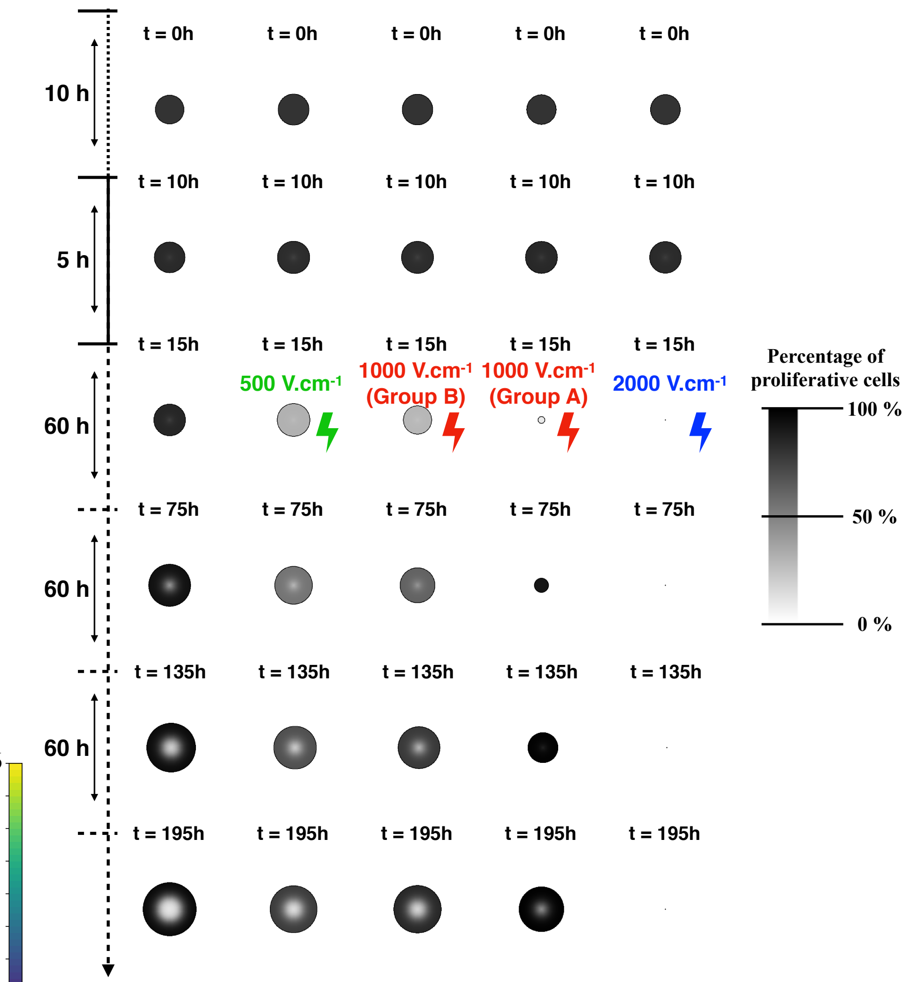

[1] G. Jankowiak, C. Taing, C. Poignard, and A. Collin. Comparison and calibration of different electroporation models. Application to rabbit livers experiments. ESAIM 2020.
[2] A. Collin, H. Bruhier, J. Kolosnjaj, M. Golzio, M.-P. Rols, and C. Poignard. Spatial mechanistic modeling for prediction of 3D multicellular spheroids behavior upon exposure to high intensity pulsed electric fields. AIMS Bioengineering 2022.

Mathematical challenges

Different challenges …

- … determined after exchanges with clinicians.

Atrial fibrillation | Surgery | Months

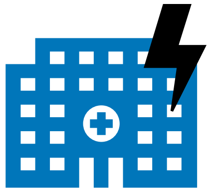

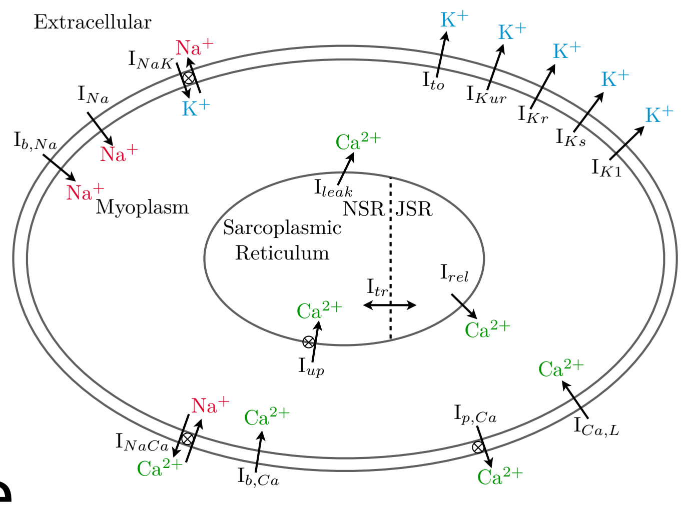

- <u>Cell scale</u>
  Better understand how the cardiac cells die.
  Model cardiac electroporation at the cellular scale (and in particular Ca^{2+} uptake).
  Validate model with data.

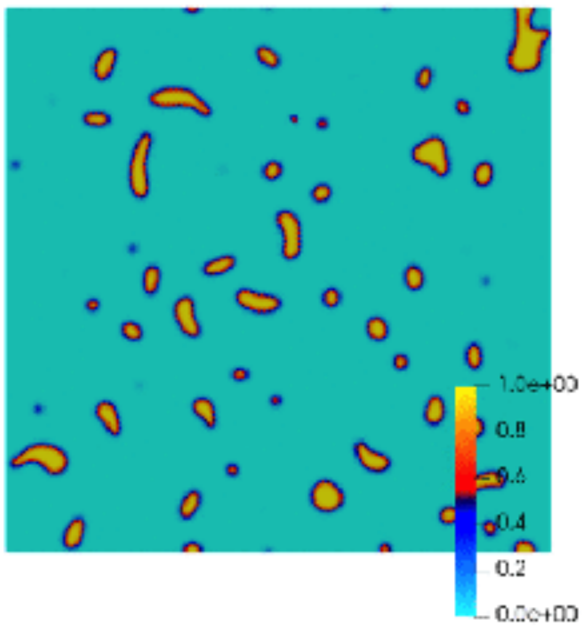

Pore formation at the cell membrane. Simulation of a phase-field model [1].

Techniques	RFA	PFA
Type of ablation	Thermal	Non-thermal
Tissue scaffold	Destruction	Preservation

[1] Phase-field model of bilipid membrane electroporation. P. Jaramillo-Aguayo, A. Collin, C. Poignard. JOMB (accepted), 2023.

Different challenges …

- … determined after exchanges with clinicians.

Atrial fibrillation — Surgery — Months

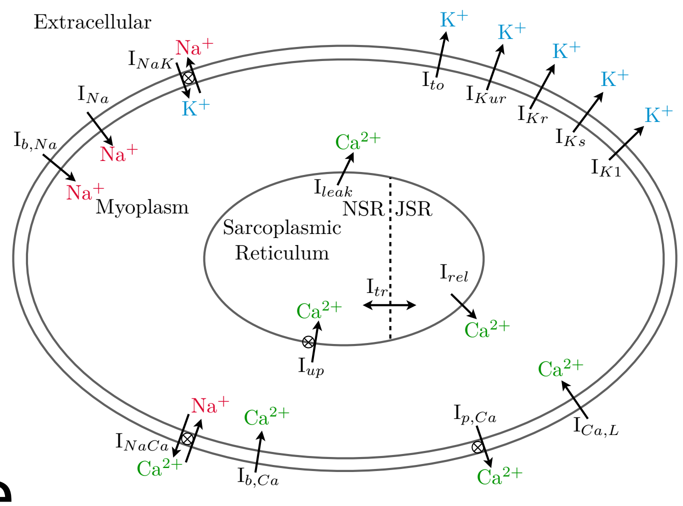

- <u>Cell scale</u>
  Better understand how the cardiac cells die.
  Model cardiac electroporation at the cellular scale (and in particular Ca^{2+} uptake).
  Validate model with data.

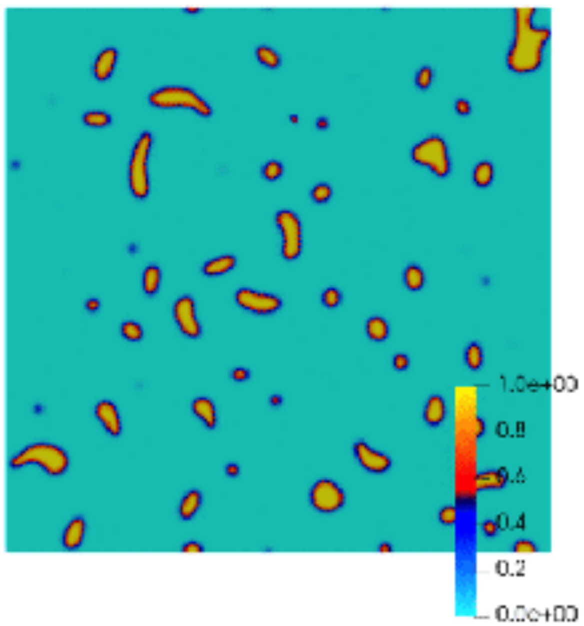

Pore formation at the cell membrane. Simulation of a phase-field model [1].

Techniques	RFA	PFA
Type of ablation	Thermal	Non-thermal
Tissue scaffold	Destruction	Preservation

[1] Phase-field model of bilipid membrane electroporation. P. Jaramillo-Aguayo, A. Collin, C. Poignard. JOMB (accepted), 2023.

Different challenges …

- … determined after exchanges with clinicians.

- <u>Tissue scale</u>
  Build equations to model the electroporation process at the tissue scale.
  Validate them with animal or patient data.
  Provide patient specific simulation.

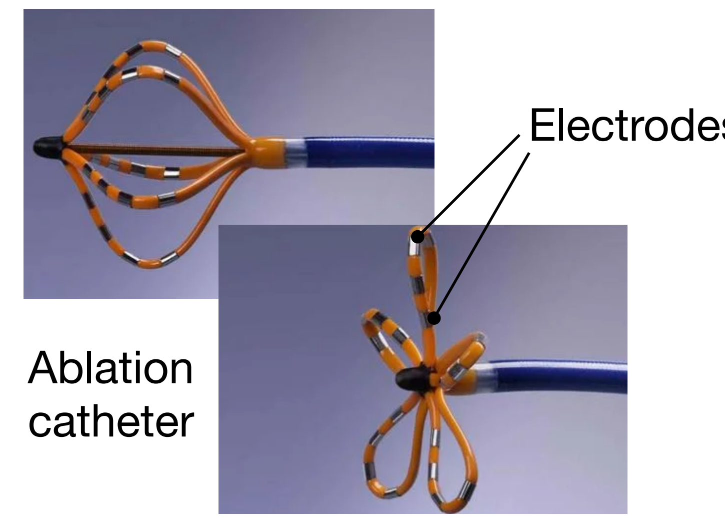

Techniques	RFA	PFA
Type of ablation	Thermal	Non-thermal
Tissue scaffold	Destruction	Preservation

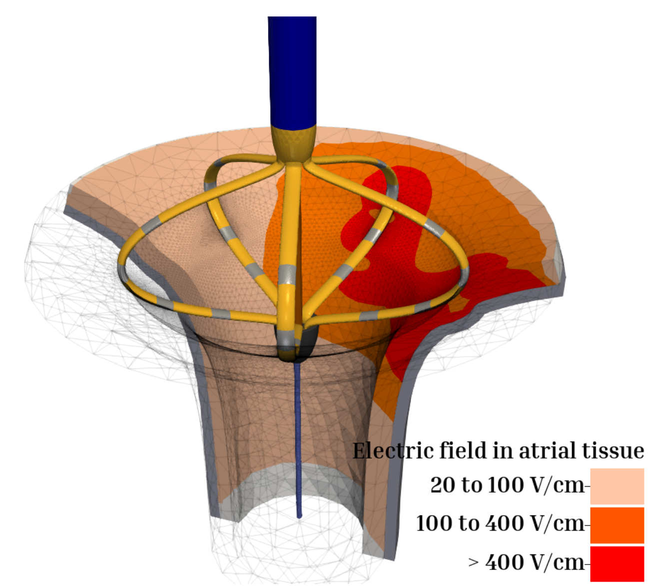

Different challenges …

- … determined after exchanges with clinicians.

Atrial fibrillation

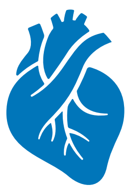

Surgery

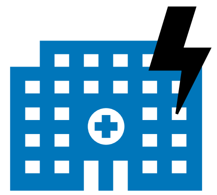

Months

- <u>Tissue scale</u>

PFA catheter in Right Superior Pulmonary Vein

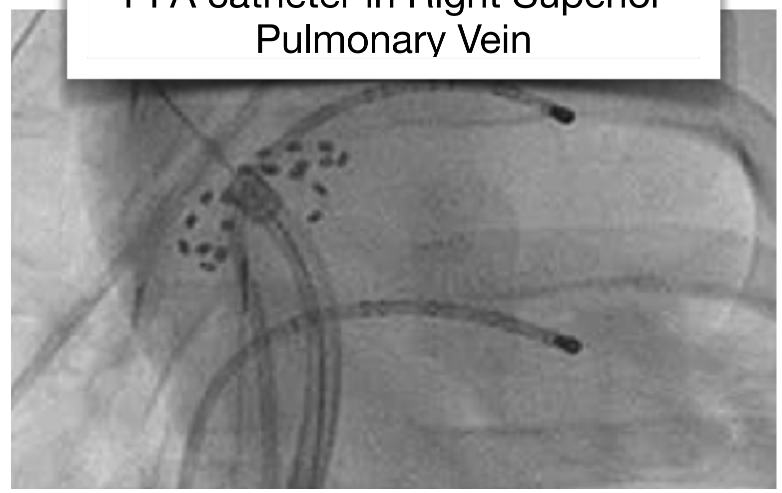

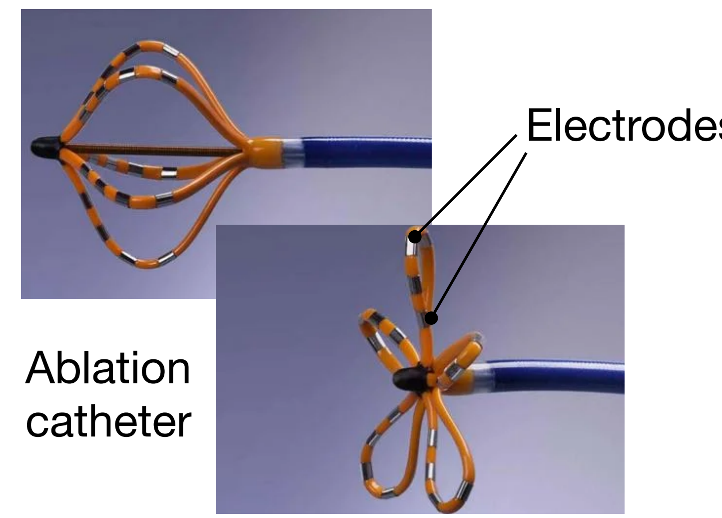

Pulmonary vein electrograms from a multipolar circular catheter

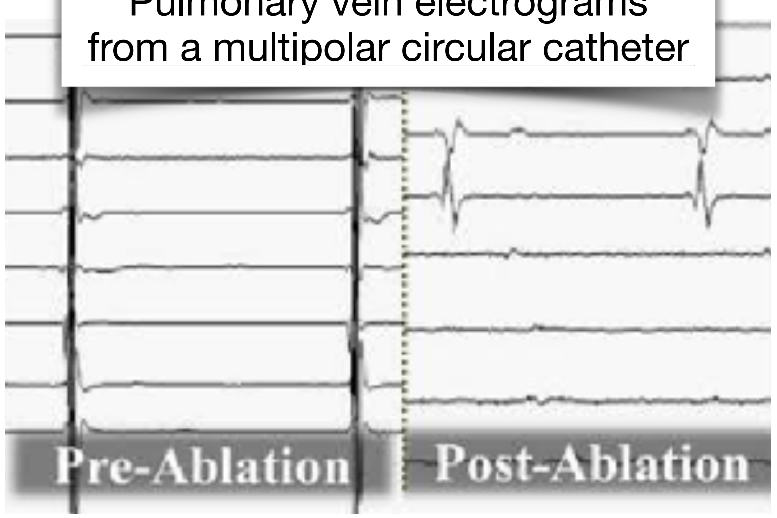

Voltage maps performed at follow-up

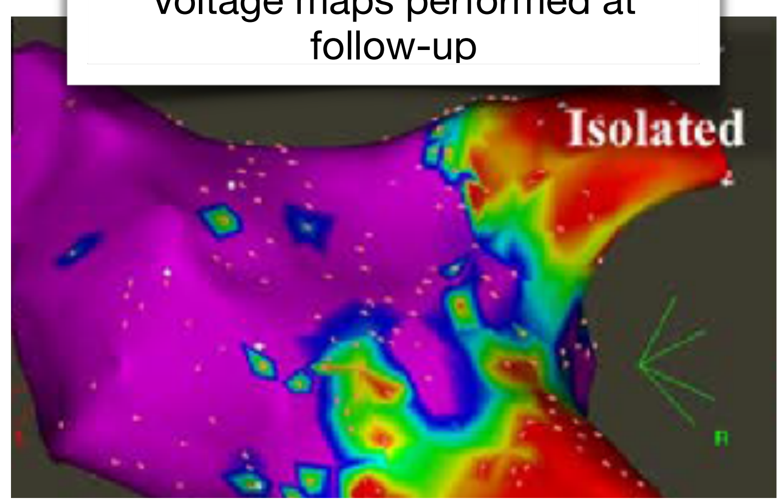

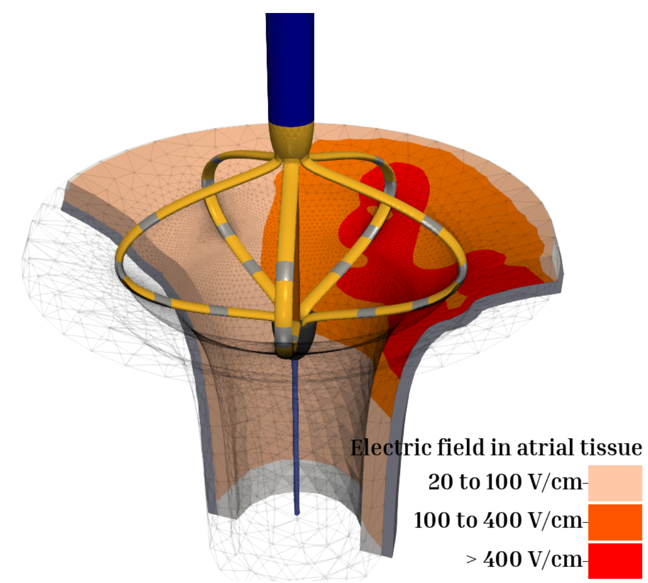

[1]Preclinical Evaluation of Pulsed Field Ablation. Electrophysiological and Histological Assessment of Thoracic Vein Isolation. J. Koruth *et al.* Circulation: Arrhythmia and Electrophysiology, 2019.

Different challenges …

- … determined after exchanges with clinicians.

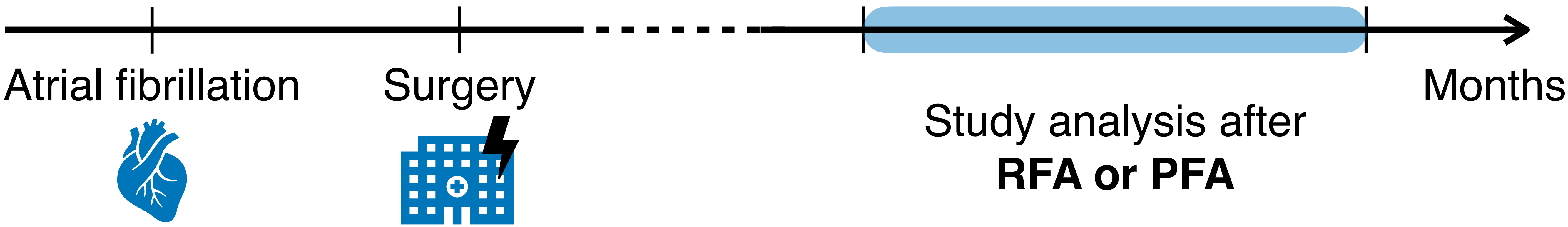

Techniques	RFA	PFA
Type of ablation	Thermal	Non-thermal
Tissue scaffold	Destruction	Preservation
Induced fibrosis	More	Few
Recurrency of AF	30% [1]	15% [2]

[1] Reddy VY, Dukkipati SR, Neuzil P, et al. Pulsed Field Ablation of Paroxysmal Atrial Fibrillation. JACC Clin Electrophysiol 2021; 7: 614–627.
[2] Wittkampf FH m., Nakagawa H. RF Catheter Ablation: Lessons on Lesions. Pacing Clin Electrophysiol 2006; 29: 1285– 1297.

Electrocardiology Modeling after PFA

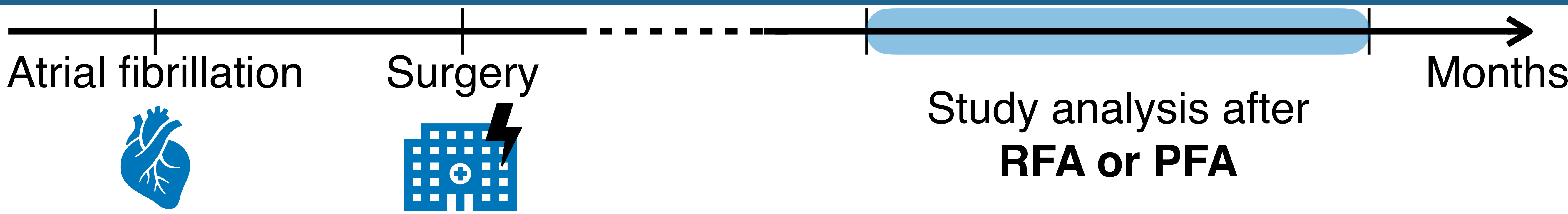

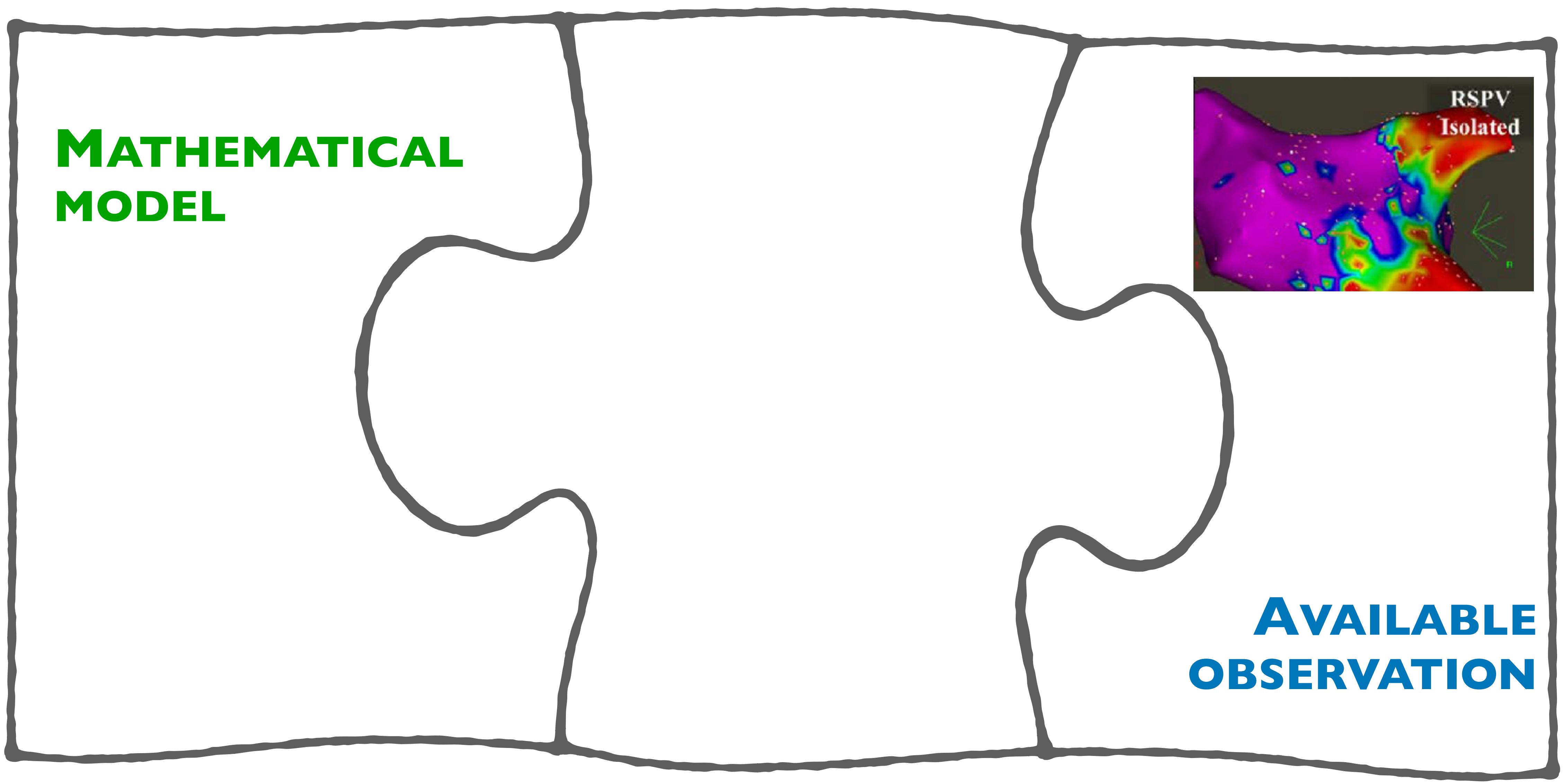

Electrocardiology Modeling after PFA

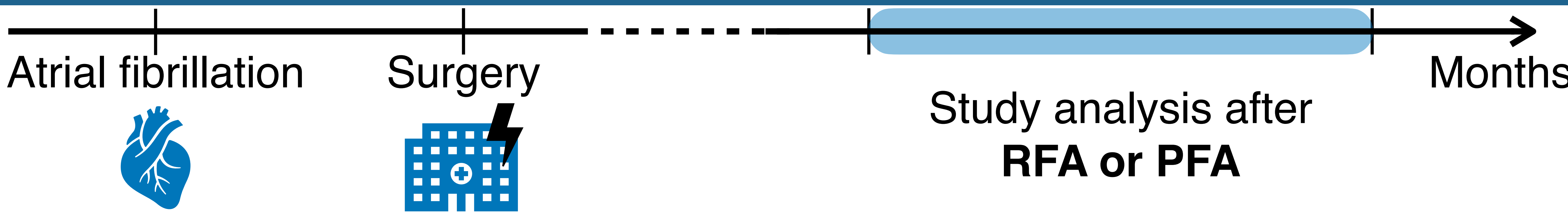

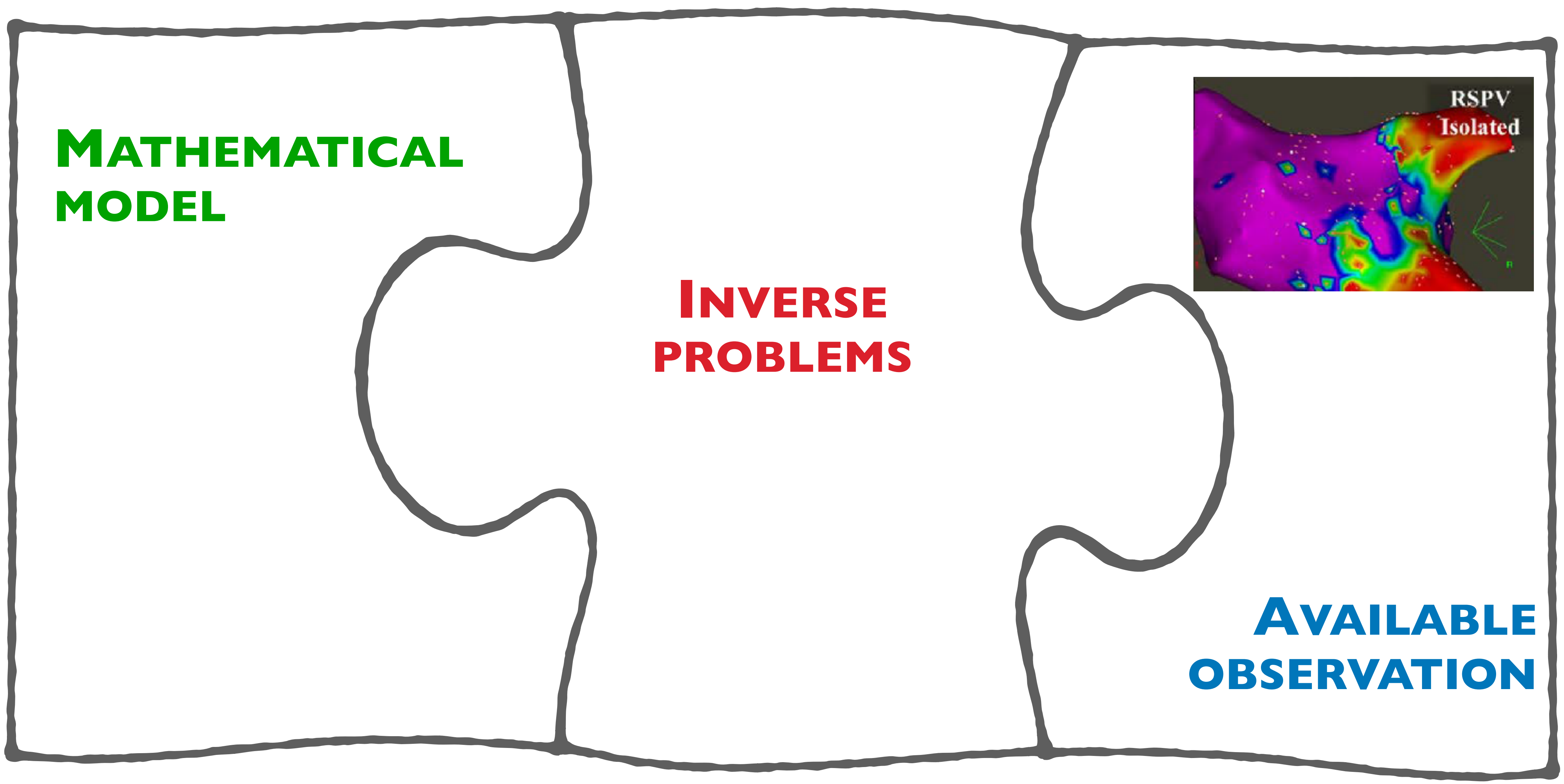

Electrocardiology Modeling after PFA

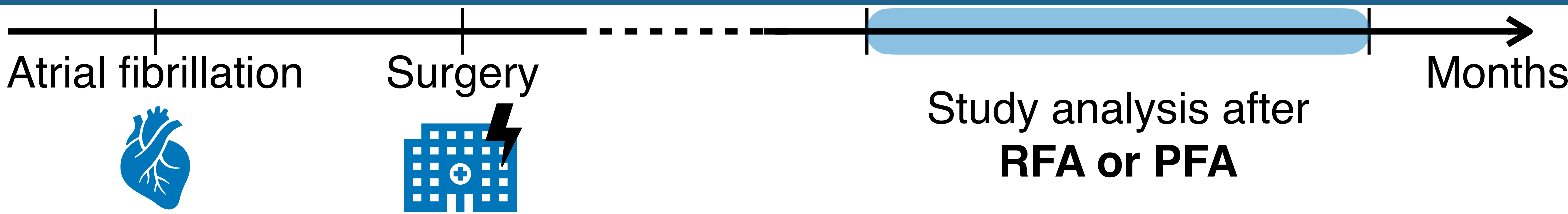

- Bidomain model

$$A_m(C_m\partial_t v_m + I_{ion}(v_m,\cdots)) - \nabla\cdot(\sigma_i\cdot\nabla v_m) - \nabla\cdot(\sigma_i\cdot\nabla u_e) = 0,\ \ \Omega,$$
$$\nabla\cdot((\sigma_i+\sigma_e)\cdot\nabla u_e) + \nabla\cdot(\sigma_i\cdot\nabla v_m) = 0,\ \ \Omega\,.$$

- Hypothesis:
  - The size of the electroporated (EP) area is considered to be thin.
  - Almost all cardiomyocytes were ablated by PFA:

    (1) intra-cellular conductivity (containing the volume fraction of cells) decreases: $\sigma_i^{ep} = \varepsilon^2\sigma_i$,

    (2) and there is no more ionic current inside the EP area.

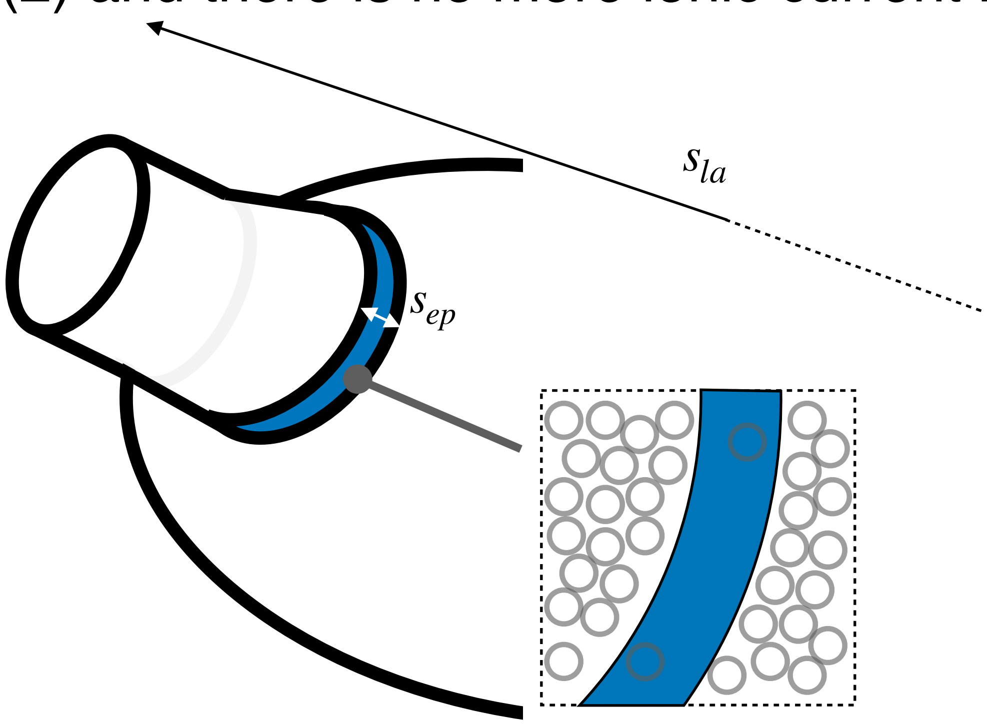

Electrocardiology Modeling after PFA

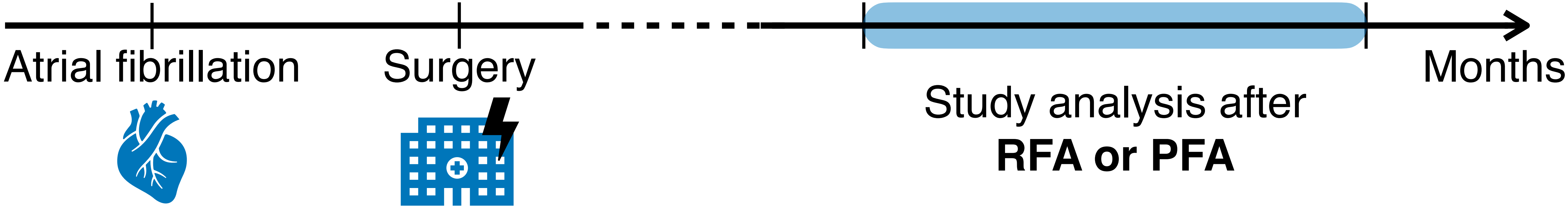

- Bidomain model

$$A_m(C_m\partial_t v_m + I_{ion}(v_m,\cdots)) - \nabla\cdot(\sigma_i\cdot\nabla v_m) - \nabla\cdot(\sigma_i\cdot\nabla u_e) = 0,\ \ \Omega,$$
$$\nabla\cdot((\sigma_i+\sigma_e)\cdot\nabla u_e) + \nabla\cdot(\sigma_i\cdot\nabla v_m) = 0,\ \ \Omega\,.$$

- Hypothesis:
  - The size of the electroporated (EP) area is considered to be thin.
  - Almost all cardiomyocytes were ablated by PFA:
    (1) intra-cellular conductivity (containing the volume fraction of cells) decreases: $\sigma_i^{ep} = \varepsilon^2\sigma_i$,
    (2) and there is no more ionic current inside the EP area.

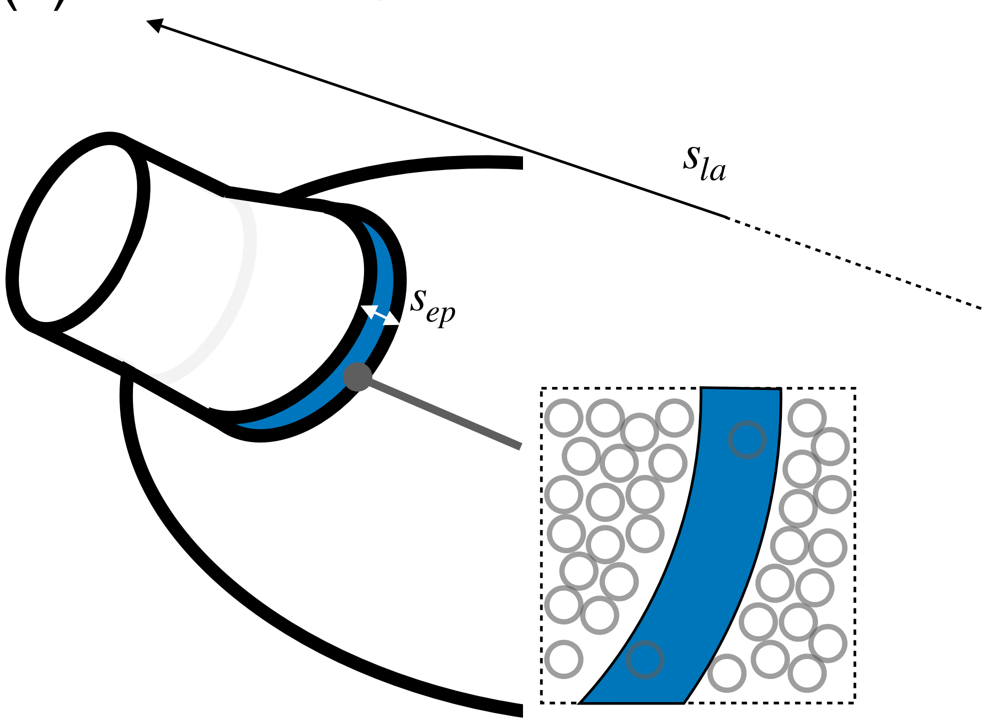

$$\varepsilon = \frac{s_{ep}}{s_{la}} \to 0$$

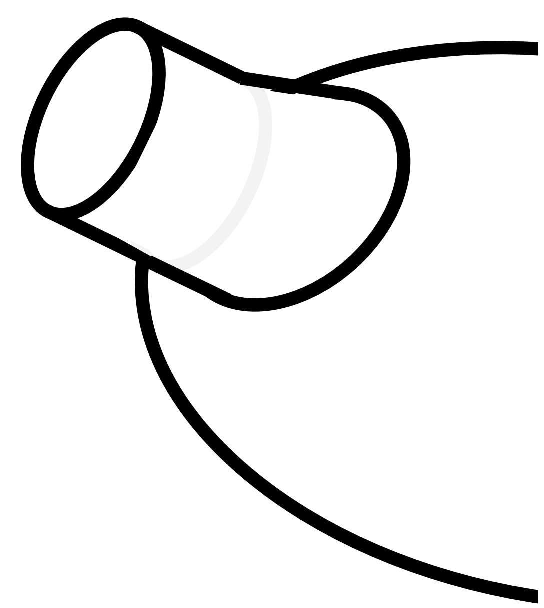

Electrocardiology Modeling after PFA

Electrocardiology Modeling after PFA

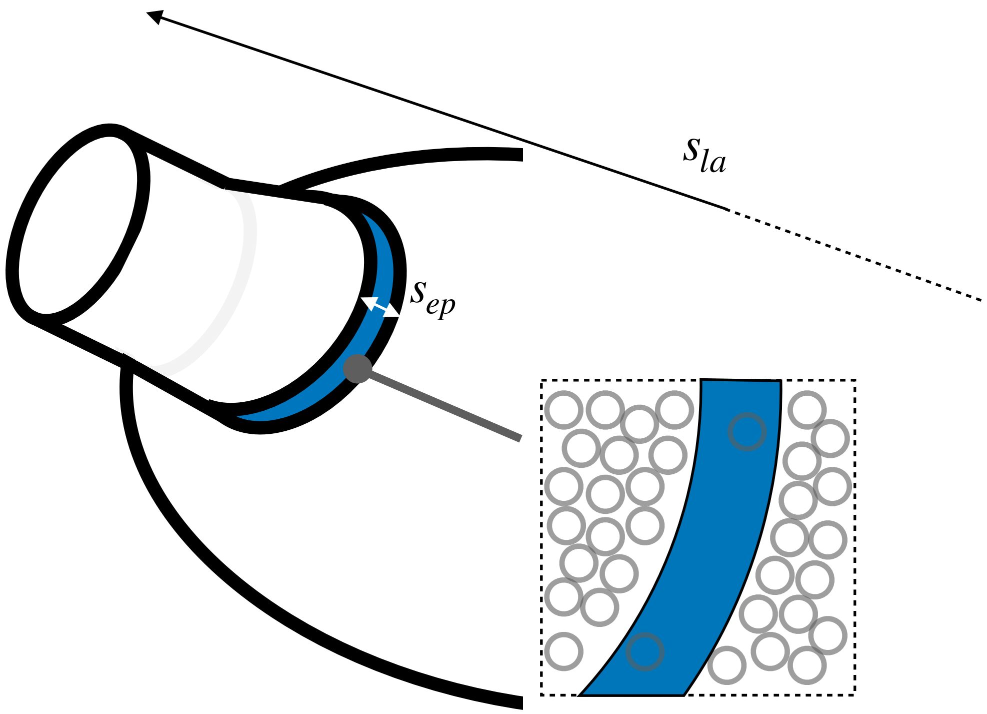

$$\varepsilon = \frac{s_{ep}}{s_{la}} \to 0$$

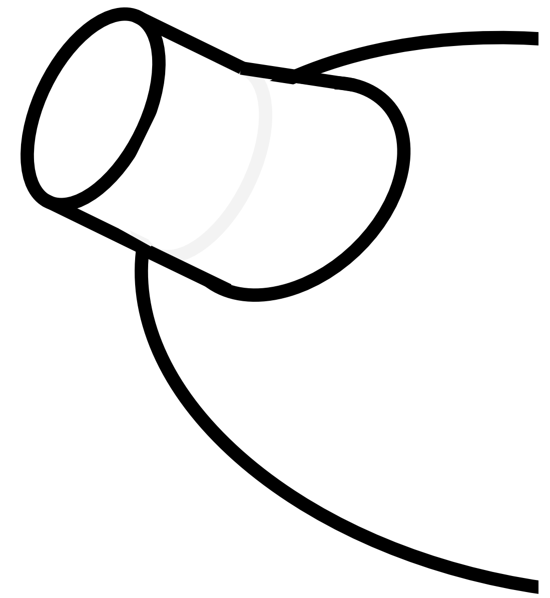

Objective:
Determine the transmission conditions at the interface Γ when $\varepsilon \to 0$.

Static case

$$
\begin{aligned}
-\nabla\cdot(\sigma_i \nabla u_i^\varepsilon) + A_m I_{ion}(u_i^\varepsilon - u_e^\varepsilon) &= 1_{\Omega_L} f, && \Omega_L \cup \Omega_R^\varepsilon,\\
-\nabla\cdot(\sigma_e \nabla u_e^\varepsilon) - A_m I_{ion}(u_i^\varepsilon - u_e^\varepsilon) &= -\, 1_{\Omega_L} f, && \Omega_L \cup \Omega_R^\varepsilon,\\
-\nabla\cdot(\sigma_i^{ep} \nabla u_i^\varepsilon) + A_m I_{ion}\,(u_i^\varepsilon - u_e^\varepsilon) &= 0, && \Omega_{ep}^\varepsilon,\\
-\nabla\cdot(\sigma_e^{ep} \nabla u_e^\varepsilon) - A_m I_{ion};(u_i^\varepsilon - u_e^\varepsilon) &= 0, && \Omega_{ep}^\varepsilon\,.
\end{aligned}
$$

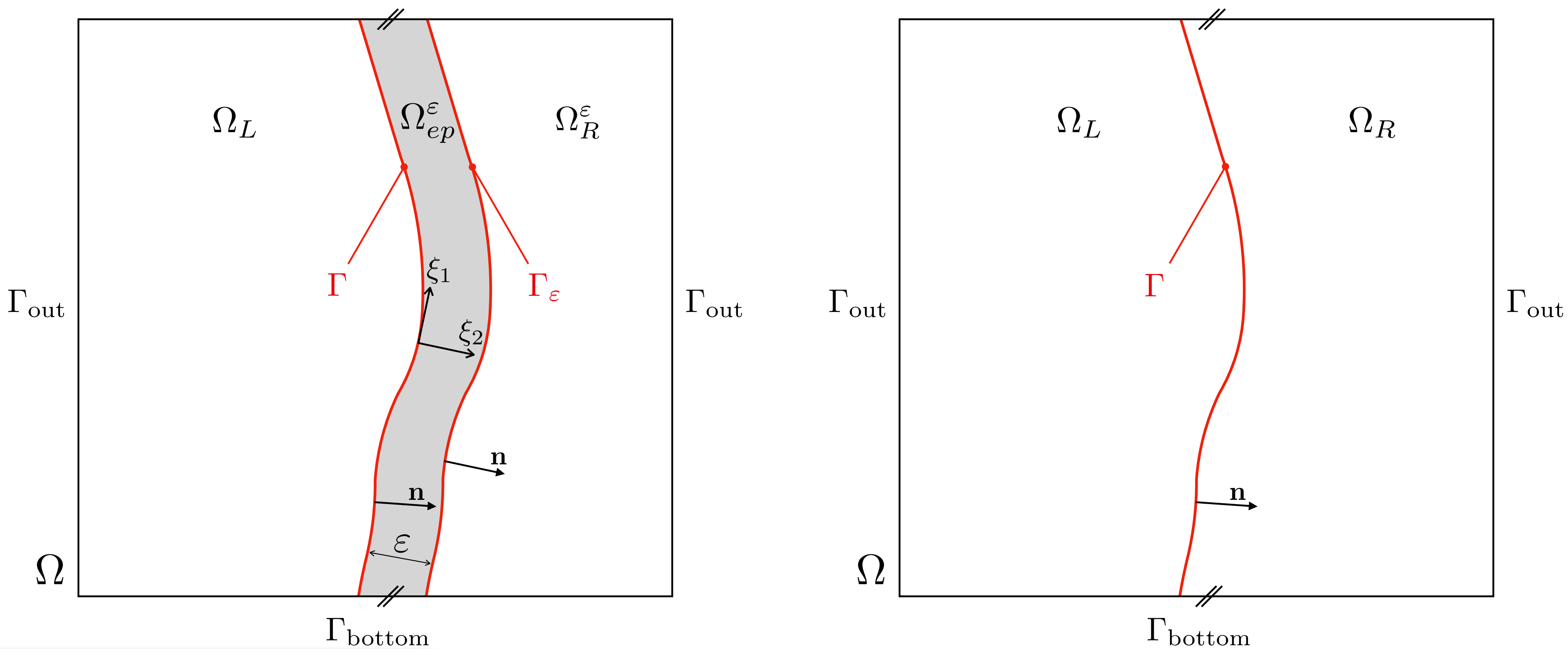

Static case

$$
\begin{aligned}
-\nabla\cdot(\sigma_i\nabla u_i^\varepsilon) + A_m I_{ion}(u_i^\varepsilon - u_e^\varepsilon) &= 1_{\Omega_L} f, && \Omega_L \cup \Omega_R^\varepsilon,\\
-\nabla\cdot(\sigma_e\nabla u_e^\varepsilon) - A_m I_{ion}(u_i^\varepsilon - u_e^\varepsilon) &= -1_{\Omega_L} f, && \Omega_L \cup \Omega_R^\varepsilon,\\
-\nabla\cdot(\varepsilon^2\sigma_i\nabla u_i^\varepsilon) + A_m I_{ion}\,(u_i^\varepsilon - u_e^\varepsilon) &= 0, && \Omega_{ep}^\varepsilon,\\
-\nabla\cdot(\sigma_e\nabla u_e^\varepsilon) - A_m I_{ion}\,(u_i^\varepsilon - u_e^\varepsilon) &= 0, && \Omega_{ep}^\varepsilon\,.
\end{aligned}
$$

Ablation of cardiomyocytes

(1) very weak intra-cellular conductivity,

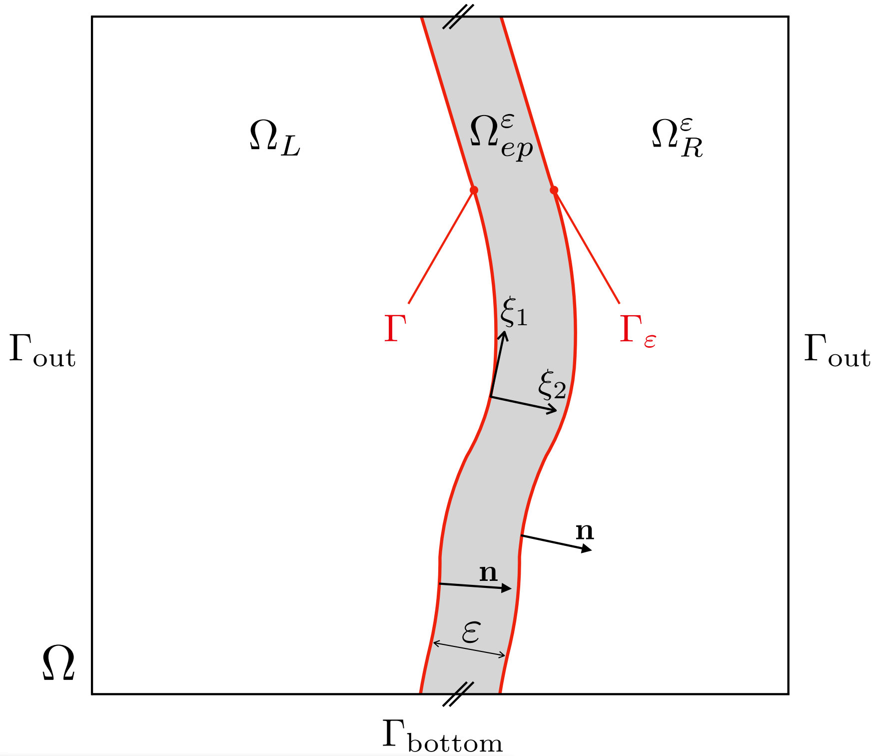

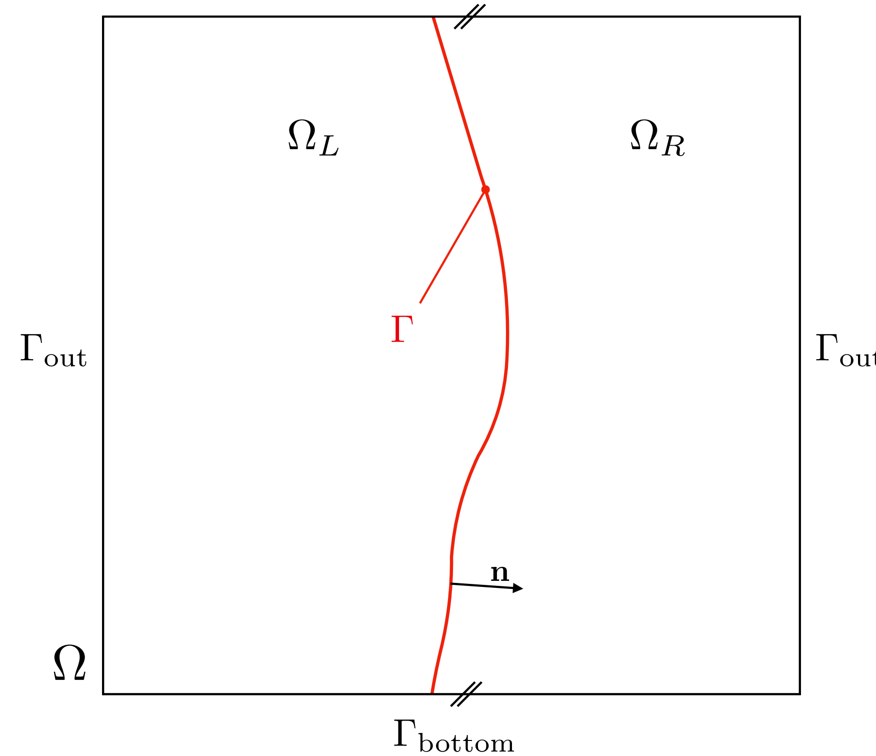

Static case

$$
\begin{aligned}
-\nabla\cdot(\sigma_i\nabla u_i^\varepsilon)+A_m I_{ion}(u_i^\varepsilon-u_e^\varepsilon) &= 1_{\Omega_L} f, && \Omega_L\cup\Omega_R^\varepsilon,\\
-\nabla\cdot(\sigma_e\nabla u_e^\varepsilon)-A_m I_{ion}(u_i^\varepsilon-u_e^\varepsilon) &= -1_{\Omega_L} f, && \Omega_L\cup\Omega_R^\varepsilon,\\
-\nabla\cdot(\varepsilon^2\sigma_i\nabla u_i^\varepsilon)+A_m S_0\,(u_i^\varepsilon-u_e^\varepsilon) &= 0, && \Omega_{ep}^\varepsilon,\\
-\nabla\cdot(\sigma_e\nabla u_e^\varepsilon)-A_m S_0\,(u_i^\varepsilon-u_e^\varepsilon) &= 0, && \Omega_{ep}^\varepsilon\,.
\end{aligned}
$$

Ablation of cardiomyocytes

(1) very weak intra-cellular conductivity,

(2) no ionic current inside the EP area.

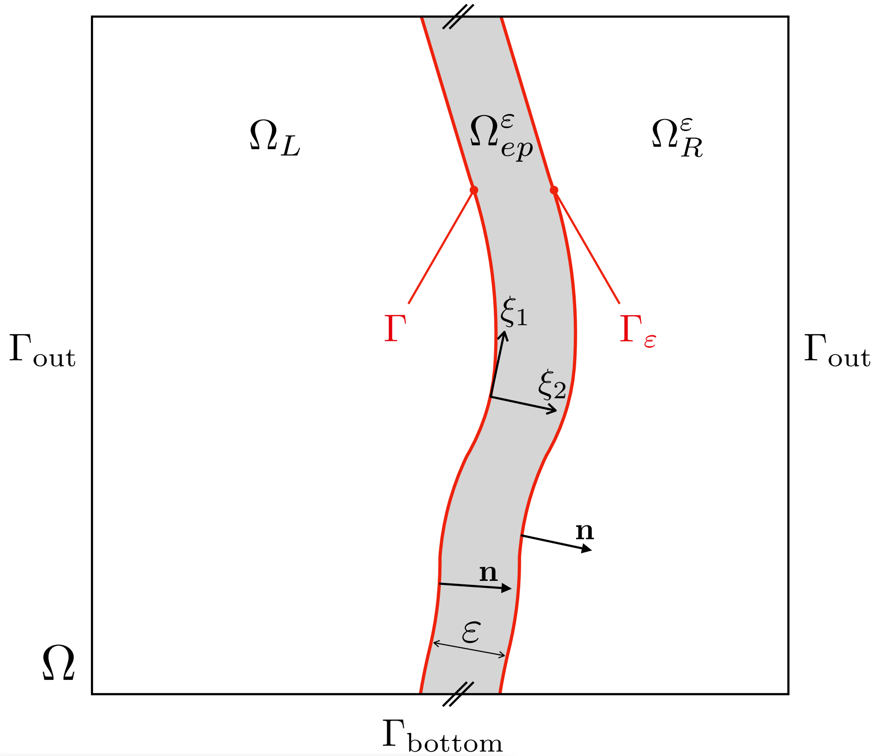

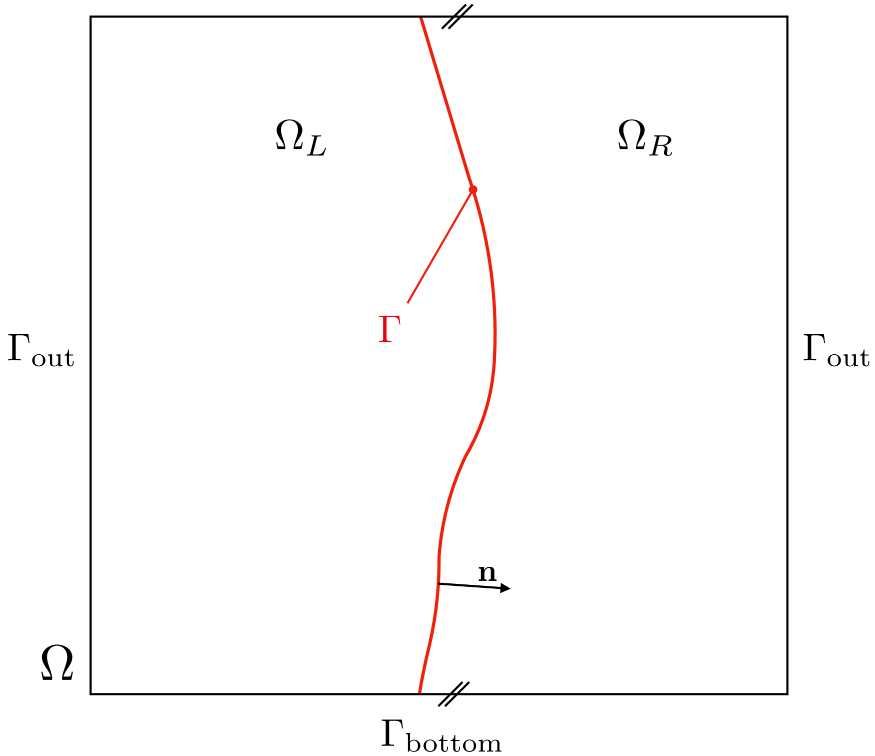

Static case

$$-\nabla\cdot(\sigma_i\nabla u_i^\varepsilon) + A_m I_{ion}(u_i^\varepsilon - u_e^\varepsilon) = 1_{\Omega_L} f, \quad \Omega_L \cup \Omega_R^\varepsilon,$$
$$-\nabla\cdot(\sigma_e\nabla u_e^\varepsilon) - A_m I_{ion}(u_i^\varepsilon - u_e^\varepsilon) = -1_{\Omega_L} f, \quad \Omega_L \cup \Omega_R^\varepsilon,$$
$$-\nabla\cdot(\varepsilon^2\sigma_i\nabla u_i^\varepsilon) + A_m S_0\,(u_i^\varepsilon - u_e^\varepsilon) = 0, \quad \Omega_{ep}^\varepsilon,$$
$$-\nabla\cdot(\sigma_e\nabla u_e^\varepsilon) - A_m S_0\,(u_i^\varepsilon - u_e^\varepsilon) = 0, \quad \Omega_{ep}^\varepsilon\,.$$

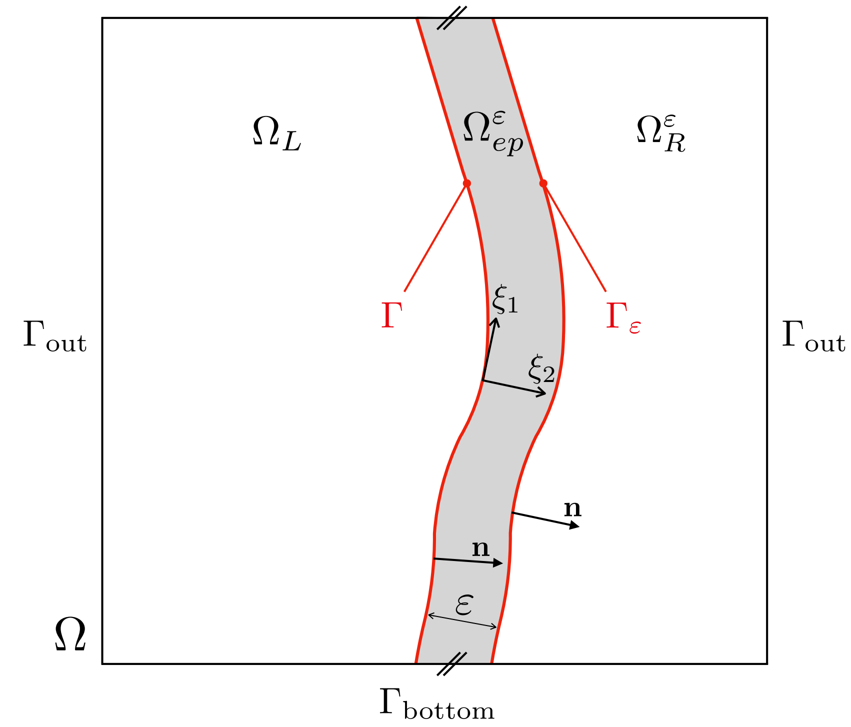

coupled to transmission conditions,

$$[u_i^\varepsilon]_{|_\Gamma} = 0, \quad [\sigma_i^\varepsilon\partial_{\mathbf{n}}u_i^\varepsilon]_{|_\Gamma} = 0, [u_e^\varepsilon]_{|_\Gamma} = 0, \quad [\sigma_e\partial_{\mathbf{n}}u_e^\varepsilon]_{|_\Gamma} = 0,$$
$$[u_i^\varepsilon]_{|_{\Gamma_\varepsilon}} = 0, \quad [\sigma_i^\varepsilon\partial_{\mathbf{n}}u_i^\varepsilon]_{|_{\Gamma_\varepsilon}} = 0, [u_e^\varepsilon]_{|_{\Gamma_\varepsilon}} = 0, \quad [\sigma_e\partial_{\mathbf{n}}u_e^\varepsilon]_{|_{\Gamma_\varepsilon}} = 0,$$

boundary conditions,

$$u_i^\varepsilon{}_{|_{\Gamma_{up}}} = u_i^\varepsilon{}_{|_{\Gamma_{bottom}}}, \; u_e^\varepsilon{}_{|_{\Gamma_{up}}} = u_e^\varepsilon{}_{|_{\Gamma_{bottom}}}, \; \partial_{\mathbf{n}}u_i^\varepsilon{}_{|_{\Gamma_{out}}} = 0, \; \partial_{\mathbf{n}}u_e^\varepsilon{}_{|_{\Gamma_{out}}} = 0,$$

and Gauge condition

$$\int_\Omega u_e^\varepsilon\,dx = 0.$$

Static case

$$-\nabla \cdot (\sigma_i \nabla u_i^\varepsilon) + A_m I_{ion}(u_i^\varepsilon - u_e^\varepsilon) = 1_{\Omega_L} f, \quad \Omega_L \cup \Omega_R^\varepsilon,$$
$$-\nabla \cdot (\sigma_e \nabla u_e^\varepsilon) - A_m I_{ion}(u_i^\varepsilon - u_e^\varepsilon) = -1_{\Omega_L} f, \quad \Omega_L \cup \Omega_R^\varepsilon,$$
$$-\nabla \cdot (\varepsilon^2 \sigma_i \nabla u_i^\varepsilon) + A_m S_0 \,(u_i^\varepsilon - u_e^\varepsilon) = 0, \quad \Omega_{ep}^\varepsilon,$$
$$-\nabla \cdot (\sigma_e \nabla u_e^\varepsilon) - A_m S_0 \,(u_i^\varepsilon - u_e^\varepsilon) = 0, \quad \Omega_{ep}^\varepsilon\,.$$
$$[u_i^\varepsilon]_{|_\Gamma} = 0, \quad [\sigma_i^\varepsilon \partial_{\mathbf{n}} u_i^\varepsilon]_{|_\Gamma} = 0, [u_e^\varepsilon]_{|_\Gamma} = 0, \quad [\sigma_e \partial_{\mathbf{n}} u_e^\varepsilon]_{|_\Gamma} = 0,$$
$$[u_i^\varepsilon]_{|_{\Gamma_\varepsilon}} = 0, \quad [\sigma_i^\varepsilon \partial_{\mathbf{n}} u_i^\varepsilon]_{|_{\Gamma_\varepsilon}} = 0, [u_e^\varepsilon]_{|_{\Gamma_\varepsilon}} = 0, \quad [\sigma_e \partial_{\mathbf{n}} u_e^\varepsilon]_{|_{\Gamma_\varepsilon}} = 0,$$
$$\int_\Omega u_e^\varepsilon \, dx = 0.$$

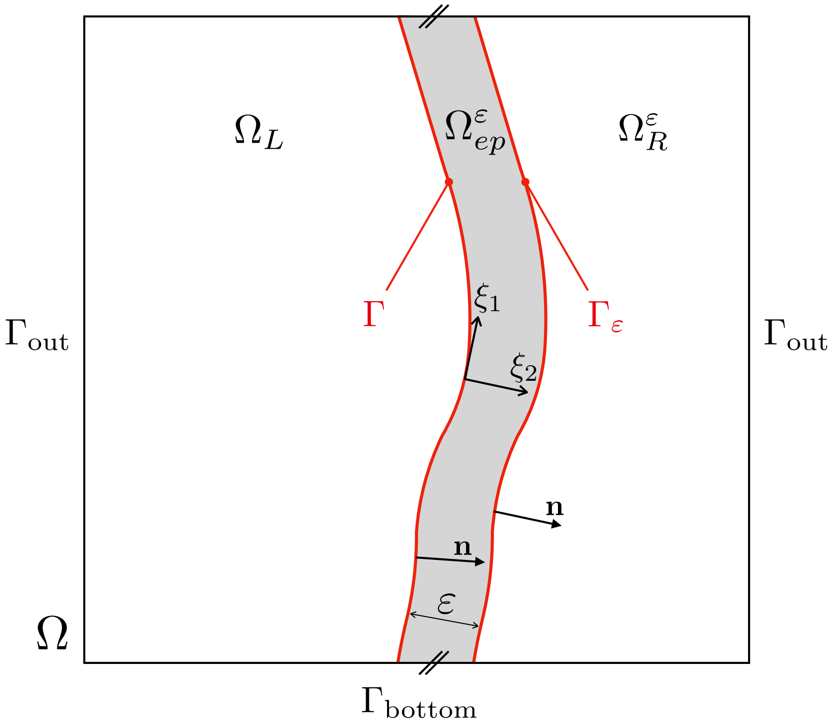

Existence & Uniqueness: under conditions on the ionic term.

Apriori estimates: allows the convergence.

Few numerical illustrations

$$-\nabla\cdot(\sigma_i\nabla u_i^\varepsilon)+A_m I_{ion}(u_i^\varepsilon-u_e^\varepsilon)=1_{\Omega_L}f,\quad \Omega_L\cup\Omega_R^\varepsilon,$$
$$-\nabla\cdot(\sigma_e\nabla u_e^\varepsilon)-A_m I_{ion}(u_i^\varepsilon-u_e^\varepsilon)=-1_{\Omega_L}f,\quad \Omega_L\cup\Omega_R^\varepsilon,$$
$$-\nabla\cdot(\varepsilon^2\sigma_i\nabla u_i^\varepsilon)+A_m S_0\,(u_i^\varepsilon-u_e^\varepsilon)=0,\quad \Omega_{ep}^\varepsilon,$$
$$-\nabla\cdot(\sigma_e\nabla u_e^\varepsilon)-A_m S_0\,(u_i^\varepsilon-u_e^\varepsilon)=0,\quad \Omega_{ep}^\varepsilon\,.$$

$$[u_i^\varepsilon]_{|_\Gamma}=0,\quad [\sigma_i^\varepsilon\partial_{\mathbf{n}}u_i^\varepsilon]_{|_\Gamma}=0,[u_e^\varepsilon]_{|_\Gamma}=0,\quad [\sigma_e\partial_{\mathbf{n}}u_e^\varepsilon]_{|_\Gamma}=0,$$
$$[u_i^\varepsilon]_{|_{\Gamma_\varepsilon}}=0,\quad [\sigma_i^\varepsilon\partial_{\mathbf{n}}u_i^\varepsilon]_{|_{\Gamma_\varepsilon}}=0,[u_e^\varepsilon]_{|_{\Gamma_\varepsilon}}=0,\quad [\sigma_e\partial_{\mathbf{n}}u_e^\varepsilon]_{|_{\Gamma_\varepsilon}}=0,$$
$$\int_\Omega u_e^\varepsilon\,dx=0.$$

Few numerical illustrations

$$-\nabla\cdot(\sigma_i \nabla u_i^\varepsilon) + A_m I_{ion}(u_i^\varepsilon - u_e^\varepsilon) = 1_{\Omega_L} f, \quad \Omega_L \cup \Omega_R^\varepsilon,$$
$$-\nabla\cdot(\sigma_e \nabla u_e^\varepsilon) - A_m I_{ion}(u_i^\varepsilon - u_e^\varepsilon) = -1_{\Omega_L} f, \quad \Omega_L \cup \Omega_R^\varepsilon,$$
$$-\nabla\cdot(\boxed{\varepsilon^2\sigma_i} \nabla u_i^\varepsilon) + A_m S_0\,(u_i^\varepsilon - u_e^\varepsilon) = 0, \quad \Omega_{ep}^\varepsilon,$$
$$-\nabla\cdot(\sigma_e \nabla u_e^\varepsilon) - A_m S_0\,(u_i^\varepsilon - u_e^\varepsilon) = 0, \quad \Omega_{ep}^\varepsilon\,.$$

$$[u_i^\varepsilon]_{|_\Gamma} = 0, \quad [\sigma_i^\varepsilon \partial_{\mathbf{n}} u_i^\varepsilon]_{|_\Gamma} = 0, [u_e^\varepsilon]_{|_\Gamma} = 0, \quad [\sigma_e \partial_{\mathbf{n}} u_e^\varepsilon]_{|_\Gamma} = 0,$$
$$[u_i^\varepsilon]_{|_{\Gamma_\varepsilon}} = 0, \quad [\sigma_i^\varepsilon \partial_{\mathbf{n}} u_i^\varepsilon]_{|_{\Gamma_\varepsilon}} = 0, [u_e^\varepsilon]_{|_{\Gamma_\varepsilon}} = 0, \quad [\sigma_e \partial_{\mathbf{n}} u_e^\varepsilon]_{|_{\Gamma_\varepsilon}} = 0,$$
$$\int_\Omega u_e^\varepsilon\, dx = 0.$$

"Numerical Justification"

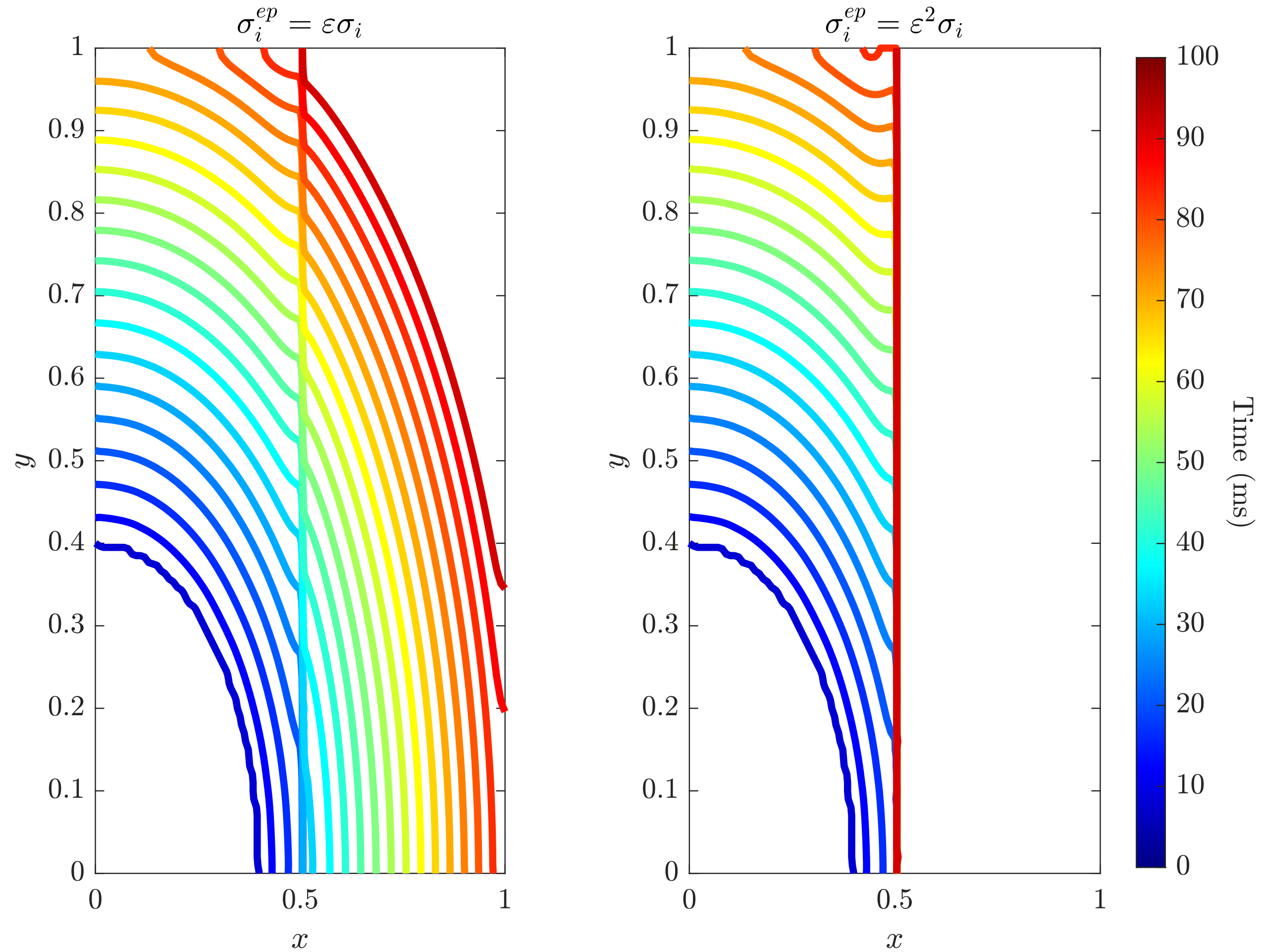

Few numerical illustrations

$$-\nabla\cdot(\sigma_i\nabla u_i^\varepsilon)+A_m I_{ion}(u_i^\varepsilon-u_e^\varepsilon)=1_{\Omega_L}f,\quad \Omega_L\cup\Omega_R^\varepsilon,$$
$$-\nabla\cdot(\sigma_e\nabla u_e^\varepsilon)-A_m I_{ion}(u_i^\varepsilon-u_e^\varepsilon)=-1_{\Omega_L}f,\quad \Omega_L\cup\Omega_R^\varepsilon,$$
$$-\nabla\cdot(\varepsilon^2\sigma_i\nabla u_i^\varepsilon)+A_m S_0\,(u_i^\varepsilon-u_e^\varepsilon)=0,\quad \Omega_{ep}^\varepsilon,$$
$$-\nabla\cdot(\sigma_e\nabla u_e^\varepsilon)-A_m S_0\,(u_i^\varepsilon-u_e^\varepsilon)=0,\quad \Omega_{ep}^\varepsilon\,.$$

$$[u_i^\varepsilon]_{|_\Gamma}=0,\quad [\sigma_i^\varepsilon\partial_{\mathbf{n}}u_i^\varepsilon]_{|_\Gamma}=0,[u_e^\varepsilon]_{|_\Gamma}=0,\quad [\sigma_e\partial_{\mathbf{n}}u_e^\varepsilon]_{|_\Gamma}=0,$$
$$[u_i^\varepsilon]_{|_{\Gamma_\varepsilon}}=0,\quad [\sigma_i^\varepsilon\partial_{\mathbf{n}}u_i^\varepsilon]_{|_{\Gamma_\varepsilon}}=0,[u_e^\varepsilon]_{|_{\Gamma_\varepsilon}}=0,\quad [\sigma_e\partial_{\mathbf{n}}u_e^\varepsilon]_{|_{\Gamma_\varepsilon}}=0,$$
$$\int_\Omega u_e^\varepsilon\,dx=0.$$

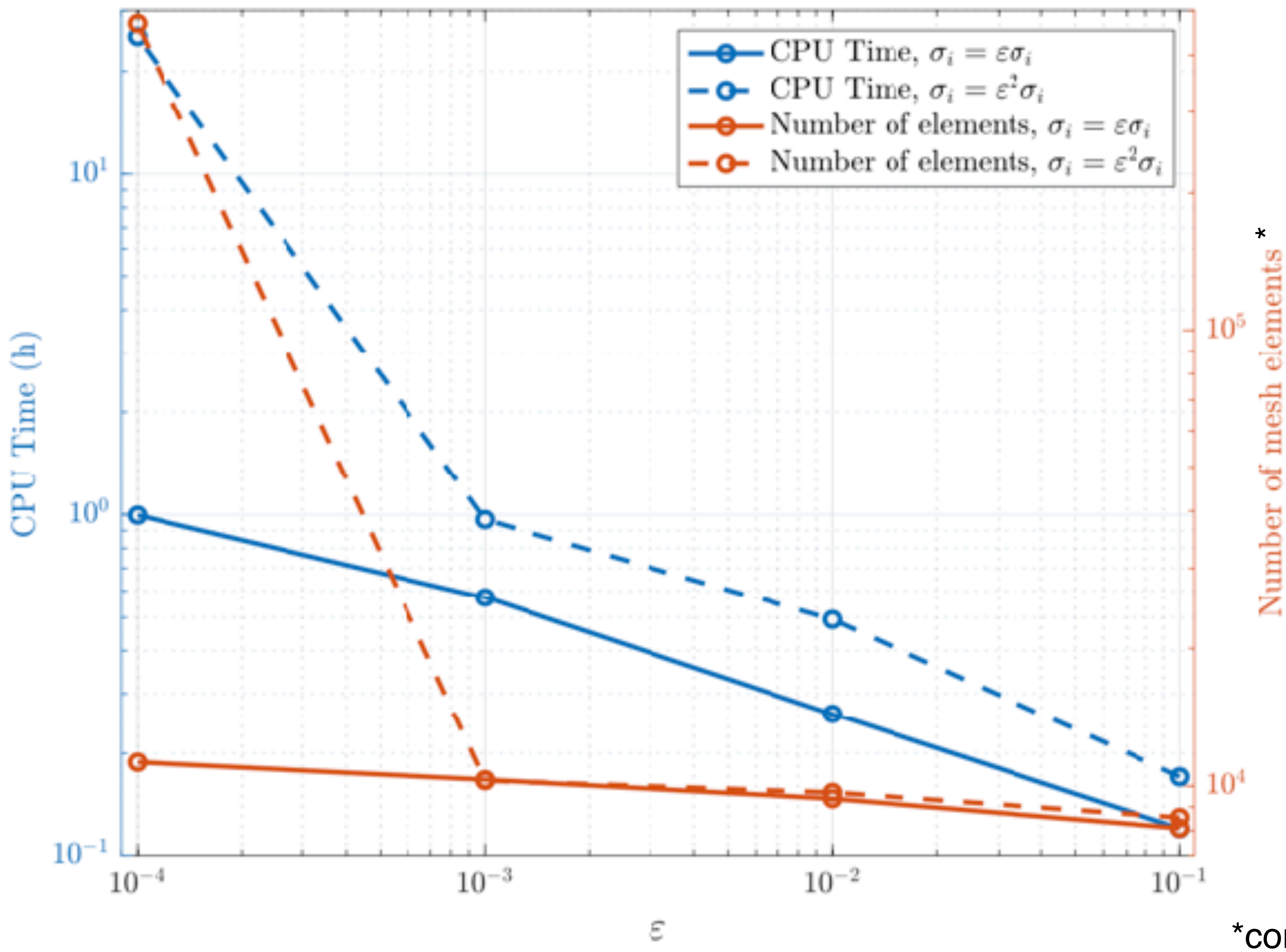

*considering an adapted mesh

Static case

$$-\nabla \cdot (\sigma_i \nabla u_i^\varepsilon) + A_m I_{ion}(u_i^\varepsilon - u_e^\varepsilon) = 1_{\Omega_L} f, \quad \Omega_L \cup \Omega_R^\varepsilon,$$
$$-\nabla \cdot (\sigma_e \nabla u_e^\varepsilon) - A_m I_{ion}(u_i^\varepsilon - u_e^\varepsilon) = -1_{\Omega_L} f, \quad \Omega_L \cup \Omega_R^\varepsilon,$$
$$-\nabla \cdot (\varepsilon^2 \sigma_i \nabla u_i^\varepsilon) + A_m S_0 \, (u_i^\varepsilon - u_e^\varepsilon) = 0, \quad \Omega_{ep}^\varepsilon,$$
$$-\nabla \cdot (\sigma_e \nabla u_e^\varepsilon) - A_m S_0 \, (u_i^\varepsilon - u_e^\varepsilon) = 0, \quad \Omega_{ep}^\varepsilon \, .$$
$$[u_i^\varepsilon]|_\Gamma = 0, \quad [\sigma_i^\varepsilon \partial_{\mathbf{n}} u_i^\varepsilon]|_\Gamma = 0, [u_e^\varepsilon]|_\Gamma = 0, \quad [\sigma_e \partial_{\mathbf{n}} u_e^\varepsilon]|_\Gamma = 0,$$
$$[u_i^\varepsilon]|_{\Gamma_\varepsilon} = 0, \quad [\sigma_i^\varepsilon \partial_{\mathbf{n}} u_i^\varepsilon]|_{\Gamma_\varepsilon} = 0, [u_e^\varepsilon]|_{\Gamma_\varepsilon} = 0, \quad [\sigma_e \partial_{\mathbf{n}} u_e^\varepsilon]|_{\Gamma_\varepsilon} = 0,$$
$$\int_\Omega u_e^\varepsilon \, dx = 0.$$

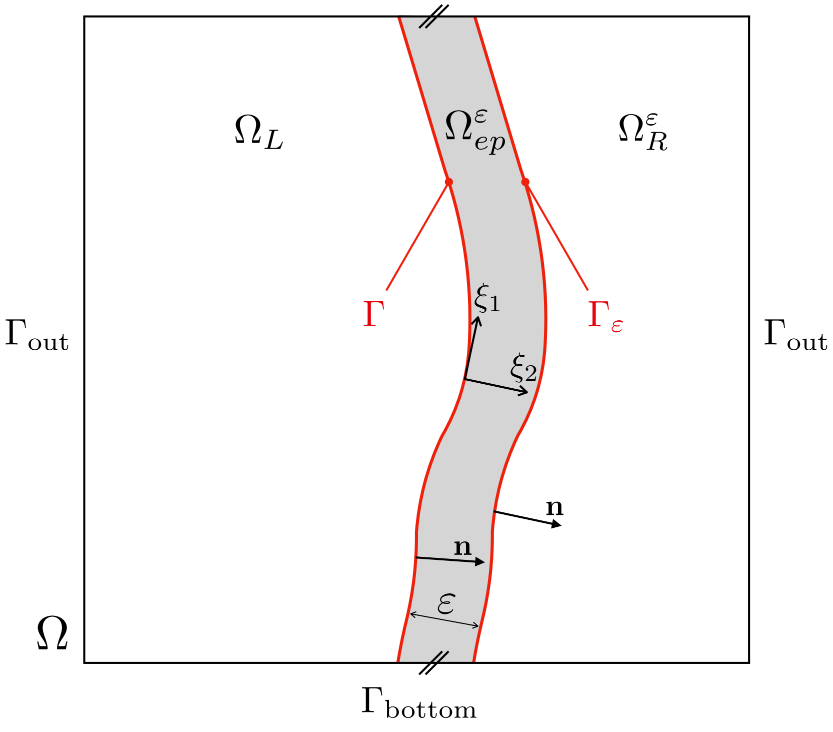

Classical ansatz

$$u_{i,e}^\varepsilon(x,y) = \sum_{p \geq 0} \varepsilon^p u_{i,e}^p(x,y), \qquad \Omega_L \cup \Omega_R^\varepsilon,$$
$$\mathrm{U}_{i,e}^\varepsilon(\xi_1, \eta) = \sum_{p \geq 0} \varepsilon^p \mathbf{u}_{i,e}^p(\xi_1, \eta), \qquad \Gamma \times (0,1) \, .$$

Problem at order 0

Inside the healthy heart

$$-\nabla \cdot (\sigma_i \nabla u_i^0) + A_m I_{ion}(u_i^0 - u_e^0) = 1_{\Omega_L} f, \quad \Omega_L \cup \Omega_R,$$

$$-\nabla \cdot (\sigma_e \nabla u_e^0) - A_m I_{ion}(u_i^0 - u_e^0) = -1_{\Omega_L} f, \quad \Omega_L \cup \Omega_R,$$

$$\partial_{\mathbf{n}} u^0_{i\,|_{\Gamma_{out}}} = 0, \quad \partial_{\mathbf{n}} u^0_{e\,|_{\Gamma_{out}}} = 0, \quad u^0_{i\,|_{\Gamma_{bottom}}} = u^0_{i\,|_{\Gamma_{up}}},$$

$$\int_{\Omega_L \cup \Omega_R} u_e^0 dx = 0.$$

CLASSICAL BIDOMAIN MODEL

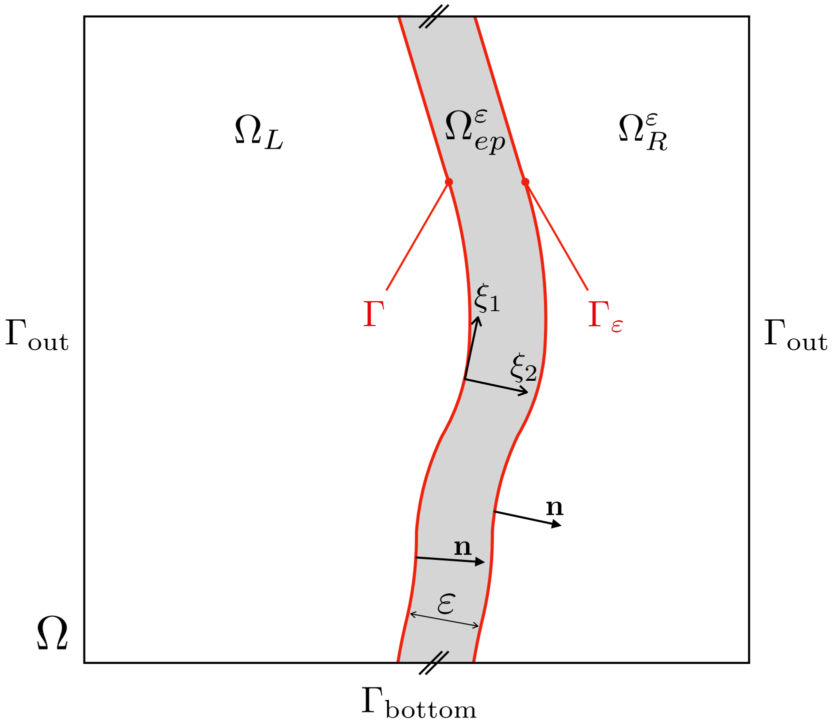

Problem at order 0

Inside the healthy heart

$$-\nabla\cdot(\sigma_i\nabla u_i^0)+A_m I_{ion}(u_i^0-u_e^0)=1_{\Omega_L}f,\quad \Omega_L\cup\Omega_R,$$

$$-\nabla\cdot(\sigma_e\nabla u_e^0)-A_m I_{ion}(u_i^0-u_e^0)=-1_{\Omega_L}f,\quad \Omega_L\cup\Omega_R,$$

$$\partial_{\mathbf{n}}u_i^0{}_{|\Gamma_{out}}=0,\quad \partial_{\mathbf{n}}u_e^0{}_{|\Gamma_{out}}=0,\quad u_i^0{}_{|\Gamma_{bottom}}=u_i^0{}_{|\Gamma_{up}},$$

$$\int_{\Omega_L\cup\Omega_R}u_e^0dx=0.$$

Classical Bidomain model

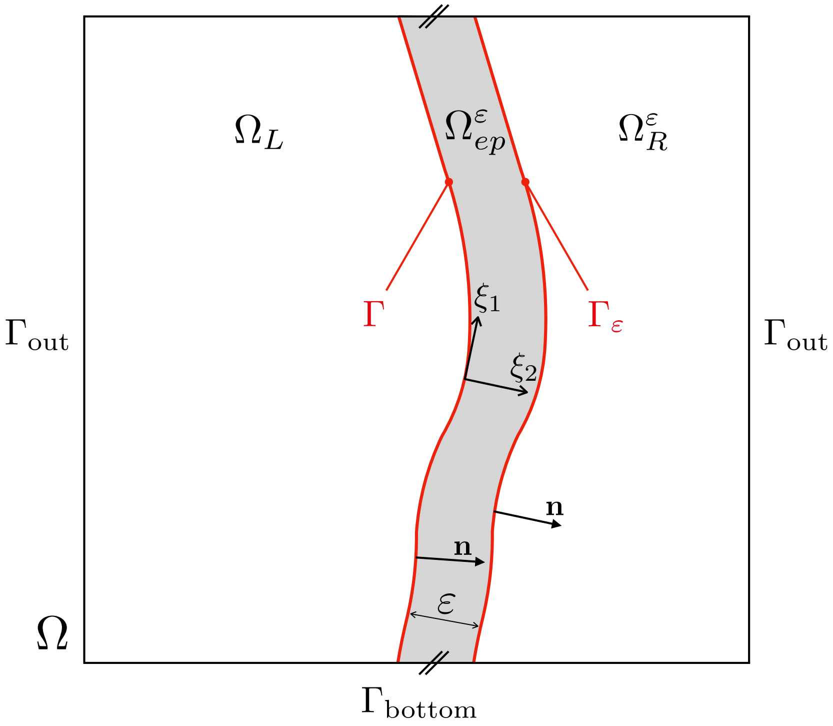

Interface Γ

$\partial_{\mathbf{n}}u_i^0{}_{|\Gamma-}=\partial_{\mathbf{n}}u_i^0{}_{|\Gamma+}=0,$ Neumann Boundary Condition on intra-cellular potential

$[u_e^0]_{|\Gamma}=0,\quad [\partial_{\mathbf{n}}u_e^0]_{|\Gamma}=0.$ Continuity on extra-cellular potential

Fully Isolated

Problem at order 0

Inside the healthy heart

$$-\nabla\cdot(\sigma_i\nabla u_i^0)+A_m I_{ion}(u_i^0-u_e^0)=1_{\Omega_L}f,\quad \Omega_L\cup\Omega_R,$$

$$-\nabla\cdot(\sigma_e\nabla u_e^0)-A_m I_{ion}(u_i^0-u_e^0)=-1_{\Omega_L}f,\quad \Omega_L\cup\Omega_R,$$

$$\partial_{\mathbf{n}}u^0_{i}{}_{|_{\Gamma_{out}}}=0,\quad \partial_{\mathbf{n}}u^0_{e}{}_{|_{\Gamma_{out}}}=0,\quad u^0_{i}{}_{|_{\Gamma_{bottom}}}=u^0_{i}{}_{|_{\Gamma_{up}}},$$

$$\int_{\Omega_L\cup\Omega_R}u_e^0dx=0.$$

CLASSICAL BIDOMAIN MODEL

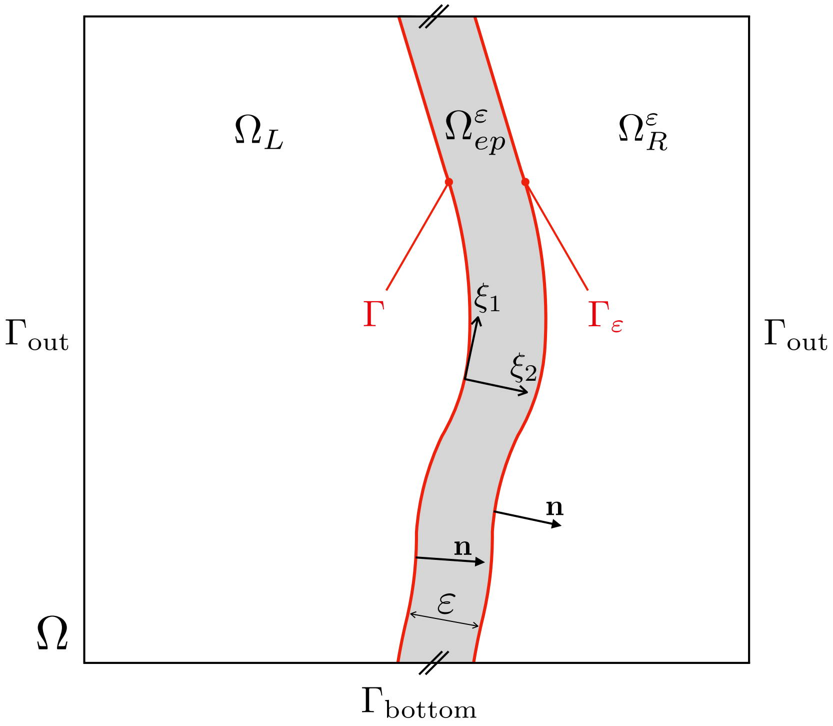

Interface Γ

$\partial_{\mathbf{n}}u^0_{i}{}_{|_{\Gamma-}}=\partial_{\mathbf{n}}u^0_{i}{}_{|_{\Gamma+}}=0,$ Neumann Boundary Condition on intra-cellular potential

$[u_e^0]_{|_\Gamma}=0,\quad[\partial_{\mathbf{n}}u_e^0]_{|_\Gamma}=0.$ Continuity on extra-cellular potential

FULLY ISOLATED

In the EP area (profile solutions)

$$\mathbf{u}_e^0=u^0_{e}{}_{|_{\Gamma-}},$$

$$\mathbf{u}_i^0=u^0_{e}{}_{|_{\Gamma-}}+\mu_0(\xi_1)e^{-\omega\eta}+\lambda_0(\xi_1)e^{\omega\eta}.$$

Map Φ_ε
Local coordinates: (ξ_1,ξ_2)
Variable change: $\eta=\xi_2/\varepsilon$
Rescaled membrane: $\Gamma\times(0,1)$

Problem at order 1

Interface Γ

$$\partial_{\mathbf{n}} u_i^1{}_{|_{\Gamma-}} = \partial_\eta \mathbf{u}_i^0{}_{|_{\eta=0}},$$

$$\partial_{\mathbf{n}} u_i^1{}_{|_{\Gamma+}} = \partial_\eta \mathbf{u}_i^0{}_{|_{\eta=1}},$$

NOT FULLY ISOLATED

$$[u_e^1]_{|_\Gamma} = \partial_{\mathbf{n}} u_e^0{}_{|_{\Gamma-}} - \int_0^1 \int_0^{\bar\eta} \kappa(\xi_1) \partial_s \mathbf{u}_e^0,$$

$$[\partial_{\mathbf{n}} u_e^1]_{|_\Gamma} = \kappa(\xi_1)\Big[-\partial_{\mathbf{n}} u_e^0{}_{|_{\Gamma-}} + \int_0^1 \int_0^{\bar\eta} \kappa(\xi_1)\partial_s \mathbf{u}_e^0\Big] - \int_0^1 \Big[\frac{S_0}{\sigma_e}(\mathbf{u}_i^0 - \mathbf{u}_e^0) - (\kappa(\xi_1))^2 \eta \partial_\eta \mathbf{u}_e^0 + S_\Gamma^0 \mathbf{u}_e^0\Big] d\eta\,.$$

Problem at order 1

Interface Γ

$$\partial_{\mathbf{n}} u_i^1{}_{|_{\Gamma-}} = \partial_\eta \mathbf{u}_i^0{}_{|_{\eta=0}},$$

NOT FULLY ISOLATED

$$\partial_{\mathbf{n}} u_i^1{}_{|_{\Gamma+}} = \partial_\eta \mathbf{u}_i^0{}_{|_{\eta=1}},$$

$$[u_e^1]_{|_\Gamma} = \partial_{\mathbf{n}} u_e^0{}_{|_{\Gamma-}} - \int_0^1 \int_0^{\bar\eta} \kappa(\xi_1) \partial_s \mathbf{u}_e^0,$$

$$[\partial_{\mathbf{n}} u_e^1]_{|_\Gamma} = \kappa(\xi_1)\left[-\partial_{\mathbf{n}} u_e^0{}_{|_{\Gamma-}} + \int_0^1 \int_0^{\bar\eta} \kappa(\xi_1)\partial_s \mathbf{u}_e^0\right] - \int_0^1 \left[\frac{S_0}{\sigma_e}(\mathbf{u}_i^0 - \mathbf{u}_e^0) - (\kappa(\xi_1))^2 \eta \partial_\eta \mathbf{u}_e^0 + S_\Gamma^0 \mathbf{u}_e^0\right] d\eta\,.$$

Interesting in the case where the parameter ε is not so small ...

Problem at order 1

Interface Γ

$$\partial_{\mathbf{n}} u_i^1{}_{|_{\Gamma-}} = \partial_\eta \mathbf{u}_i^0{}_{|_{\eta=0}},$$

$$\partial_{\mathbf{n}} u_i^1{}_{|_{\Gamma+}} = \partial_\eta \mathbf{u}_i^0{}_{|_{\eta=1}},$$

NOT FULLY ISOLATED

$$[u_e^1]_{|_\Gamma} = \partial_{\mathbf{n}} u_e^0{}_{|_{\Gamma-}} - \int_0^1 \int_0^{\bar\eta} \kappa(\xi_1)\partial_s \mathbf{u}_e^0,$$

$$[\partial_{\mathbf{n}} u_e^1]_{|_\Gamma} = \kappa(\xi_1)\Big[-\partial_{\mathbf{n}} u_e^0{}_{|_{\Gamma-}} + \int_0^1 \int_0^{\bar\eta} \kappa(\xi_1)\partial_s \mathbf{u}_e^0\Big] - \int_0^1 \Big[\frac{S_0}{\sigma_e}(\mathbf{u}_i^0 - \mathbf{u}_e^0) - (\kappa(\xi_1))^2 \eta \partial_\eta \mathbf{u}_e^0 + S_\Gamma^0 \mathbf{u}_e^0\Big] d\eta\,.$$

Interesting in the case where the parameter ε is not so small ...

Solutions at any order are then determined by induction.

Convergence theorem

THEOREM [1]

Assuming the well-posedness of all the PDE systems and let $(u_i^{\varepsilon,N}, u_e^{\varepsilon,N})$ be the functions defined by

$$u_{i,e}^{\varepsilon,N} = \begin{cases} \sum_{k=0}^{N} \varepsilon^k u_{i,e}^k, & \Omega_L \cup \Omega_R^\varepsilon, \\ \sum_{k=0}^{N} \varepsilon^k \mathbf{u}_{i,e}^k \circ \Phi_\varepsilon^{-1}, & \Omega_{ep}^\varepsilon, \end{cases}$$

for all $N \geq 0$, there exists a constant C_N independent of ε such that

$$\|u_i^\varepsilon - u_i^{\varepsilon,N}\|_{H^1(\Omega_L \cup \Omega_R^\varepsilon)} + \|u_e^\varepsilon - u_e^{\varepsilon,N}\|_{H^1(\Omega)} + \varepsilon \|\nabla (u_i^\varepsilon - u_i^{\varepsilon,N})\|_{L^2(\Omega_{ep}^\varepsilon)} \leq C_N \varepsilon^{N+1} .$$

[1] A. Collin, S. Nati Poltri, C. Poignard. Electrocardiology modeling after pulsed field ablation relying on asymptotic analysis. To be submitted. 2023.

Come back to bidomain equations

- Bidomain model

$$
\begin{aligned}
A_m(C_m\partial_t v_m + I_{ion}(v_m, w)) - \nabla \cdot (\sigma_i \cdot \nabla u_i) &= 0, \ \ \Omega,\\
A_m(C_m\partial_t v_m + I_{ion}(v_m, w)) + \nabla \cdot (\sigma_e \cdot \nabla u_e) &= 0, \ \ \Omega,\\
\partial_t w + g(v_m, w) &= 0, \ \ \Omega,\\
\partial_{\mathbf{n}} u_{i|_{\partial\Omega\setminus\Gamma}} = \partial_{\mathbf{n}} u_{e|_{\partial\Omega\setminus\Gamma}} &= 0.\\
\int_\Omega u_e &= 0.
\end{aligned}
$$

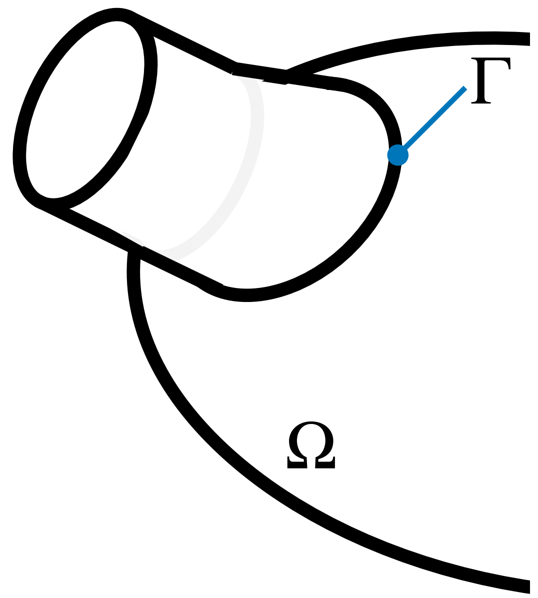

- Neumann Boundary Condition on intra-cellular potential

$$\partial_{\mathbf{n}} u_{i|_\Gamma} = 0.$$

- Continuity on extra-cellular potential

$$[u_e]_{|_\Gamma} = 0, \quad [\partial_{\mathbf{n}} u_e]_{|_\Gamma} = 0.$$

And RFA?

- Bidomain model

$$\begin{aligned} A_m(C_m\partial_t v_m + I_{ion}(v_m, w)) - \nabla\cdot(\sigma_i\cdot\nabla u_i) &= 0, \quad \Omega, \\ A_m(C_m\partial_t v_m + I_{ion}(v_m, w)) + \nabla\cdot(\sigma_e\cdot\nabla u_e) &= 0, \quad \Omega, \\ \partial_t w + g(v_m, w) &= 0, \quad \Omega, \\ \partial_{\mathbf{n}} u_{i|_{\partial\Omega\setminus\Gamma}} = \partial_{\mathbf{n}} u_{e|_{\partial\Omega\setminus\Gamma}} &= 0. \\ \int_\Omega u_e &= 0. \end{aligned}$$

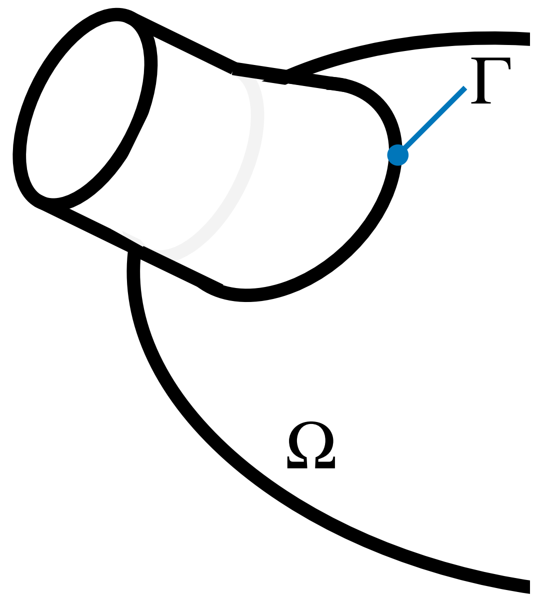

- Kedem–Katchalsky transmission condition

$$\alpha[u_e]|_\Gamma = \partial_{\mathbf{n}} u_{e|_{\Gamma-}} = \partial_{\mathbf{n}} u_{e|_{\Gamma+}}$$

$$\alpha[u_i]|_\Gamma = \partial_{\mathbf{n}} u_{i|_{\Gamma-}} = \partial_{\mathbf{n}} u_{i|_{\Gamma+}}$$

$\alpha > 0$ homogeneous to a surface conductance models the fact that treated region has a higher resistance due to RFA than the healthy tissue.

$\alpha = 0$	Isolation (perfect RFA)
$0 < \alpha \ll 1$	Fibrosis
$\alpha \gg 1$	Continuity

Numerical illustration

- Very realistic left atrium

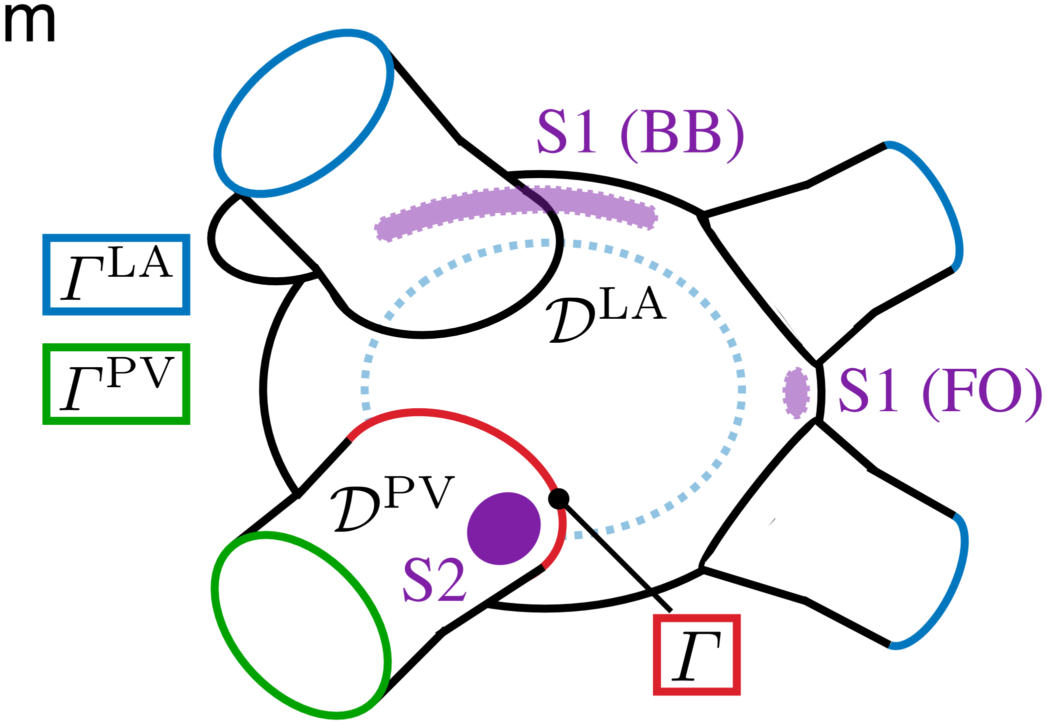

- Bidomain surface model [1]

$$\sigma_{i,e} = \sigma_{i,e}^{t} I_d + (\sigma_{i,e}^{l} - \sigma_{i,e}^{t})(f(\theta)\ \tau_0 \otimes \tau_0 + (1 - f(\theta))\ \tau_0^{\perp} \otimes \tau_0^{\perp})$$

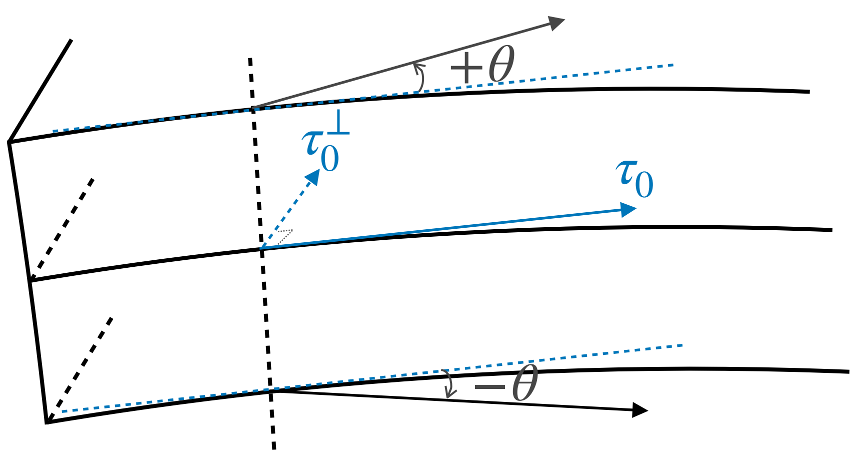

[1] Chapelle, D., Collin, A., & Gerbeau, J. F. (2013). A surface-based electrophysiology model relying on asymptotic analysis and motivated by cardiac atria modeling. *Mathematical Models and Methods in Applied Sciences*, *23*(14), 2749-2776.

Numerical illustration

- Fibers architecture

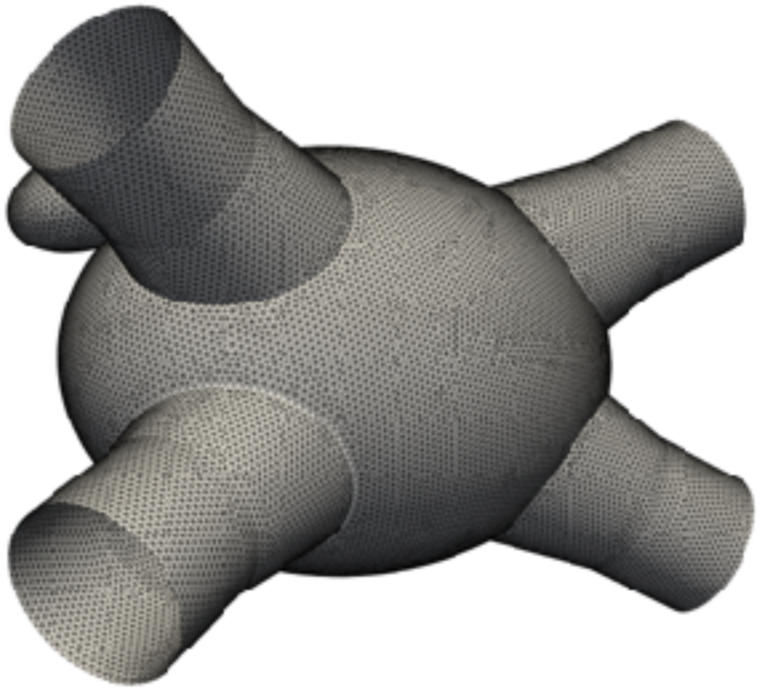

Computational mesh

Fiber orientation at the **endocardium**, see [1]

Fiber orientation at the **epicardium**, see [1]

[1] Ho, S. Y., Anderson, R. H., & Sánchez-Quintana, D. (2002). Atrial structure and fibres: morphologic bases of atrial conduction. Cardiovascular research, 54(2), 325-336.

Numerical illustration

- Numerical resolution: Finite Element Method, BDF 2, FreeFEM++
- Non-overlapping Schwarz-type algorithm for PFA
  (penalty parameter chosen very carefully through a mathematical study)
- Weak coupling for RFA
- Mesh, fibers and codes are available here:
  https://gitlab.inria.fr/snatipol/af-pfa-rfa

Numerical results

RFA (long term)

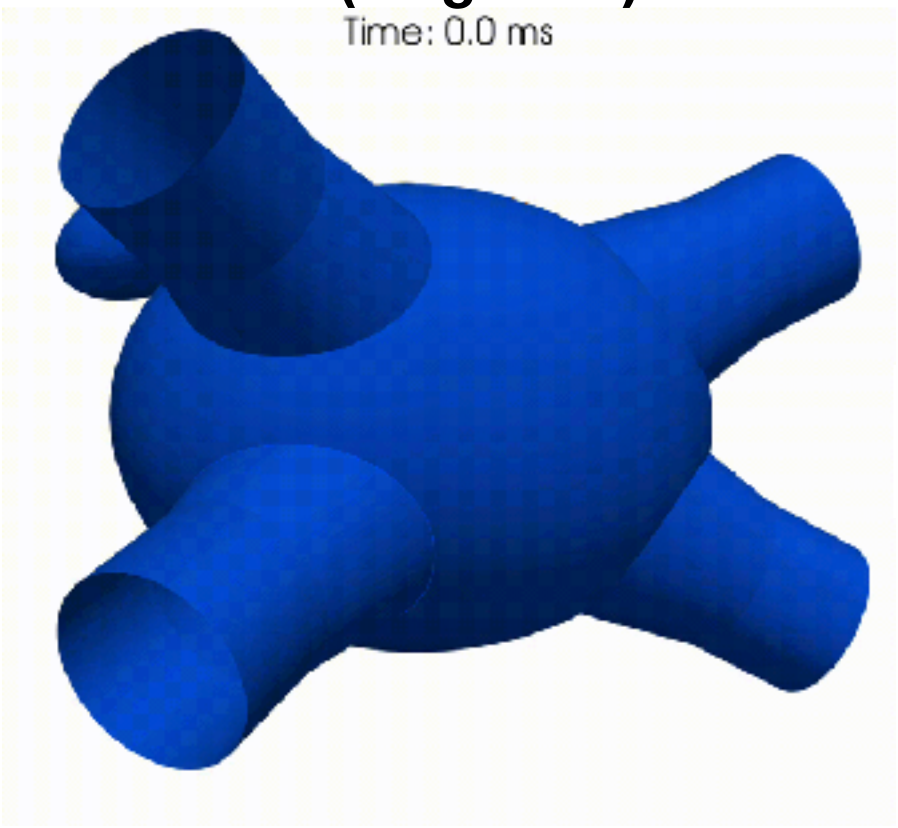

Well-designed transmission conditions

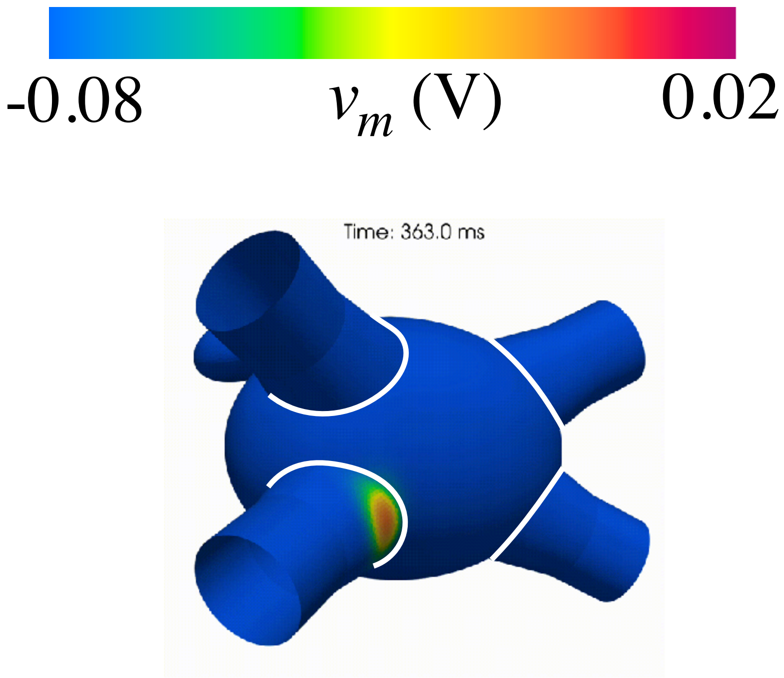

PFA (long term)

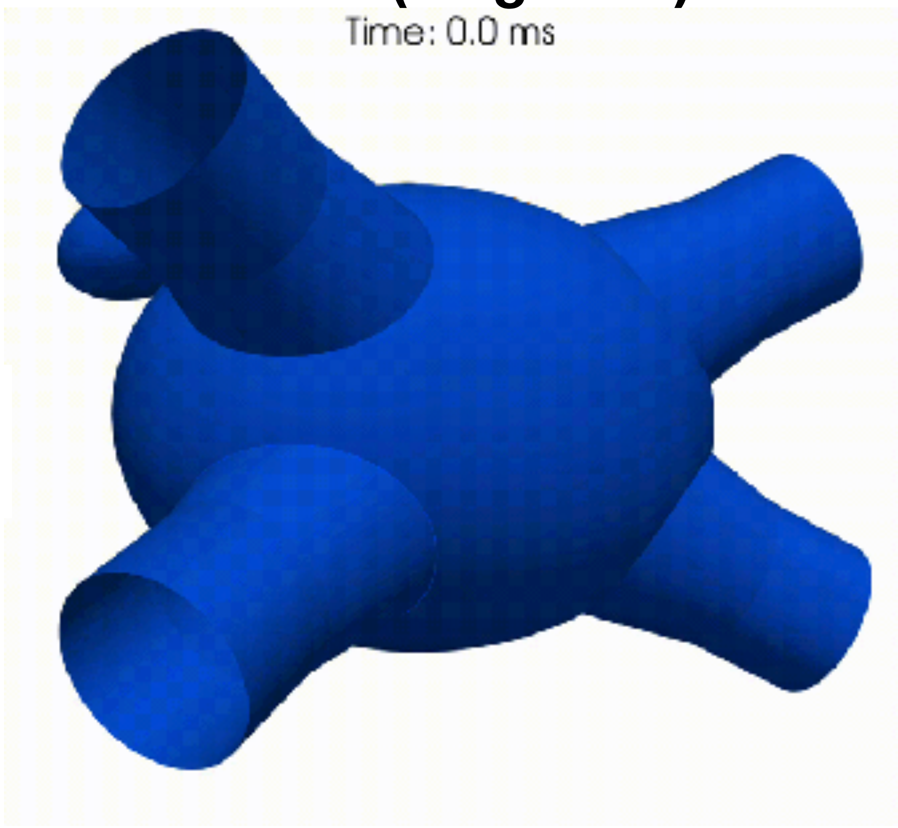

[1] Electrocardiology Modeling after Catheter Ablations for Atrial Fibrillation. S. Nati Poltri, G. Caluori, P. Jaïs, A. Collin, C. Poignard. FIMH 2023.

Numerical results

RFA (long term)

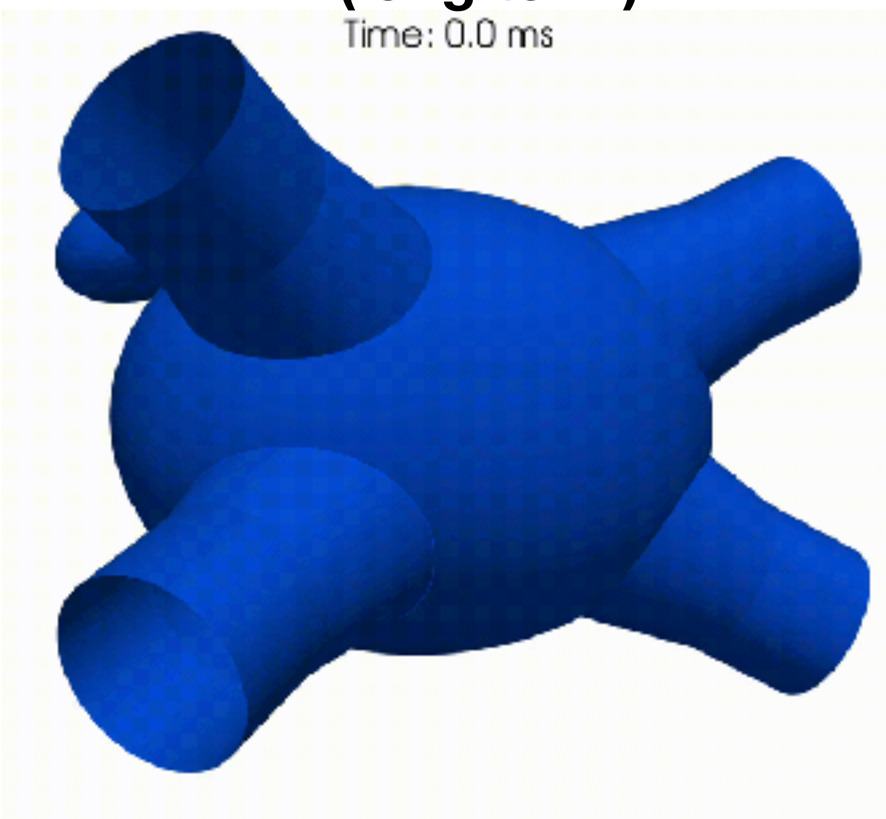

Well-designed transmission conditions

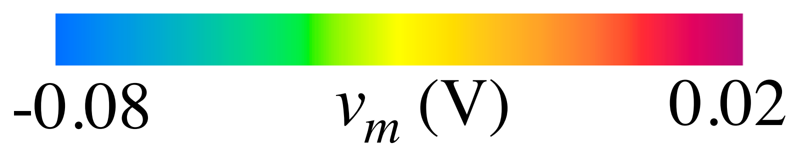

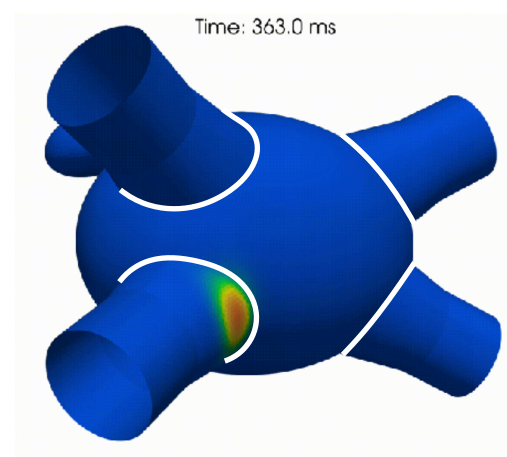

PFA (long term)

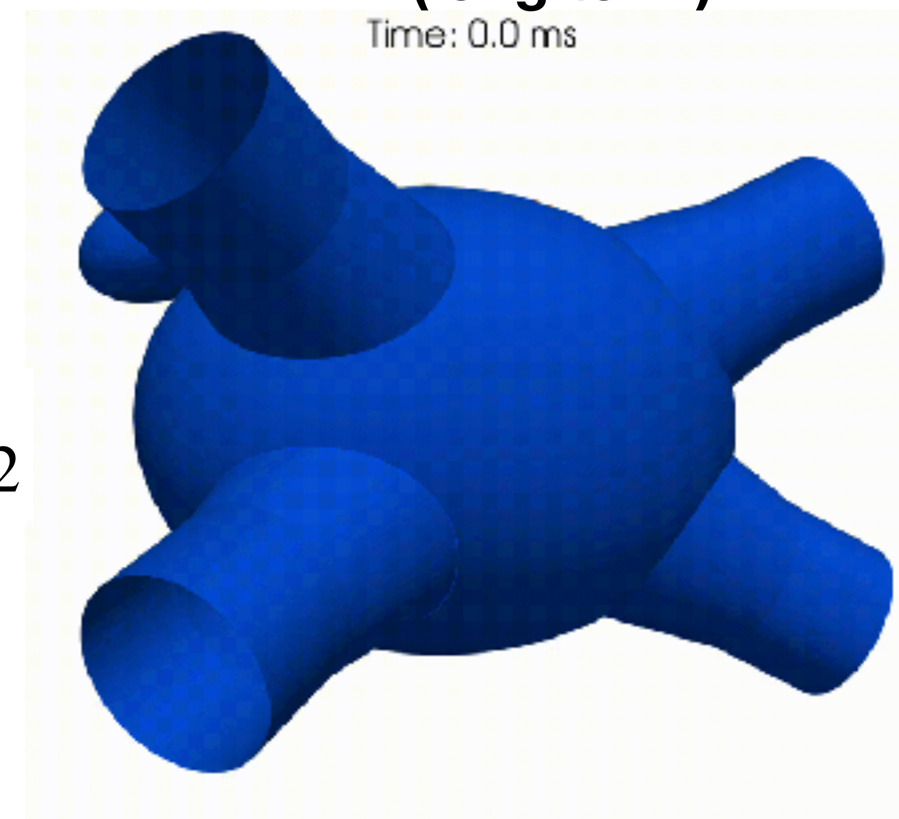

[1] Electrocardiology Modeling after Catheter Ablations for Atrial Fibrillation. S. Nati Poltri, G. Caluori, P. Jaïs, A. Collin, C. Poignard. FIMH 2023.

Numerical results

RFA (long term)

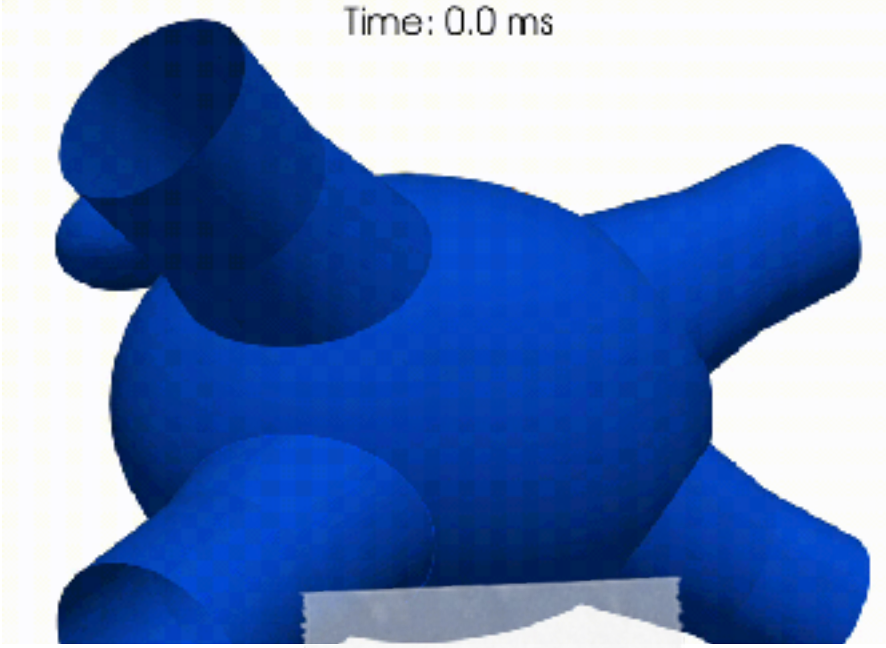

Well-designed transmission conditions

PFA (long term)

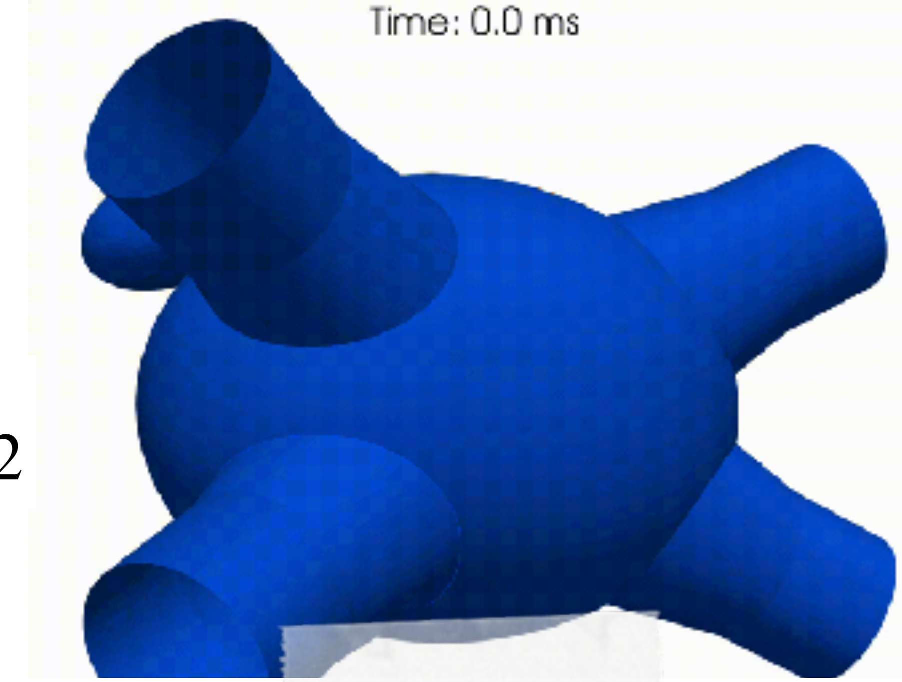

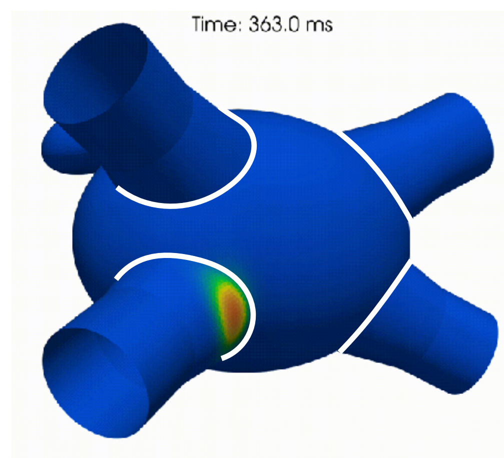

RFA: quasi-complete decoupling of the two domains for all potentials (intra- and extra-cellular potentials)

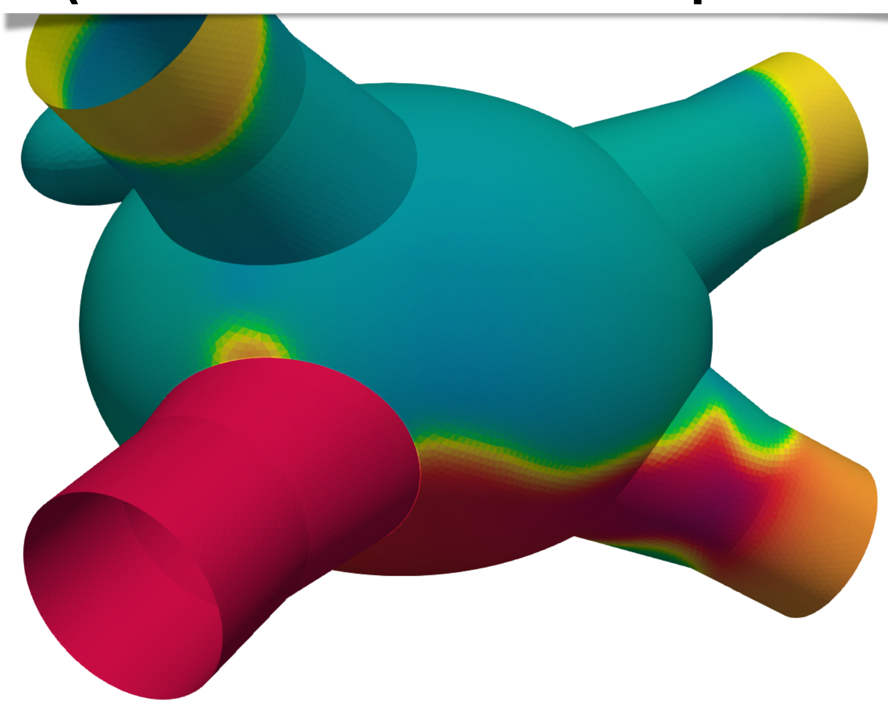

PFA: continuity of extracellular potential (Only the cardiomyocytes are impacted)

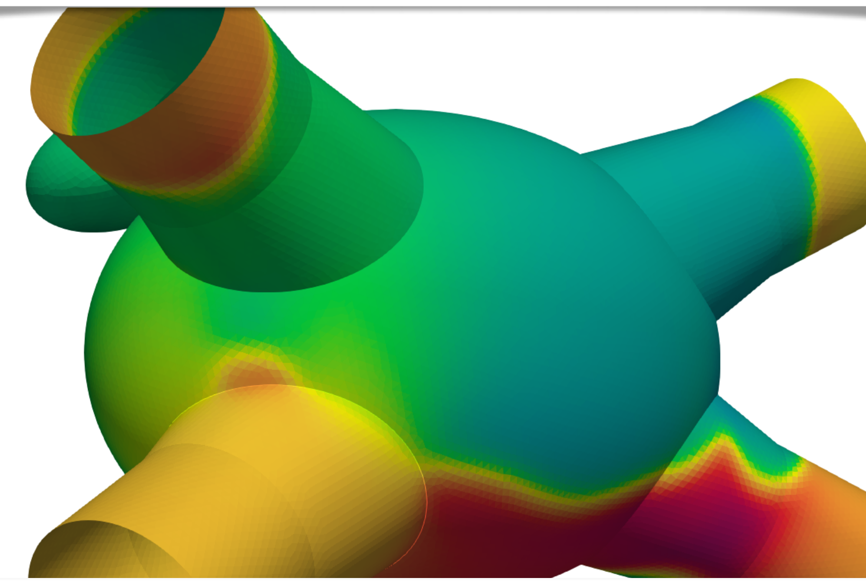

[1] Electrocardiology Modeling after Catheter Ablations for Atrial Fibrillation. S. Nati Poltri, G. Caluori, P. Jaïs, A. Collin, C. Poignard. FIMH 2023.

Numerical results

Perfect RFA

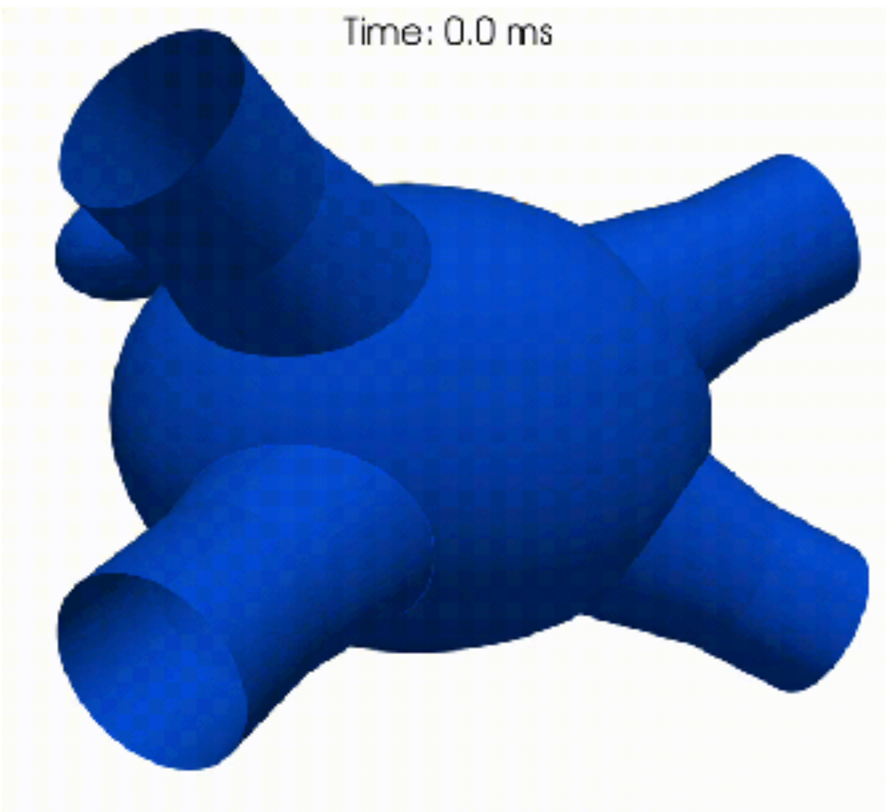

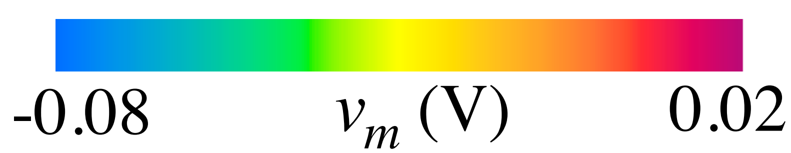

RFA with fibrosis

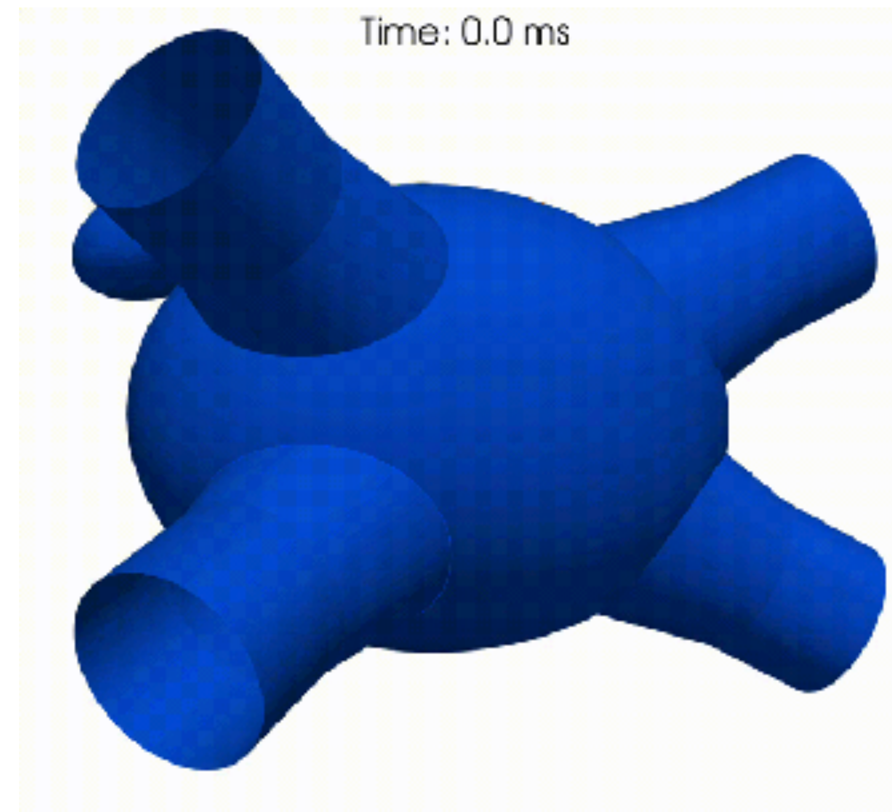

PARTIAL DISCONNECTION

[1] Electrocardiology Modeling after Catheter Ablations for Atrial Fibrillation. S. Nati Poltri, G. Caluori, P. Jaïs, A. Collin, C. Poignard. FIMH 2023.

Numerical results

Perfect RFA

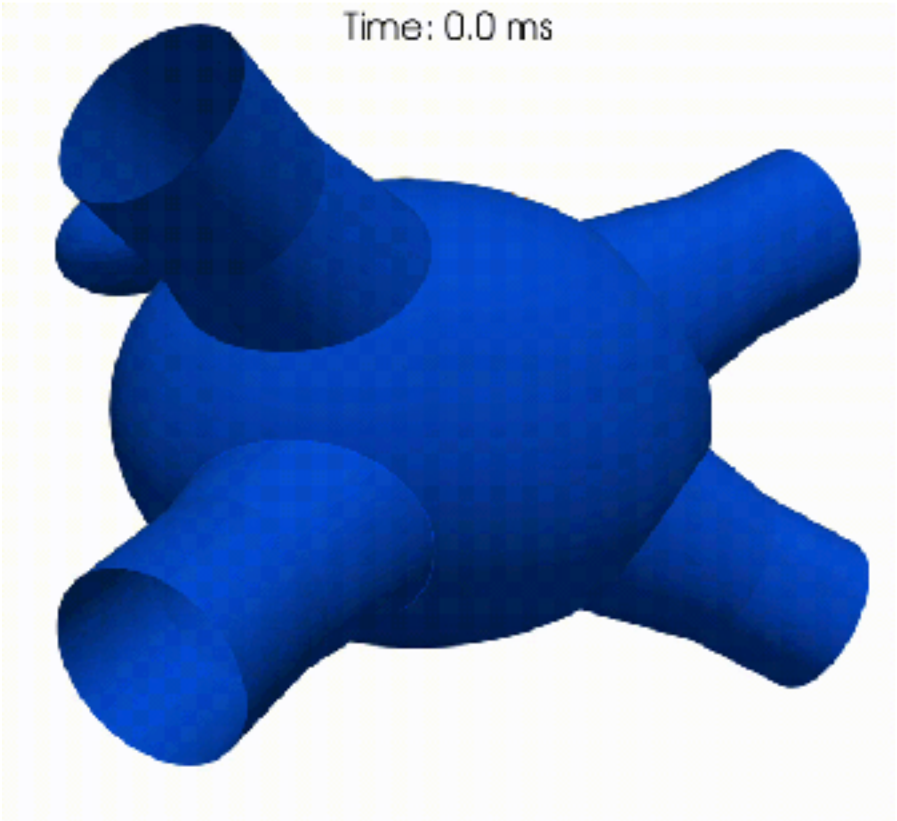

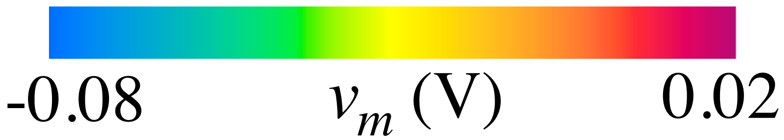

RFA with fibrosis

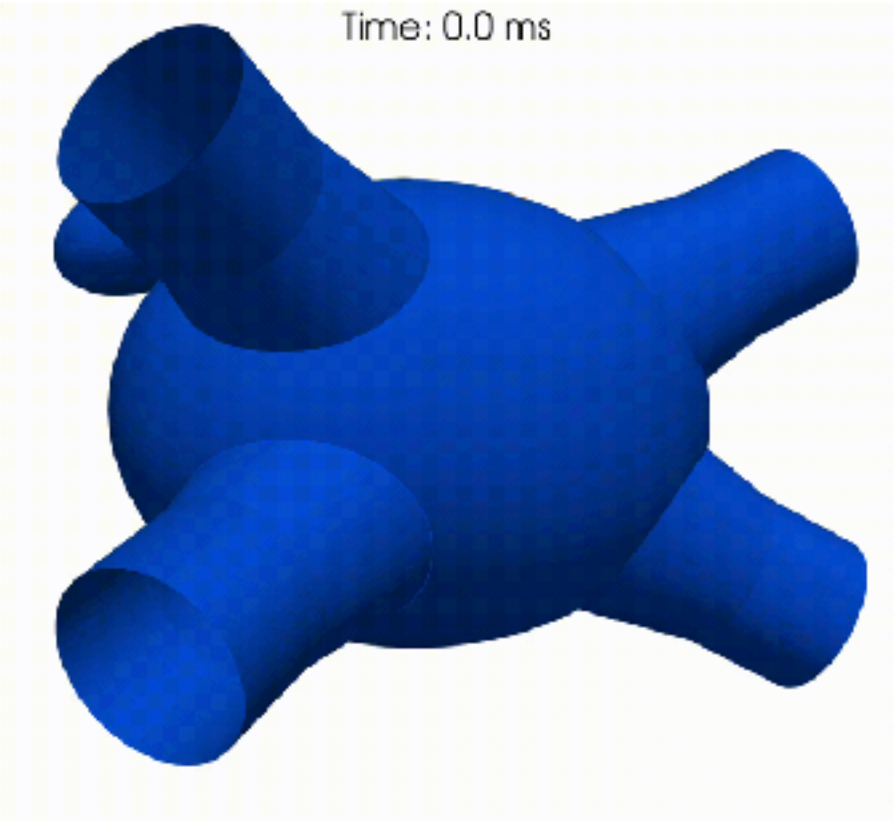

PARTIAL DISCONNECTION

[1] Electrocardiology Modeling after Catheter Ablations for Atrial Fibrillation. S. Nati Poltri, G. Caluori, P. Jaïs, A. Collin, C. Poignard. FIMH 2023.

Conclusion

- Novel non-thermal promising technique: *Pulsed electric Field Ablation (PFA)*, which takes advantage of irreversible electroporation to perform cardiac ablation.

- General context: well-designed mathematical models:
  (1) to improve understanding of irreversible electroporation on cardiac signal,
  (2) to develop numerical criteria for treatment evaluation based on clinical data.

Conclusion

- Novel non-thermal promising technique: *Pulsed electric Field Ablation (PFA)*, which takes advantage of irreversible electroporation to perform cardiac ablation.

- General context: well-designed mathematical models:
  (1) to improve understanding of irreversible electroporation on cardiac signal,
  (2) to develop numerical criteria for treatment evaluation based on clinical data.

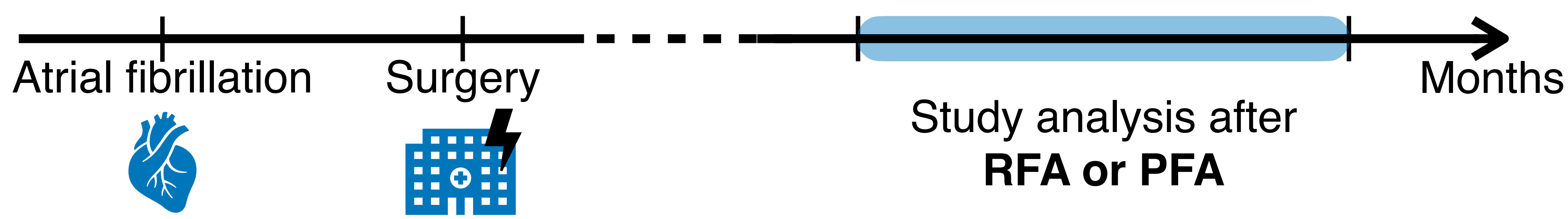

- Main results:
  (1) Derive a cardiac electrophysiological model of a cardiac domain containing an ablated region by PFA (and by RFA).
  (2) Propose a mathematical explanation for the lower recurrence of AF after PFA compared with RFA.
  (3) Both RFA and PFA lead to isolation of the pulmonary veins with respect to the electrical signal, but the nature of these isolations is very different.

Perspectives

First perspective: ventricular tachycardia (3D geometry).

- Impacts of:
  - wall thickness of the EP area,
  - fiber orientation within the EP area,

  on recurrence.

- Perform a numerical comparison between PFA and RFA to predict whether the difference in recurrence observed for AF would also be expected for ventricular tachycardia.

Second perspective: validate modeling with clinical or animal data (MRI geometry, depolarization maps, impedance data)
-> Inverse problem

Perspectives

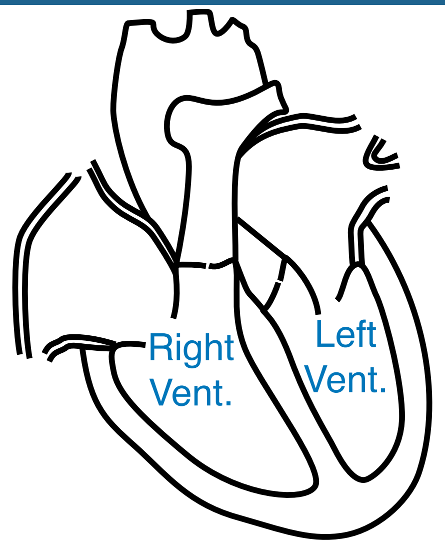

First perspective: ventricular tachycardia (3D geometry).

- Impacts of:
  - wall thickness of the EP area,
  - fiber orientation within the EP area,

  on recurrence.

- Perform a numerical comparison between PFA and RFA to predict whether the difference in recurrence observed for AF would also be expected for ventricular tachycardia.

Second perspective: validate modeling with clinical or animal data (MRI geometry, depolarization maps, impedance data)
-> Inverse problem